APPENDIX A

NRC MATERIALS LICENSE SUB-1435

Depleted Uranium Impact Area
Jefferson Proving Ground, Madison, Indiana

THIS PAGE WAS INTENTIONALLY LEFT BLANK

MATERIALS LICENSE

Pursuant to the Atomic Energy Act of 1954, as amended, the Energy Reorganization Act of 1974 (Public Law 93-438), and the applicable parts of Title 10, Code of Federal Regulations, Chapter I, Parts 19, 20, 30, 31, 32, 33, 34, 35, 36, 39, 40, 51, 70, and 71, and in reliance on statements and representations heretofore made by the licensee, a licensee is hereby issued authorizing the licensee to receive, acquire, possess, and transfer byproduct, source, and special nuclear material designated below; to use such material for the purpose(s) and at the place(s) designated below; to deliver or transfer such material to persons authorized to receive it in accordance with the regulations of the applicable Part(s). This license shall be deemed to contain the conditions specified in Section 183 of the Atomic Energy Act of 1954, as amended, and is subject to all applicable rules, regulations, and orders of the Nuclear Regulatory Commission now or hereafter in effect and to any conditions specified below.

	Licensee					
1	U.S. Department of Army			3.	License Number	SUB-1435
2.	Rock Island Arsenal 1 Rock Island Arsenal Rock Island, IL 61299-5000			4.	Expiration Date	Until Terminated
				5.	Docket or Reference Number	40-08838
6.	Byproduct, Source, and/or Special Nuclear Material: Source	7.	Chemical and/or Physical Form: Any	8.	Maximum Amount that Licensee May Possess at Any One Time Under This License: No Limit	
	Uranium		Depleted uranium metal, alloy, and/or other forms		80,000 kilograms	

9. Authorized Use: For possession only for decommissioning. License renewal applications dated August 29, 1994.

CONDITIONS

10. Authorized place of use:

A. The licensed material shall be kept onsite, for the purpose of decommissioning, in the restricted area known as the "Depleted Uranium Impact Area". This area is located north of the firing line, at the Jefferson Proving Ground, in Madison, Indiana 47250.

B. This license has been transferred from the "U.S. Department of the Army, U.S. Army Soldier and Biological Chemical Command, Aberdeen Proving Ground, Maryland 21010-5424" to "U.S. Department of the Army, 1 Rock Island Arsenal, Rock Island, Illinois 61299-5000."

[Applicable Amendments: 9, 10, 11]

11. A. Licensed materials shall be kept under the supervision of the Radiation Safety Officer, who shall have the following education, training, and experience:

1. Education: A Bachelors degree in the physical sciences, industrial hygiene, or engineering from an accredited college or university or an equivalent combination of training and relevant experience in radiological protection. Two years of relevant experience are generally considered equivalent to 1 year of academic study.

2. Health physics experience: At least 1 year of work experience in applied health physics, industrial hygiene, or similar work relevant to radiological hazards associated with site remediation. This experience should involve actually working with radiation detection and measurement equipment, not strictly administrative or "desk" work.

Enclosure

MATERIALS LICENSE

MATERIALS LICENSE SUPPLEMENTARY SHEET

License Number: SUB-1435

Docket or Reference Number: 40-08838

Amendment No. 17

3. Specialized knowledge: A thorough knowledge of the proper application and use of all health physics equipment used for depleted uranium and its daughters, the chemical and analytical procedures used for radiological sampling and monitoring, methodologies used to calculate personnel exposure to depleted uranium and its daughters, and a thorough understanding of how the depleted uranium was used at the location and how the hazards are generated and controlled.

B. The licensee, without prior NRC approval, may appoint a RSO provided: a) the licensee maintains documentation demonstrating that the requirements of condition 11A are met; and b) the NRC is informed of the name of the new RSO within 30 days of the appointment by letter to Document Control Desk, Director, Office of Federal and State Materials and Environmental Management Programs, U.S. Nuclear Regulatory Commission, Washington, D.C. 20555-0001.

[Applicable Amendments: 8, 9, 10, 16]

12. Except as specifically provided otherwise in this license, the licensee shall conduct its program in accordance with the statements, representations, and procedures contained in the documents, including any enclosures, listed below. The NRC regulations shall govern unless the statements, representations, and procedures in the licensee's application and correspondence are more restrictive than the regulation.

A. Letter and attachments for license renewal dated August 29, 1994,

B. Letter dated May 25, 1995,

C. Application with attachments dated September 29, 1995, and

D. JPG Security Plan included with the letter dated December 10, 2003.

E. Request for change of licensing official and signed NRC Form 313 dated November 8, 2004.

F. Request for change of licensing official and signed NRC Form 313 dated October 25, 2007.

G. Request for change of licensing official and signed NRC Form 313 dated February 4, 2008.

[Applicable Amendments: 3, 4, 6, 9, 10, 11, 12, 13, 14, 15]

MATERIALS LICENSE

MATERIALS LICENSE SUPPLEMENTARY SHEET

License Number: SUB-1435

Docket or Reference Number: 40-08838

Amendment No. 17

13. The Army shall submit a Decommissioning Plan for NRC review and approval under an alternate schedule identified in its May 25, 2005, Field Sampling Plan; its responses to action items from a September 8, 2005, public meeting by letter dated October 26, 2005; its Field Sampling Plan addendum dated November 2005 and all subsequent addendums; its responses to NRC's request for additional information by letter dated February 9, 2006; and its May 2, 2012 letter. The Army will also submit an Environmental Report using the guidance in NUREG-1748 for NRC to use in preparing an Environmental Impact Statement. The Decommissioning Plan and Environmental Report will be submitted no later than August 30, 2013.

[Applicable Amendments: 9, 10, 13, 14, 15, 17]

FOR THE U.S. NUCLEAR REGULATORY COMMISSION

Date: 12/27 /12

/RA/
Andrew Persinko, Deputy Director
Decommissioning and Uranium Recovery
Licensing Directorate
Division of Waste Management
and Environmental Protection
Office of Federal and State Materials
and Environmental Management Programs

THIS PAGE WAS INTENTIONALLY LEFT BLANK

APPENDIX B

GROUNDWATER MODELING

Depleted Uranium Impact Area
Jefferson Proving Ground, Madison, Indiana

THIS PAGE WAS INTENTIONALLY LEFT BLANK

TABLE OF CONTENTS

Page

1. INTRODUCTION ... 1-1
   1.1 OBJECTIVE ... 1-1
   1.2 SITE BACKGROUND ... 1-1
      1.2.1 Location ... 1-4
      1.2.2 Site Description ... 1-4
   1.3 SITE INVESTIGATIONS ... 1-5
      1.3.1 Scoping Survey ... 1-5
      1.3.2 Characterization Survey ... 1-6
      1.3.3 Remedial Investigation South of the Firing Line ... 1-7
      1.3.4 Fracture Trace Report ... 1-7
      1.3.5 Well Location Selection Report ... 1-7
      1.3.6 Well Construction and Surface Water Data Report ... 1-8
      1.3.7 Slug Test Report ... 1-10
      1.3.8 USGS Age Dating Report ... 1-11
   1.4 REPORT OUTLINE ... 1-12
2. DATA SUMMARY ... 2-1
   2.1 METEOROLOGICAL DATA ... 2-1
   2.2 TOPOGRAPHY ... 2-1
   2.3 HYDROGEOLOGY ... 2-2
      2.3.1 Surface Water ... 2-2
      2.3.2 Hydrostratigraphy ... 2-2
         2.3.2.1 Overburden ... 2-2
         2.3.2.2 Bedrock ... 2-5
      2.3.3 Water Levels ... 2-7
      2.3.4 Hydraulic Conductivity ... 2-11
      2.3.5 Geotechnical Properties ... 2-13
      2.3.6 Groundwater Use ... 2-13
      2.3.7 Water Budget ... 2-13
   2.4 ANALYTICAL DATA SUMMARY ... 2-14
3. CONCEPTUAL SITE MODEL ... 3-1
   3.1 CHARACTERISTICS OF URANIUM AND DEPLETED URANIUM ... 3-2
      3.1.1 Uranium ... 3-2
      3.1.2 Depleted Uranium ... 3-2
      3.1.3 Radioactivity ... 3-4
   3.2 TRANSPORT MECHANISMS ... 3-4
      3.2.1 Groundwater Pathway ... 3-4
         3.2.1.1 Overburden ... 3-6
         3.2.1.2 Shallow Bedrock Zone ... 3-6
         3.2.1.3 Deep Bedrock Zone ... 3-6
         3.2.1.4 Karst Development ... 3-6
         3.2.1.5 Recharge and Groundwater Flow ... 3-7
      3.2.2 Surface Water Pathway ... 3-7
      3.2.3 Biotransfer Pathways ... 3-7
   3.3 EXPOSURE PATHWAYS ... 3-8
4. VADOSE ZONE COLUMN MODEL ... 4-1
   4.1 CURRENT DU ACTIVITY IN SOIL ... 4-1

TABLE OF CONTENTS (Continued)

Page

4.2 SOURCE TERM EVALUATION 4-2
4.2.1 Penetrator Distribution 4-2
4.2.2 DU Corrosion and Dissolution Rates 4-2
4.2.3 Laboratory Derived K_d Values 4-4
4.3 MODEL SELECTION AND DESCRIPTION 4-5
4.4 MODEL DESIGN 4-6
4.4.1 Model Domain and Discretization 4-6
4.4.2 Boundary Conditions 4-6
4.4.3 Layer Properties 4-8
4.5 MODELING RESULTS OF THE BASE CASE SIMULATION 4-9
4.6 SENSITIVITY ANALYSIS 4-10
4.7 UNCERTAINTIES IN MODELING SIMULATIONS 4-11
5. GROUNDWATER FLOW MODEL 5-1
5.1 MODEL DESIGN 5-1
5.1.1 Model Selection and Description 5-1
5.1.2 Model Domain and Discretization 5-1
5.1.3 Boundary Conditions 5-3
5.1.3.1 External Boundary Conditions 5-3
5.1.3.2 Internal Boundary Conditions 5-6
5.1.4 Layer Elevations 5-6
5.2 FLOW CALIBRATION 5-7
5.2.1 Groundwater Calibration Targets 5-7
5.2.2 Hydraulic Conductivity 5-8
5.2.3 Recharge 5-11
5.2.4 Calibration Results 5-11
5.3 MODEL UNCERTAINTY AND SENSITIVITY ANALYSIS 5-13
6. GROUNDWATER MODELING SUMMARY AND CONCLUSIONS 6-1
6.1 SOIL TO GROUNDWATER RESULTS 6-1
6.2 GROUNDWATER FLOW RESULTS 6-1
7. REFERENCES 7-1

LIST OF ATTACHMENTS

Attachment 1. Water Level Hydrographs and Continuous Recorder Data for DU Impact Area Wells
Attachment 2. DU Transport Through FEHM Soil Column Model
Attachment 3. Groundwater Model Sensitivity Analysis

LIST OF FIGURES

Page

Figure 1-1 Location of JPG in Southern Indiana 1-2
Figure 1-2 Location of DU Impact Area at the Former Jefferson Proving Ground 1-3
Figure 1-3 Well Locations Within and Near DU Impact Area 1-9
Figure 2-1 Top of Bedrock Elevations 2-6
Figure 2-2 Locations of Wells With Continuous Recorders and Collected Data 2-9
Figure 2-3 Particle Size Comparison of JPG Soil Types 2-13
Figure 2-4 Environmental Radiation Monitoring Locations 2-15
Figure 2-5 JPG Sediment Total Uranium April 2008-February 2009 2-17
Figure 2-6 JPG Surface Water Total Uranium April 2008-February 2009 2-18
Figure 2-7 JPG Background Soil Sampling Locations 2-20
Figure 2-8 JPG Soil Sampling Locations Within and Around the DU Impact Area 2-21
Figure 2-9 JPG Soil Sampling Locations Under Penetrators Within the DU Impact Area 2-22
Figure 2-10 JPG Soil Sampling for K_d Study 2-23
Figure 3-1 Revised Conceptual Site Model of DU Transport Through the Environment at and in Close Proximity to the DU Impact Area 3-5
Figure 4-1 Estimated DU Mass Release Into Soil From Penetrator Corrosion/Dissolution 4-3
Figure 4-2 Example Soil Density Profile Through Loess Soil and Glacial Till at Well Location JP-DU-06 4-5
Figure 4-3 Schematic of Vadose Zone Column Model 4-7
Figure 4-4 Base Case Results Showing Predicted Concentrations with Depth 4-9
Figure 5-1 Groundwater Model Domain 5-2
Figure 5-2 Water Bearing Units in Groundwater Flow Model 5-3
Figure 5-3 Layer 1 Boundary Conditions 5-4
Figure 5-4 Layer 2 Boundary Conditions 5-5
Figure 5-5 Layer 1 Hydraulic Conductivity Distribution 5-9
Figure 5-6 Layer 2 Hydraulic Conductivity Distribution 5-10
Figure 5-7 Layer 3 Hydraulic Conductivity Distribution 5-10
Figure 5-8 Model Recharge Distribution 5-11
Figure 5-9 Modeled Groundwater Elevations in Layer 1 5-12
Figure 5-10 Observed Versus Modeled Water Levels 5-13

LIST OF TABLES

Page

Table 2-1 Monthly Precipitation and Temperature at Madison, Indiana 2-1
Table 2-2 Depth to Bedrock at DU Impact Area and Vicinity 2-3
Table 2-3 Soil Series at the DU Impact Area 2-4
Table 2-4 Depths to Groundwater in Overburden Wells 2-8

LIST OF TABLES (Continued)

Page

Table 2-5 Overburden Slug Test Results 2-11
Table 2-6 Shallow Bedrock Slug Test Results 2-11
Table 3-1 Percent U-235 by Mass in Different Types of Uranium 3-3
Table 3-2 Amount of Isotope Present by Activity in Natural Uranium 3-3
Table 3-3 Relative Isotopic Activity in DU 3-3
Table 4-1 DU Activity with Depth in Shallow Loess Soils 4-1
Table 4-2 Most Likely Estimate Values for Corrosion and Dissolution Rates 4-3
Table 4-3 Summary of DU Batch Testing Results 4-4
Table 4-4 FEHM Input Parameters 4-8
Table 4-5 FEHM Model Predicted Percentage of Source Concentration at End of 1,000 Years 4-9
Table 4-6 Summary of Sensitivity Analysis for FEHM Column Modeling 4-12
Table 5-1 Layer Elevation Summary 5-7
Table 5-2 February 2009 Calibration Targets 5-8
Table 5-3 Calibration Statistics 5-12

LIST OF ACRONYMS AND ABBREVIATIONS

ac	Acre
ADAMS	Agencywide Documents Access and Management System
BGS	Below Ground Surface
BRAC	Base Realignment and Closure
CFC	Chlorofluorocarbon
cfs	Cubic Feet per Second
cm	Centimeter
cm^2	Square Centimeter
CSM	Conceptual Site Model
DEM	Digital Elevation Model
DU	Depleted Uranium
Eh	Redox Potential
EOD	Explosive Ordnance Disposal
ERM	Environmental Radiation Monitoring
FEHM	Finite Element Heat and Mass Transfer
ft	Feet
ft/day	Feet per Day
FWS	U.S. Fish and Wildlife Service
g/cm^3	Gram per Cubic Centimeter
$gal/day/ft^2$	Gallon per Day per Square Foot
GHB	General Head Boundary
GIS	Geographic Information System
in	Inch
in/y	Inch per Year
INANG	Indiana Air National Guard
JPG	Jefferson Proving Ground
K_d	Distribution Coefficient
kg	Kilogram
km	Kilometer
km^2	Square Kilometer
L/kg	Liter per Kilogram
LEU	Low Enriched Uranium
μg	Microgram
μg/L	Microgram per Liter
μR/hr	MicroRoentgen per Hour
m	Meter
m/y	Meter per Year
m^2	Square Meter
mg/kg	Milligram per Kilogram
mg/L	Milligram per Liter
mi	Mile
mi^2	Square Mile
mL/g	Milliliter per Gram
mm	Millimeter
MOA	Memorandum Of Agreement
MPa	Megapascal
msl	Mean Sea Level
NaI	Sodium Iodide
NARA	U.S. National Archives and Records Administration

LIST OF ACRONYMS AND ABBREVIATIONS (Continued)

NRC	Nuclear Regulatory Commission
NRCS	Natural Resources Conservation Service
pCi/g	Picocurie per Gram
pCi/L	Picocurie per Liter
R_d	Distribution Ratio
RI	Remedial Investigation
RI/FS	Remedial Investigation/Feasibility Study
RQD	Rock Quality Designation
SAIC	Science Applications International Corporation
SSR	Sum of Squared Residuals
SVS	Soil Verification Study
TOC	Total Organic Carbon
U-234	Uranium-234
U-235	Uranium-235
U-238	Uranium-238
USAF	U.S. Air Force
USDA	U.S. Department of Agriculture
USGS	U.S. Geological Survey
UXO	Unexploded Ordnance

1. INTRODUCTION

Depleted Uranium (DU) fate and transport via the groundwater pathway was assessed through integration of site data within numerical models. The soil to groundwater pathway was evaluated using a one-dimensional column model to assess potential transport through the vadose zone. A three-dimensional groundwater flow and transport model was constructed to assess potential migration within the saturated zone beneath the former Jefferson Proving Ground (JPG). The groundwater model extent is constrained within the boundaries of the former JPG. As such, the model permits evaluation of DU transport beneath JPG as well as the potential for off-site migration (defined here as off the former JPG property).

1.1 OBJECTIVE

The objective consists of developing and calibrating a groundwater model for use in assessing DU fate and transport. The model, in conjunction with site investigation data, is then used to evaluate the potential for DU migration at the former JPG. The results of this study, in conjunction with results from the surface water pathway evaluation, will be used to support decisions regarding the restricted release license termination of the Nuclear Regulatory Commission (NRC) license for DU at JPG, NRC Materials License SUB-1435.

1.2 SITE BACKGROUND

JPG, located in southeast Indiana, was established in 1941 as a proving ground for the production line acceptance test firing of a wide variety of conventional military ordnance (Figure 1-1). The Defense Secretary's Commission on Base Realignment and Closure (BRAC) recommended JPG for closure in December 1988, and in April 1989, the Congress mandated that JPG be closed (Public Law 100-526). The U.S. Army used JPG until 1994. JPG was closed in September 1995 under the Defense Authorization Amendments and Base Closure and Realignment Act of 1988 (Public Law 100-526). The area south of the firing line, where DU was stored, was surveyed at that time to determine the extent of DU contamination. Following decontamination efforts, the total area south of the firing line was released for unrestricted use (i.e., released from radiological controls) in 1996 (see NRC press release dated 13 May 1996, NRC Agencywide Documents Access and Management System (ADAMS), accession number ML003705136). The NRC license for the area north of the firing line was amended for possession of DU only in May 1996.

The mission at JPG was to plan and conduct production line acceptance tests, reconditioning tests, surveillance tests, and other studies of ammunition and weapons systems for conventional military ordnance. Impact areas at JPG included high impact targets, asphalt and sediment-bottom ponds for testing proximity fuses, a gunnery range, mine fields, and the DU Impact Area (SEC Donahue 1992, see also the Archives Search Report for Ordnance and Explosive Waste Chemical Warfare Materials, Jefferson Proving Ground, Madison, Indiana, Volume I Record Review and Interviews, Appendix D – Comprehensive List of Ammunition Tested at Jefferson Proving Ground, June 1995). DU remaining within the DU Impact Area is the focus of fate and transport assessment efforts.

The DU Impact Area (Figure 1-2) is a rectangular shaped area approximately 17,280 feet (ft) (5,270 meters [m]) long and 5,240 ft (1,600 m) wide that is positioned lengthwise, north to south, from F Road to just south of C Road, approximately 2,080 acres (ac). The western and eastern boundaries of the area are at Morgan and Wonju Roads, respectively. Active testing of DU munitions was conducted at the DU Impact Area between 18 March 1984 and 2 May 1994. DU penetrators were test fired through soft cloth targets at 1,000 m intervals from 3 firing points (J, 500 Center, and K5), with the majority occurring along the 500 Center firing point. The Army estimates the mass of DU remaining in the DU Impact Area to be approximately 162,040 pounds (lb) (73,500 kilograms [kg]). See Section 1 of the Decommissioning Plan (U.S. Army 2013) for additional details.

Location of JPG in Southern Indiana

Figure 1-1

Date: 8/5/2013

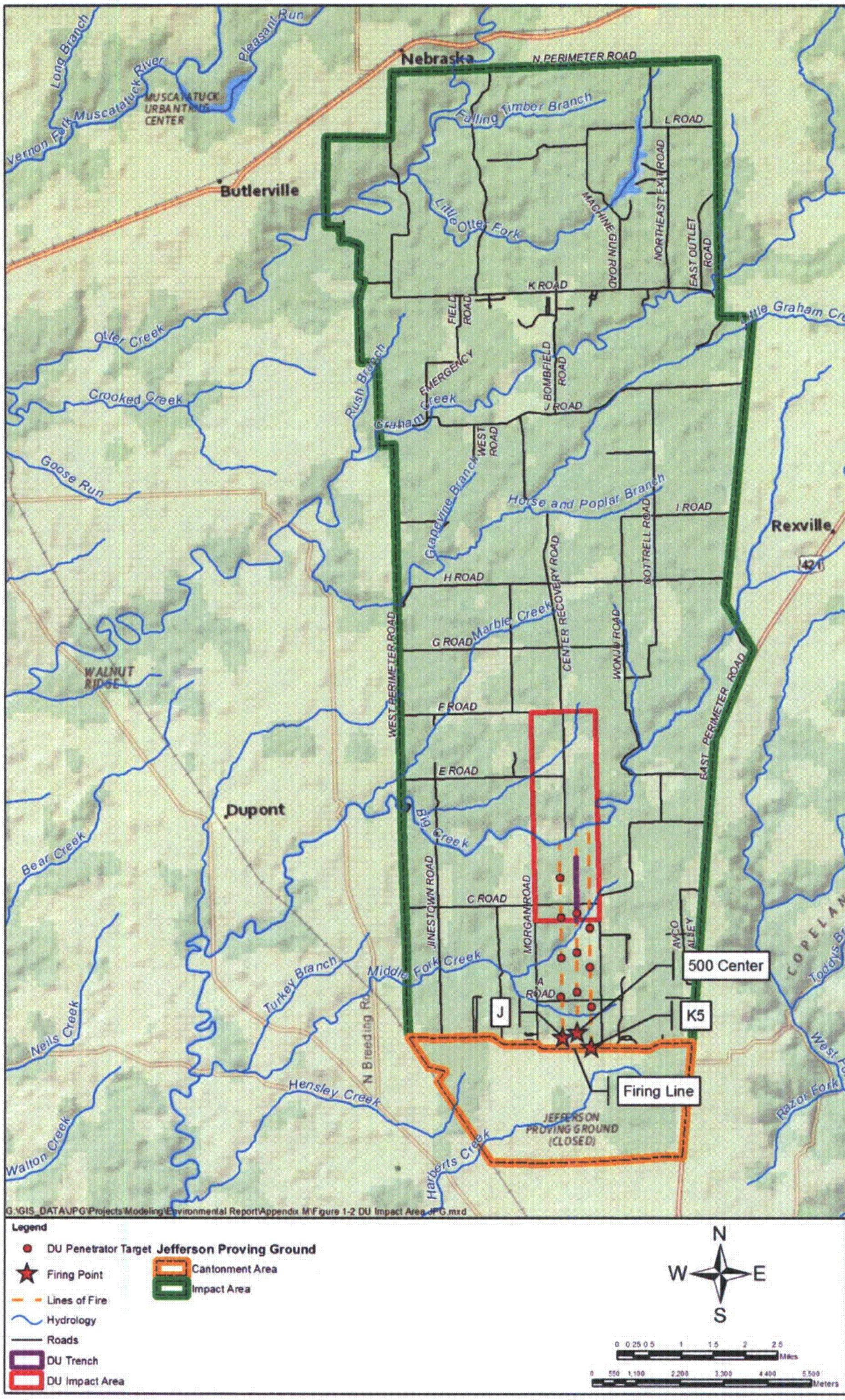

Location of DU Impact Area at the Former Jefferson Proving Ground

Figure 1-2

Date: 8/5/2013

1.2.1 Location

JPG occupies approximately 55,264 ac (224 square kilometers [km^2]) within parts of north central Jefferson, southwestern Ripley, and southeastern Jennings counties in the southeastern portion of Indiana. The DU Impact Area is situated entirely within Jefferson County.

JPG is located 8 miles (mi) (13 kilometers [km]) north of the Indiana/Kentucky border (SAIC 1997) and the Ohio River. The nearest population center is the city of Madison, Indiana, which has a population of 11,967 (U.S. Census Bureau 2010), and is approximately one-third of the population of Jefferson County. The location of the site and nearby communities is shown in Figure 1-1. Major metropolitan areas include Louisville, Kentucky, approximately 45 mi (72 km) southwest; Cincinnati, Ohio, approximately 75 mi (121 km) northeast; and Indianapolis, Indiana, approximately 85 mi (137 km) north-northwest.

The property surrounding the site is predominantly farmlands, woodlands, and rural residential areas (U.S. Army 2002). Public water from deep wells is used by nearby communities or individuals, with well depths ranging from 50 ft (15 m) to 300 ft (90 m) completed in the limestone formations underlying the site (Rust E&I 1994, 1998; MWH 2002).

1.2.2 Site Description

A firing line with 268 gun positions directed to the north was used for testing conventional military ordnance. This firing line separates JPG into two areas: an approximate 4,000 ac (16.1 km^2) southern portion and an approximate 51,000 ac (206 km^2) northern portion (SAIC 1997). The DU Impact Area, consisting of approximately 2,080 ac (8.4 km^2) within the 51,000 ac (206 km^2) area north of the firing line, was used for testing of DU munitions. Firings of DU projectiles were directed toward the DU Impact Area from three gun positions along the firing line; the three gun positions were designated as Firing Points J, 500 Center, and K. DU projectiles were fired from tank guns at high velocities through soft cloth targets and, upon impact, projectiles penetrated the earth, ricocheted, or broke into pieces.

The firing protocol caused the DU projectiles to impact in approximately the same location each time along the firing line trajectories (SEG 1996). Repeated impacts in the same areas resulted in the formation of north to south trending trenches north of the lines-of-fire. Eighty-nine percent of the DU penetrators were fired from 500 Center. Repetitive impacts from the 500 Center firing line position formed a trench approximately 3.4 ft (1 m) deep by 16.4 to 26.3 ft (5 to 8 m) wide extending for approximately 3,937 ft (1,200 m). Similar patterns occurred at the other two firing positions but to a lesser extent and magnitude because a smaller quantity of DU was fired from these locations (SEG 1996). Only about seven percent of the total DU was fired from firing point J. Firing point K, the easternmost DU firing point, was used to fire only 4 percent of the total DU.

Explosive ordnance disposal (EOD) personnel would sweep the area twice a year to recover DU. The residual DU varies in size from microscopic particles to complete projectiles (SEG 1996). The distribution of this DU is nonhomogeneous because of the variability in the projectile trajectory and projectile fragmentation, but site radiological investigations have indicated that most of the contamination is along the firing lines (SEG 1995, 1996; Section 6).

During the period that JPG was operational (1941 to 1994), more than 24 million rounds of conventional explosive ammunition were fired into the area north of the firing line, including within the DU Impact Area. Approximately 1.5 million rounds did not detonate upon impact, remaining as high-explosive unexploded ordnance (UXO) either on or beneath the ground surface and resulting in approximately 85 high-explosive rounds of UXO per acre within the DU Impact Area. This remaining UXO is a hazard that has been a major factor in decisions concerning management of the area north of the firing line (SAIC 1997).

The 51,000-ac area north of the firing line remains under Army ownership. The U.S. Fish and Wildlife Service (FWS) manages JPG's natural resources under a memorandum of agreement (MOA) (U.S. Army 2000). Also under the MOA, the Indiana Air National Guard (INANG) for the U.S. Air Force (USAF) operates an air to ground training range north of the firing line for several Air National Guard units. All ordnance utilized by the various Air National Guard units is inert with small spotting charges. Public use of the area is limited due to the potential for contact with UXO, exposure to DU, and the INANG training mission.

The cantonment area, located south of the firing line, houses the support facilities that were used for administrative ammunition assembly and testing, vehicle maintenance, and residential housing (U.S. Army 2002). This area has been leased for farming, and buildings in the former military housing area have been subleased to private companies and individuals. Ownership of the entire area south of the firing line has been transferred to a local farmer with the exception of approximately 1,200 ac, which are expected to be transferred within the next 24 months, two park parcels transferred to Jefferson County, one building, and the approximate 17 miles of railroad tracks sold to the Madison Port Authority.

1.3 SITE INVESTIGATIONS

In compiling information and data for the conceptual model of the site, several pertinent reports were used and are summarized here.

1.3.1 Scoping Survey

Areas potentially affected by facility operations include the firing lines and the DU Impact Area. A radiological scoping survey of these areas was conducted between 8 October and 23 December 1994. The objective of the study was to confirm and document areas affected by DU projectiles and to identify areas to be included in further studies (SEG 1995).

The approach to data collection involved measurement of exposure rates at grid locations and collection of soil, groundwater, surface water, sediment, and vegetation samples at locations referenced to a similar grid.

For exposure rate measurements in the DU Impact Area, grid lines were established at separations of 164 ft (50 m) in the north-south direction, and measurements were taken 3.3 ft (1 m) above the ground at intervals of 33 ft (10 m) along each grid line.

For the exposure rate measurements in the firing line area, three north-south grid lines were established for each of the three firing points. A central grid line was located along the firing point, and two additional grid lines were located 164 ft (50 m) to the east and west of the central firing point. Exposure rate measurements were taken 3.3 ft (1 m) above ground level at an interval of 33 ft (10 m) along each grid line. Prior to performance of exposure measurements in the DU Impact Area, a background study was performed. Thirty-five locations south of the firing line were measured to determine an average background exposure rate of 12 microRoentgen per hour (μR/hr). The result is consistent with results of the site environmental monitoring program.

As part of the survey, 62 soil, 11 groundwater, 14 surface water, 13 sediment, and 20 vegetation locations were sampled. Details on the sampling methods and results can be found in the scoping survey report (SEG 1995).

Gamma dose rate surveys indicate that areas most affected by the testing of DU munitions are the 500 Center line-of-fire and adjacent areas (SEG 1995). The majority of the affected area runs from south to north along the 500 Center line-of-fire, but the affected area becomes broader north of D Road where DU penetrators impacted the upslope (SEG 1996). This conclusion is supported by soil sample results that show that areas along the 500 Center line-of-fire are the only areas exhibiting soil contamination above the guideline value of 35 picocuries per gram (pCi/g). Elevated levels of uranium-238 (U-238) and uranium-234 (U-234) (up to 176 pCi/g and 24 pCi/g, respectively) were observed in soil samples collected along the 500 Center firing point (SEG 1995). Soil samples collected throughout the remainder of the survey area exhibited uranium levels consistent with the background levels associated with natural uranium.

Survey results for groundwater, surface water, and sediment samples indicated no uranium contamination associated with these media in the DU Impact Area when compared to guideline and background values. Although no guideline value for uranium in vegetation is available, analytical results for vegetation samples were consistent with results obtained during the baseline environmental survey.

1.3.2 Characterization Survey

The scoping survey conducted in late 1994 confirmed classification of the DU Impact Area as a radiologically affected area. Additional information on residual contamination in the DU Impact Area was collected in a characterization study conducted in mid-1995 (SEG 1995). The purpose of the characterization survey was to confirm and document the contamination in a 1,300-ac (5.3 km^2) portion of the DU Impact Area and to estimate costs and techniques for decontamination of the area. Due to the potential presence of UXO, suitable precautions (utilization of EOD escorts) were taken in the field to prevent the occurrence of any accidents involving such UXO; however, no areas or surfaces within the 1,300-ac (5.3 km^2) DU Impact Area were inaccessible for this survey.

The survey design utilized a combination of randomly and judgmentally selected locations to estimate the size of the affected area and the volume of contaminated soil and to confirm prior results of environmental sampling.

Samples of soil, groundwater, surface water, sediment, fish, freshwater clam, turtle, and deer liver, kidney, and bone samples were collected in affected and unaffected areas and analyzed using alpha spectroscopy to determine concentrations of U-234, uranium-235 (U-235), U-238, and the ratio of U-234 to U-238. Random- and judgment-selected soil samples were collected at three depths: 0 to 5.9 inches (in), 5.9 to 11.8 in, and 11.8 to 17.7 in (0 to 15 centimeters [cm], 15 to 30 cm, and 30 to 45 cm). Background surface and subsurface soil samples were collected from 10 sites in known unaffected areas. The average total uranium concentration in background soils was 1.94 pCi/g.

Total uranium concentrations in soil collected beneath penetrators ranged from 1.5 pCi/g to 12,000 pCi/g, with an average concentration of 757 pCi/g. Decreasing concentrations of total uranium were observed with increasing depths (15 to 30 cm and 30 to 45 cm). Random soil samples collected in the affected area, but not in the impact trenches, indicate that soil contamination outside the primary impact trenches is associated with proximity to penetrator fragments.

With the exception of two surface water samples, all groundwater and surface water samples exhibited total uranium concentrations consistent with background levels. The two elevated surface water samples were collected from static pools of water, in otherwise dry streams.

Total uranium concentrations in sediment samples ranged from 0.75 pCi/g to 6.2 pCi/g. Total uranium concentrations in vegetation samples ranged from 17.0 pCi/g to 3,447 pCi/g. Results of uranium analyses performed on vegetation root wash samples ranged from 50.4 pCi/sample to 14,258 pCi/sample. Total uranium concentrations in biological samples ranged from 0.91 pCi/g (deer liver) to 0.774 pCi/g (freshwater clam).

Results of *in situ* gamma spectroscopy measurements and soil sampling were used to determine the following:

- The average depth of the DU contamination is approximately 11 cm

- The affected area is approximately 500,000 square meters (m^2) (125 ac)
- The total volume estimate for remediation is approximately 55,000 cubic meters.

The average depth of the DU contamination (11 cm) is not the depth to which remediation may be performed, if soil remediation were actually performed. Survey data indicate that remediation of soils near projectiles should reach to about 45 cm in the horizontal (radially) and vertical directions.

1.3.3 Remedial Investigation South of the Firing Line

A Remedial Investigation/Feasibility Study (RI/FS) was conducted for the area south of the Firing Line for environmental contamination. Initially, 50 potential contaminant-release sites were identified for investigation. Phase I (Rust E&I 1994) and Phase 2 (Rust E&I 1998) were completed. Characterization data (e.g., soil and lithologic descriptions, hydraulic conductivity testing) collected as part of these investigations were used to support the DU fate and transport assessment.

1.3.4 Fracture Trace Report

An aerial photograph fracture trace analysis (SAIC 2006a) was completed for the JPG site to identify possible fracture locations and fracture orientations in the carbonate limestone aquifer in the DU Impact Area. Fractures were identified as natural linear features consisting of topographic (including straight stream segments), vegetal, or soil tonal alignments, visible primarily on aerial photographs, and expressed continuously for less than 1 mi were identified. Only natural linear features not obviously related to outcrop pattern or tilted beds, lineation and foliation, and stratigraphic contacts are classified as fracture traces (Lattman 1958).

Stereo-paired aerial photographs were obtained from the U.S. National Archives and Records Administration (NARA) showing the site prior to construction of JPG and the DU testing range. Historical (1937) aerial photographs were used to map fracture traces and lineaments to identify enhanced groundwater flow pathways in the aquifer. An area of approximately 22 square miles (mi^2) including the DU projectile testing range and immediate surrounding area was analyzed. A total number of 110 numbered fracture trace lines were identified from the aerial photographs.

Fracture traces were grouped based on similar orientation and color coded into nine groups. Seventy percent of the mapped traces were oriented either North 27° to 59° West (33 fracture traces) or North 31° to 56° East (43 fracture traces). Because of the registration and distortion associated with the aerial photographs, compounded by the paucity of useful features that survived since 1937, the accuracy of the fracture trace locations is approximately ± 100 ft. The distribution of fracture traces was used to select the locations and extent of electrical imaging geophysical survey traverse lines, which in turn were used to select locations for installation of clustered groundwater monitoring wells in potential groundwater conduits.

1.3.5 Well Location Selection Report

This section summarizes the results of a soil verification survey, installation of surface water gauging stations, surface geophysical (electrical imaging) survey, and well location selection (SAIC 2007):

- The soil verification study was completed to determine if published soil survey maps were representative and applicable for use in completing future soil sampling efforts. Results from the verification survey indicated the maps were reasonably accurate and applicable for their planned use. The majority of soils were identified as somewhat poorly and poorly drained soils exhibiting redoximorphic features that indicate a reducing environment in shallow (<3 ft) soils for some period of time (generally late winter through spring) during the year.

- Installation of stream and cave spring gauges is documented, along with any noted conditions (e.g., beaver dams near one of the planned gauging stations locations required station to be relocated).
- Field verification of fracture trace analysis was completed and the electrical imaging survey was conducted. Evaluation of results from both efforts indicates the potential for the presence of preferential flow paths in the carbonate bedrock beneath the DU Impact Area. Fourteen sites (13 "fracture" or "conduit" and 1 deep overburden) for locations of well pairs were selected. Nine sites were selected to provide coverage in possible flow directions from the DU Impact Area and areas suspected to contain DU penetrators. The tenth well pair location was selected to evaluate an area identified in the electrical imaging results with a greater than average depth to bedrock. This location will provide information on unconsolidated materials and the zone of bedrock-soil interface in an area where deep bedrock weathering appears to have occurred.

1.3.6 Well Construction and Surface Water Data Report

As part of the phased site characterization efforts at JPG, additional monitoring wells and surface water gauging stations were installed within and adjacent to the DU Impact Area to collect data necessary to refine the conceptual site model (CSM), evaluate the potential for migration of DU from the DU Impact Area, and provide site-specific inputs for the exposure modeling.

A goal of this characterization effort was to identify the most significant groundwater flow pathways. The most significant pathways are believed to be present within fractures and solution enhanced features within the carbonate aquifer underlying the DU Impact Area. As described above, a fracture trace and lineament analysis was completed followed by surface geophysics (electrical resistivity surveys) to identify potential preferential pathways in the shallow carbonate bedrock. Groundwater monitoring wells were placed at locations having the greatest chance of intersecting preferential groundwater pathways within the carbonate aquifer. These locations represent the most likely monitoring locations to evaluate if dissolved DU oxidation products are migrating within groundwater. Some wells also were installed in saturated overburden material with sufficient permeability to provide a functional monitoring well. Twenty-three wells were installed at 10 well cluster locations (Figure 1-3). The wells were installed in May, June, November, and December 2007.

Another goal of the characterization effort was to evaluate potential interconnections between groundwater and surface water flow paths. Surface water gauging stations were installed in September 2006, consisting of automatic, continuous, recording stream gauging stations on Big Creek (three locations) and Middle Fork (four locations), selected cave springs along Big Creek (two locations) inside the DU Impact Area, and one visual staff gauge along an unnamed tributary of Big Creek.

Evaluation of hydrographs for the stream gauges indicates stream stage and flow increases rapidly and decreases rapidly after a precipitation event. The hydrographs showed a period of low- to no-flow for many of the summer months. Both conditions are indicative of a hydrologic system in which surface water runoff is high and groundwater recharge is low.

A preliminary water budget determined that 56 percent of precipitation is returned to the atmosphere via evapotranspiration and the remaining 44 percent leaves the site as runoff. The 44 percent of precipitation included in runoff is composed of surface water runoff and groundwater runoff (groundwater recharge). The component of the water budget that infiltrates the ground surface and becomes groundwater was estimated to be on the order of 8 percent of total precipitation utilizing the stream hydrographs and base flow separation techniques. The remaining 36 percent of annual precipitation that falls on the site is believed to leave the site as surface water runoff.

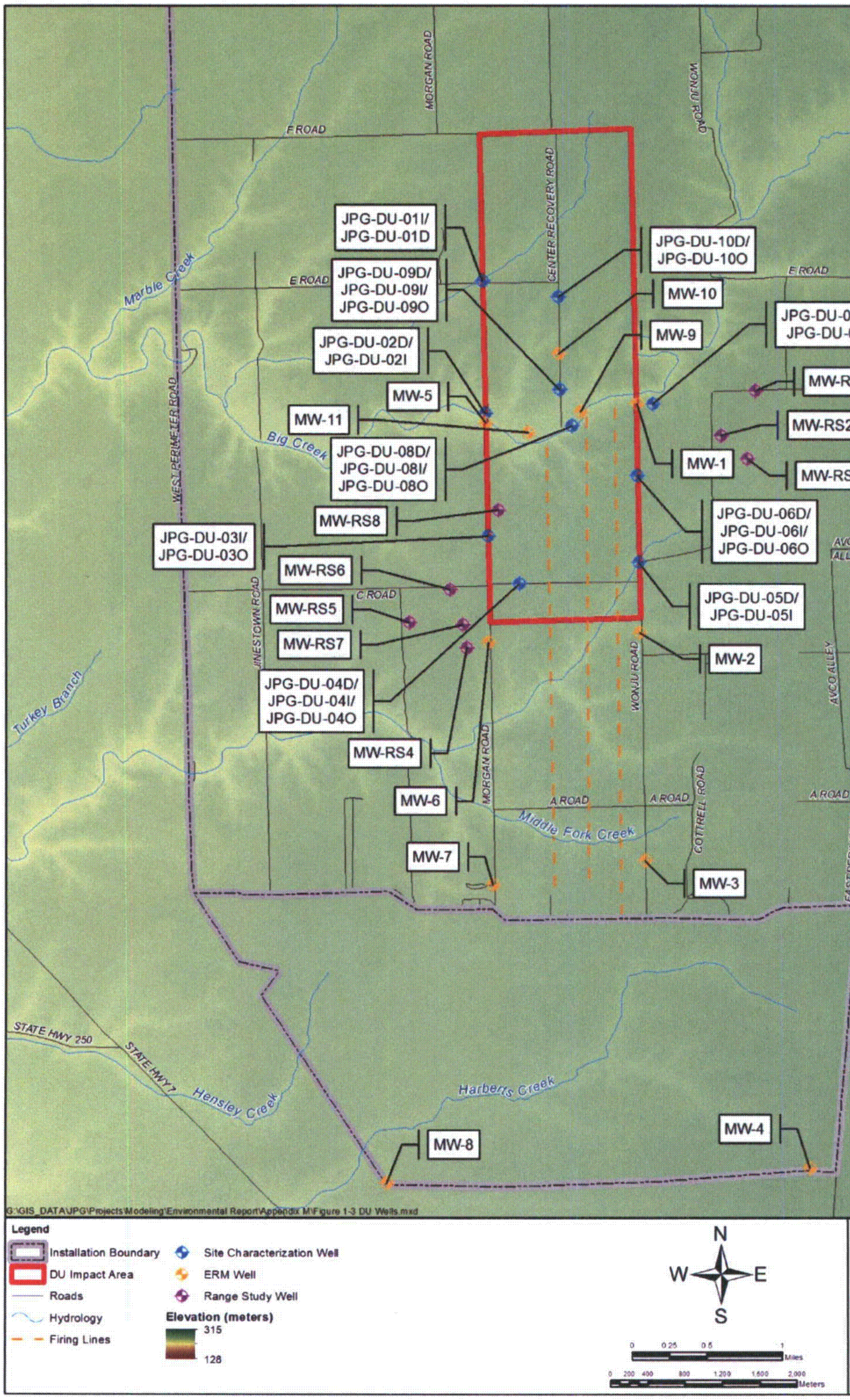

Well Locations Within and Near DU Impact Area

Figure 1-3

Date: 8/5/2013

1.3.7 Slug Test Report

The Slug Test Report (SAIC 2010) provides the hydraulic conductivity results based on aquifer testing completed in groundwater monitoring wells installed within and around the DU Impact Area. The slug testing program was successfully implemented at overburden and shallow bedrock wells; however, deep bedrock wells penetrate such low permeable rock, conclusive quantitative tests could not be performed. Preliminary review of the data indicated tests, where able to be performed, were implemented correctly and reproducibly, resulting in analyzable data sets. Trapped air in well filter packs did not appear to be a factor influencing hydraulic conductivity estimates. Overall, well construction characteristics and water column displacement data sets conformed to assumptions for use of conventional slug test analysis solutions, allowing analysis to proceed and reliable hydraulic conductivity value estimates to be achieved.

The hydraulic conductivity in the overburden and shallow bedrock is highly variable. Both zones included several wells where slug testing was not performed due to very slow water level recovery during preliminary field evaluation. The respective hydraulic conductivity in these cases is estimated to be at the low end of published literature values. As a result, the calculated hydraulic conductivities summarized below for both the overburden and shallow bedrock can be thought of as at the higher range of representative values at JPG, but representative of the transmissible portions of each hydrostratigraphic zone, as further concluded below.

The range in hydraulic conductivity values in overburden wells is from 0.01 to 5.3 gallons per day per square foot (gal/day/ft^2) with a geometric mean for all overburden wells of 0.85 gal/day/ft^2. The geometric mean for the overburden wells with JPG-DU-09O removed is 3.74 gal/day/ft^2. The published range for till is approximately 10 to 0.00001 gal/day/ft^2 (Freeze and Cherry 1979), putting the JPG average overburden hydraulic conductivity estimate in the upper range. Since the hydraulic conductivity values calculated for JPG-DU-03O, JPG DU-04O, and JPG-DU-06O are at the high end of the literature range for tills, any skin effects developed during installation of these wells are minimal and do not impact the usability of the slug test data. Hydraulic conductivity values calculated for JPG-DU-09O were approximately two orders of magnitude lower than the other overburden wells evaluated, but still at the higher end of published till conductivities.

The average hydraulic conductivity value for shallow bedrock wells, including JPG-DU-02I where a dominant solution zone is present, is 5.79 gal/day/ft^2. Without JPG-DU-02I, the average is slightly lower at 3.34 gal/day/ft^2. The published range for limestone and dolomite is approximately 10 to 0.02 gal/day/ft^2 (Freeze and Cherry 1979), putting the JPG average (without JPG-DU-02I) hydraulic conductivity value on the upper end of the published range for limestone and dolomite and at the low end of solution enhanced, or karst limestone. Factoring in the several wells that could not be tested because water levels did not recover would certainly drop the shallow bedrock average hydraulic conductivity.

Deeper bedrock permeability is clearly lower than overburden or shallow bedrock, although remains unquantified due to the incomplete recovery of wells following development or incomplete recovery following installation of the data logger transducer/slug the night before testing. The above traits have led to a qualitative estimate of permeability for the deep bedrock on the order of 0.02 gal/day/ft^2, which is at the low end of published values for limestone (Freeze and Cherry 1979).

In terms of the CSM, slug testing has quantified the permeability of overburden and shallow bedrock with values relatively similar for both hydrostratigraphic zones. Results suggest on a local scale that the overburden can transmit groundwater horizontally, possibly in discrete coarser-grained zones in the till, and that the till is likely in hydraulic communication with shallow bedrock. Slug test results confirm portions of each medium will essentially not transmit groundwater or transmit it very slowly (hydraulic properties at the low end of published values for the units of interest). Water will reside for long periods of time in these low-permeability areas, as confirmed through groundwater age dating tests conducted by the U.S. Geological Survey (USGS) (USGS 2010). The response of shallow bedrock well JPG-DU-02I to slug testing and the resultant hydraulic conductivity value estimate indicates that the shallow limestone may be more permeable on an average, large-scale basis than the overlying till, especially where the till is thin and rock is most susceptible to dissolution over time and subsequent enhanced fracture permeability.

Based on observed very slow recoveries in deeper bedrock wells (following development, sampling, etc.) and the inability to conclusively slug test these wells relative to the hydraulic conductivity values for overburden and shallow bedrock, there is a pronounced reduction in average rock permeability below an average depth of 29 to 33 ft into the bedrock. The deeper limestone bedrock may be three or more orders of magnitude lower in hydraulic conductivity than either the overburden or the shallow, solution enhanced bedrock. The lack of secondary porosity features at depth is the likely explanation for the pronounced decrease in permeability with depth in the DU Impact Area. There is little to no transmission of groundwater within this deeper rock.

1.3.8 USGS Age Dating Report

From 2007 to 2008, the USGS (USGS 2010), in cooperation with the Army, conducted a study to evaluate the relative age of groundwater in Pre-Wisconsinan till and underlying shallow and deep carbonate bedrock units in and near the DU Impact Area. The shallow carbonate unit includes about the upper 40 ft of bedrock below the bedrock-till surface; the deeper carbonate unit includes wells completed at greater depth. Samples collected during April 2008 from 15 wells were analyzed for field water quality parameters, dissolved gases, tritium, and chlorofluorocarbon (CFC) compounds; samples from 14 additional wells were analyzed for tritium only. Findings from the age dating report include:

- Groundwater gradients in the Pre-Wisconsinan till and the shallow carbonate unit were from topographically higher areas toward Big Creek and Middle Fork Creek, and their tributaries. Vertical gradients were strongly downward from the shallow carbonate unit toward the deep carbonate unit at three of four paired wells where water levels recovered after development; indicating the general lack of flow between the two units. The lack of post development recovery of water levels at four other wells in the deep carbonate unit indicates that parts of that unit have no appreciable permeability.
- Most wells in the Pre-Wisconsinan till have the potential to produce groundwater that partially was recharged during or after DU penetrator testing; their water quality can indicate the presence of DU-related contaminants.
- Five wells in the shallow carbonate bedrock produced water that was recharged, at least partially, during or after penetrator testing and are downgradient from the DU Impact Area, including:
  - The shallow carbonate unit near Big Creek is a karst flow system that may be recharged in part from areas with smaller thicknesses of overlying till or through more permeable parts of the till. This is indicated by CFC- and tritium-based piston-flow (nonmixing) model age dates of early 1980s for water from JPG-DU-02I, similar tritium-based ages of water produced from nearby wells MW-5 and MW-11, and cave development along the creek.
  - The CFC and tritium-based age dates indicate that water samples from JPG-DU-01I and JPG-DU-03I were best described as mixtures of post-1984 modern recharge and submodern (1953 or older) recharge.
- Groundwater age dates indicate that the ages of recharge sampled from shallow carbonate unit wells JPG-DU-04I, JPG-DU-05I, JPG-DU-06I, JPG-DU-09I, and JPG-DU-10D in easternmost (upgradient) and southernmost wells in the shallow carbonate unit are submodern (1953 or older) and predate the DU testing by at least 30 or more years. Water quality data from these

five wells are not likely to represent effects from DU-projectile testing or corrosion for years (possibly 30 years or more).

- Well JPG-DU-09D in the deep carbonate unit produced groundwater samples with a submodern (1953 or older) age date. The slow recovery of water levels in most wells in the deep carbonate unit is consistent with slow rates of groundwater flow and very old groundwater ages in that unit.

1.4 REPORT OUTLINE

The remainder of the report is divided into sections as follows:

- Section 2 consists of a layout of the important data used for the groundwater modeling effort. Both origins of the data, as well as a brief discussion of what the data are, are included.
- Section 3 presents the CSM. This section lays out both the conceptual view of the JPG site including an overview of geologic and hydrogeologic properties.
- Section 4 describes the development and results of vadose zone column modeling.
- Section 5 presents development of the groundwater flow model constructed to determine potential lateral movement of DU should it reach the water table. The flow model was calibrated against measured water levels at the site and a sensitivity analysis was performed to determine uncertainty in flow results. A preferential pathway was also tested to simulate a hypothetical worst case fracture placement under the trench.
- Section 6 presents the potential for DU transport, examines the relative flow contribution entering the streams from beneath the DU Impact Area trench, and the potential for movement offsite within the groundwater.
- Section 7 lists the references used to develop this report.
- Attachment 1 discusses the water level hydrographs and continuous recorder data collected from groundwater monitoring wells installed in and around the DU Impact Area.
- Attachment 2 includes more details about the Finite Element Heat and Mass Transfer (FEHM) soil column model including major input parameters, charts showing results in concentrations versus time, and a series of six sensitivity analyses.
- Attachment 3 includes details from a series of three sensitivity analyses conducted on the groundwater flow model.

2. DATA SUMMARY

In compiling the information for the modeling study, numerous data sources were used. This section describes those sources and presents the areas in which it was incorporated. Details on manipulation of these data pieces are found in the discussion of the CSM and/or modeling.

2.1 METEOROLOGICAL DATA

JPG lies within a temperate climate zone. Average annual precipitation is 47 inches per year (in/y) for the period 1976 through 2007 at Madison, Indiana (SAIC 2008). Data from this period were used to develop the water budget for JPG. During this same period, annual precipitation extremes ranged from a low of 33.2 inches in 1987 to a high of 60.9 inches in 1990. Average monthly precipitation ranges from a high of 5.08 inches in May to a low of 2.8 inches in February (Table 2-1). For comparison, the average annual precipitation from nearby Versailles, Indiana, weather station for 57 years (1949 through 2005) is 43.1 in/y, ranging from a low of 26.9 inches in 1953 to a high of 60.2 inches in 1990. Table 2-1 lists monthly temperatures and record extremes at Madison, Indiana (The Weather Channel 2013). On average, July and August are the warmest months, and January is the coldest month.

Table 2-1. Monthly Precipitation and Temperature at Madison, Indiana
Jefferson Proving Ground, Madison, Indiana

	Jan	Feb	Mar	Apr	May	Jun	Jul	Aug	Sep	Oct	Nov	Dec
Monthly Precipitation (in) for Madison, IN (1976-2007)												
Average	3.41	2.80	3.87	4.18	5.08	4.18	4.61	4.36	3.08	3.67	3.93	3.81
Min	0.52	0.22	1.04	0.88	1.31	0.34	0.94	1.16	0.24	0.83	0.94	0.50
Max	8.21	7.82	7.80	8.22	11.63	9.00	9.36	8.90	8.22	12.30	7.39	7.93
Monthly Temperature (°F)												
Average High	42	47	57	68	76	85	88	88	81	70	58	46
Average Low	23	25	32	42	53	62	66	65	57	45	35	27
Mean	33	36	45	55	65	74	77	77	69	58	47	37
Record High	75 (1950)	76 (2000)	84 (1981)	93 (1957)	97 (1953)	103 (1988)	108 (1954)	104 (1988)	108 (1953)	96 (1953)	88 (1950)	77 (1982)
Record Low	-17 (1994)	-12 (1951)	-2 (1980)	10 (2007)	27 (1963)	37 (1966)	48 (1972)	43 (1986)	33 (1995)	23 (1981)	0 (1950)	-18 (1989)

A weather station exists onsite, northeast of the DU Impact Area just off of the intersection of State Highway 421 and Old Michigan Road. This weather station served as the basis for site-specific meteorological data for the 2003 though 2011 period.

2.2 TOPOGRAPHY

Digital elevation data were obtained from the Indiana Spatial Data Portal (http://www.indiana.edu/~gisdata/statewide/05dem.html). The Indiana 2005 digital elevation and surface models were created from the 2005 Indiana Map Color Orthophotography Project collected during March and April leaf-off conditions at a minimum resolution of 1-ft statewide. The data cover the entire land area of the State of Indiana and consist of 4,000- by 4,000-ft high-resolution tiles. The entire perimeter of the State is buffered by at least 1,000 ft. The tiles covering the JPG site were downloaded and compiled into one high resolution digital elevation model (DEM) for use in areas where the increased resolution was necessary.

The DEM was compared against data from the site measured by a state licensed surveyor (e.g., ground surface elevation at well locations) and against locations where bridges crossed site streams. Minor adjustments to the DEM were made to ensure the DEM represented surveyed site data as well as topography at bridges.

2.3 HYDROGEOLOGY

Data used to describe the hydrogeology has been collected from numerous investigations. Recent site characterization data are described in Section 3 of the Decommissioning Plan.

2.3.1 Surface Water

The DU Impact Area falls within the USGS hydrologic unit (0512020701) of the Muscatatuck River and is drained by Big Creek and Middle Fork Creek. Big Creek includes two smaller tributaries: Marble Creek and Camp Creek. The total area included for the surface water model extends to the confluence of Middle Fork Creek with Big Creek, covering a total area of roughly 44,949 ac. The majority of this area consists of Big Creek with 34,060 ac; Marble Creek (3,053 ac) and Camp Creek (5,843 ac) occur downstream from the DU Impact Area. The Middle Fork Creek drainage area consists of 10,889 ac. A detailed description of the surface water features, monitoring data, and fate and transport assessment is provided in Appendix E.

The streams are flashy in nature and respond rapidly to precipitation events, especially in late fall through spring when vegetative growth is limited. During summer months, several closely spaced storm events or high intensity storms may be required to generate substantial runoff.

2.3.2 Hydrostratigraphy

Hydrostratigraphic units at the DU Impact Area include overburden and bedrock. Overburden is defined as unconsolidated sediments occurring above the bedrock and consists mainly of soils, loess, and glacial till with minor amounts of alluvium deposited along streams. The underlying bedrock consists of interbedded limestone, dolomite, and shale. The upper portion of the bedrock referred to here as shallow bedrock (upper 40 to 60 ft of bedrock) is more permeable than deep (below 40 to 60 ft) bedrock.

Monitoring well boring logs exist for the wells within the DU Impact Area as well as additional wells south of the firing line. Observations and sampling during borehole advancement serves as the primary data source on the subsurface at the JPG facility. Depth to bedrock data are summarized in Table 2-2 for the characterization wells installed in 2007, the Environmental Radiation Monitoring (ERM) wells installed in 1983 and 1988, and the Range Study Program wells installed in 2002 (Figure 1-3).

The characterization wells installed within and near the DU Impact Area were completed in the overburden (designated with "O" as part of the well identification, for example, JPG-DU-06O), shallow bedrock (designated with "I" as part of the well identification, for example JPG-DU-6I), and deep bedrock (designated with "D" as part of the well identification, for example JPG-DU-6D). Some wells were installed as clusters. Complete details on well installation can be found in the well installation and surface water data report (SAIC 2008).

2.3.2.1 Overburden

Overburden ranges from less than 1 ft to 72.5 ft based upon wells drilled in and around the DU Impact Area. The majority of soils within the DU Impact Area are somewhat poorly or poorly drained silty loam derived from the underlying loess or tills.

Seven soil series are mapped in the DU Impact Area (USDA NRCS 2005): Avonburg, Cincinnati, Cobbsfork, Grayford, Holton, Rossmoyne, and Ryker. A soil verification study (SAIC 2007) was conducted to confirm the soil series as mapped by the U.S. Department of Agriculture (USDA). All seven soil series have similar texture, consisting of silt loam derived from different parent materials and having different slopes. Table 2-3 summarizes the soil series. Six soil series are derived from parent material consisting of loess, underlying till-derived paleosols, and limestone residuum, and one soil series is derived from alluvium on floodplains.

Table 2-2. Depth to Bedrock at DU Impact Area and Vicinity Jefferson Proving Ground, Madison, Indiana

Well ID	Date Installed	Ground Surface Elevation	Top of PVC Elevation	Total Depth of Boring	Top of Bedrock		Lithology in Exposed Open Interval
		FAMSL	FAMSL		FTBGS	FAMSL	
DU Impact Area Characterization Wells							
JPG-DU-01D	6/14/2007	838.26	841.15	113.1	19.5	818.76	Limestone
JPG-DU-01I	6/15/2007	838.06	841.23	41.7	20	818.06	Limestone
JPG-DU-02D	5/20/2007	800.92	803.83	119.3	0.65	800.27	Limestone
JPG-DU-02I	5/21/2007	800.93	803.94	49.0	16	784.93	Limestone, shale
JPG-DU-03I	12/12/2007	862.14	865.6	120.6	40.6	821.54	Limestone
JPG-DU-03O	12/12/2007	862.1	865.54	25.0	>25	NA	Clay, sand, and gravel
JPG-DU-04D	11/29/2007	864.18	867.13	120.8	46.2	817.98	Limestone
JPG-DU-04I	12/3/2007	864.32	867.38	65.5	47	817.32	Limestone
JPG-DU-04O	12/4/2007	864.11	867.28	47.0	>47	NA	Gravel and clay
JPG-DU-05D	11/19/2007	843.67	847.26	130.7	5.7	837.97	Fossiliferous Limestone
JPG-DU-05I	11/27/2007	843.71	847.21	34.9	5.8	837.91	Limestone
JPG-DU-06D	6/17/2007	872.79	875.76	118.7	35.7	837.09	Limestone
JPG-DU-06I	6/18/2007	872.91	875.65	48.4	35.4	837.51	Limestone
JPG-DU-06O	11/13/2007	872.56	876.02	25.0	>25	NA	Clayey sand, sandy/gravelly clay
JPG-DU-07D	11/15/2007	842.58	846.53	120.4	5.7	836.88	Fossiliferous Limestone
JPG-DU-07I	11/18/2007	842.39	846.33	60.4	5.6	836.79	Limestone
JPG-DU-08D	5/23/2007	815.36	818.58	139.3	6	809.36	Limestone
JPG-DU-08I	5/24/2007	815.44	818.59	39.3	6	809.44	Limestone, dolomite, shale
JPG-DU-09D	6/2/2007	846.1	849.07	119.5	34	812.1	Limestone
JPG-DU-09I	6/2/2007	846.45	849.38	74.0	34	812.45	Limestone
JPG-DU-09O	6/3/2007	846.63	849.63	34.0	>34	NA	Clay with sand and gravel
JPG-DU-10D	6/6/2007	870.71	873.64	118.75	72.5	798.21	Limestone, shaley limestone
JPG-DU-10O	6/7/2007	870.39	873.51	71.8	71.8	798.59	Sand, silt, clay
ERM Program Wells							
MW-1	12/6/1983	851.75	853.58	33.2	4.5	847.25	Limestone
MW-2	12/13/1983	848.25	850.49	23.7	7	841.25	Limestone
MW-3	12/13/1983	870.96	873.64	42.8	18.5	852.46	Limestone
MW-4	12/14/1983	898.92	902.19	28	10	888.92	Siltstone/Limestone
MW-5	12/7/1983	801.91	804.36	33.4	5.6	796.31	Limestone
MW-6	12/17/1983	858.44	861.22	40	>40	NA	Silty Clay
MW-7	12/8/1983	850.99	853.7	53.7	26.5	824.49	Limestone
MW-8	12/9/1983	838.97	841.28	28.2	14.5	824.47	Limestone
MW-9	9/9/1988	819.85	819.96	38.2	3.7	816.15	Limestone & Shale
MW-10	9/18/1988	865.91	866.14	41.3	>41.3	NA	Sandy to Clayey Silt
MW-11	9/19/1988	809.49	809.89	41.9	2.1	807.39	Limestone & Shale
Range Study Program Wells							
MW-RS1	8/20/2002	865.39	867.78	13.5	8	857.39	Limestone & Clayey Silt
MW-RS2	8/16/2002	873.28	875.83	25.7	9	864.28	Limestone
MW-RS3	8/17/2002	879.19	881.57	12.5	>12.5	NA	Silty Clay
MW-RS4	8/19/2002	858.21	860.85	13	>13	NA	Silty Clay & Fine Sand
MW-RS5	8/18/2002	851.42	853.98	12.9	>12.9	NA	Silty Clay & Fine Sand
MW-RS6	8/18/2002	858.24	860.68	14.8	>14.8	NA	Silty Clay & Sand
MW-RS7	8/19/2002	859.42	862.02	12.5	>12.5	NA	Silty Clay & Sand
MW-RS8	8/21/2002	865.03	867.14	15.7	>15.7	NA	Silty Clay & Sand

- ***Cincinnati Series***—Deep, well-drained soils formed on mantle of loess
- ***Cobbsfork Series***—Poorly drained soils on broad summits of till plains; formed in loess and underlying till-derived paleosols
- ***Holton Series***—Deep, poorly drained soils formed in loaming alluvium on floodplains
- ***Grayford Series***—Deep, well-drained soils formed in loess, till of Illinoian age, and residuum from limestone on dissected till plains and sinkholes
- ***Avonburg Series***—Very deep, somewhat poorly drained soils formed in loess and underlying paleosol in till
- ***Rossmoyne Series***—Very deep, moderately well-drained soils formed on mantle of loess and underlying till of Illinoian age

Table 2-3. Soil Series at the DU Impact Area Jefferson Proving Ground, Madison, Indiana

Soil Series[a]	Map Symbol[a]	Slope[a]	Depth[a]	Drainage Class	Taxonomic Classification[a]	Total Acreage as Mapped[a]	Percent of Total Acres[a]	Saturated Hydraulic Conductivity (m/s)[b]
Avonburg	Av	0-6%	Very Deep	Somewhat Poorly Drained	Fine-silty, mixed, active, mesic Aeric Fragic Glossaqualf	311.97	14.8	Upper solum moderately high to high 4.23×10^{-2} to 1.41×10^{-1}
Cincinnati	Cn	1-18%	Very Deep	Well Drained	Fine-silty, mixed, active, mesic Oxyaquic Fragiudalf	409.12	19.4	Moderate permeability
Cobbsfork	Co	0-1%	Very Deep	Poorly Drained	Fine-silty, mixed, active, mesic Fragic Glossaqualf	861.47	40.7	Upper solum 1.41×10^{-2} to 1.41×10^{-1}
Grayford	Gr	2-35%	Deep	Well Drained	Fine-silty, mixed, active, mesic Ultic Hapludalf	144.81	6.8	Moderately high to high 4.23×10^{-2} to 1.41×10^{-1}
Holton	Ho	0-2%	Very Deep	Somewhat Poorly Drained	Coarse-loamy, mixed, active, nonacidic, mesic, Aeric Endoaquept	36.22	1.7	Moderately high to high
Rossmoyne	Ro	0-25%	Very Deep	Moderately Well Drained	Fine-silty, mixed, superactive, mesic Aquic Fragiudalf	259.85	12.3	Moderate above fragipan, moderately slow below fragipan
Ryker	Ry	0-18%	Very Deep	Well Drained	Fine-silty, mixed, active, mesic Typic Paleudalf	90.8	4.3	NA

[a]From Tables 2-1 through 2-3 of the Final Well Location Selection Report (SAIC 2007).
[b]From Appendix A of the Final Well Location Selection Report – official soil series descriptions (SAIC 2007).
NA – Not available, no description provided.

- ***Ryker Series***—Very deep, well-drained soils formed in loess, underlying drift, and residuum from limestone on till plains.

Results from the field observations indicate the soil mapping units delineated on the Natural Resources Conservation Service (NRCS) map are reasonably accurate. From the soil borings observed, the site soil conditions may be wetter than indicated by the NRCS soil survey map. The field data indicate that the somewhat poorly drained Avonburg series may be grouped together with the poorly drained Cobbsfork series for the purpose of interpretation. Combined, these two soil series would comprise approximately 55 percent of the DU Impact Area. The well-drained Cincinnati and Rossmoyne series also may be grouped together, since both have a fragipan subsurface diagnostic horizon, which tends to perch water during parts of the year, and this combination would account for another 32 percent of the DU Impact Area. The well-drained Grayford, Ryker, and somewhat poorly drained Holton series all have somewhat unique soil conditions.

The portion of the DU Impact Area (>55 percent) with somewhat poorly and poorly drained soil exhibits redoximorphic features (soil mottling) that indicate a reducing environment exists in the shallow (<3 ft) subsurface for some period of time (generally late winter through spring) during the year. Redoximorphic features or soil drainage mottling are color patterns in the soil formed by the oxidation and reduction of iron and/or manganese caused by saturated or near saturated conditions within the soil. This reducing environment is sufficient to reduce the ferric iron to ferrous iron. The presence of ferrous or ferric iron is an indicator of the oxidative state. No direct measurements of redox potential (Eh) were obtained during this investigation. Corrosion of metals and, therefore, DU penetrators can be greatly affected by the environment in which it is located. As discussed in greater detail in Appendix C, DU penetrator corrosion rates and processes are much lower under reducing conditions than those present under oxidation (Parkhurst et al. 2012).

Loess occurs above the glacial till. The boundary between the loess and glacial till is transitional and not sharply defined due to similar lithology; most loess is derived from the underlying glacial till. The presence of gravel and split spoon blow counts (a substantial increase in blow counts was used to indicate presence of till) is used in this effort to differentiate loess from the underlying glacial till. Review of the site characterization well logs shows loess thickness to range from 0 to 11 ft with an average of 6.3 ft. ERM and Range Study well logs show slightly greater depth to the glacial till, but with less precision as split spoons (and therefore lithology descriptions) were collected at 5-ft intervals in the overburden.

2.3.2.2 Bedrock

The depth to carbonate bedrock ranges from less than 1 ft below ground surface (BGS) to 72.5 ft BGS. Relief on the top of bedrock is nearly 100 ft with the top of bedrock ranging in elevation from 784.93 to 888.92 ft above mean sea level (msl). In addition to the bedrock picks developed in the boring logs, additional information was obtained from a bedrock topographic map of the state of Indiana downloaded from the Indiana geographic information system (GIS) Atlas (http://inmap.indiana.edu/dload_page/geology.html). Bedrock topography in this file was converted from the original published map, Indiana Geological Survey Miscellaneous Map 36. The contours define the elevation/topography of the bedrock surface in Indiana. As the date of the bedrock map predates the monitor well boring logs, the map was adjusted in the vicinity of the model to take into account the additional information gained from the site-specific data (ERM wells, Range Study Wells and site characterization wells within and around the DU Impact Area; environmental investigation wells for sites south of the firing line [Figure 2-1]).

Karst features have been observed at JPG and specifically within the DU Impact Area consisting of surface expressions of small sinkholes, caves along Big Creek, and weathered jointing (fracturing) of bedrock observed at outcrops along Big Creek. Caves and solution features appear to be most commonly

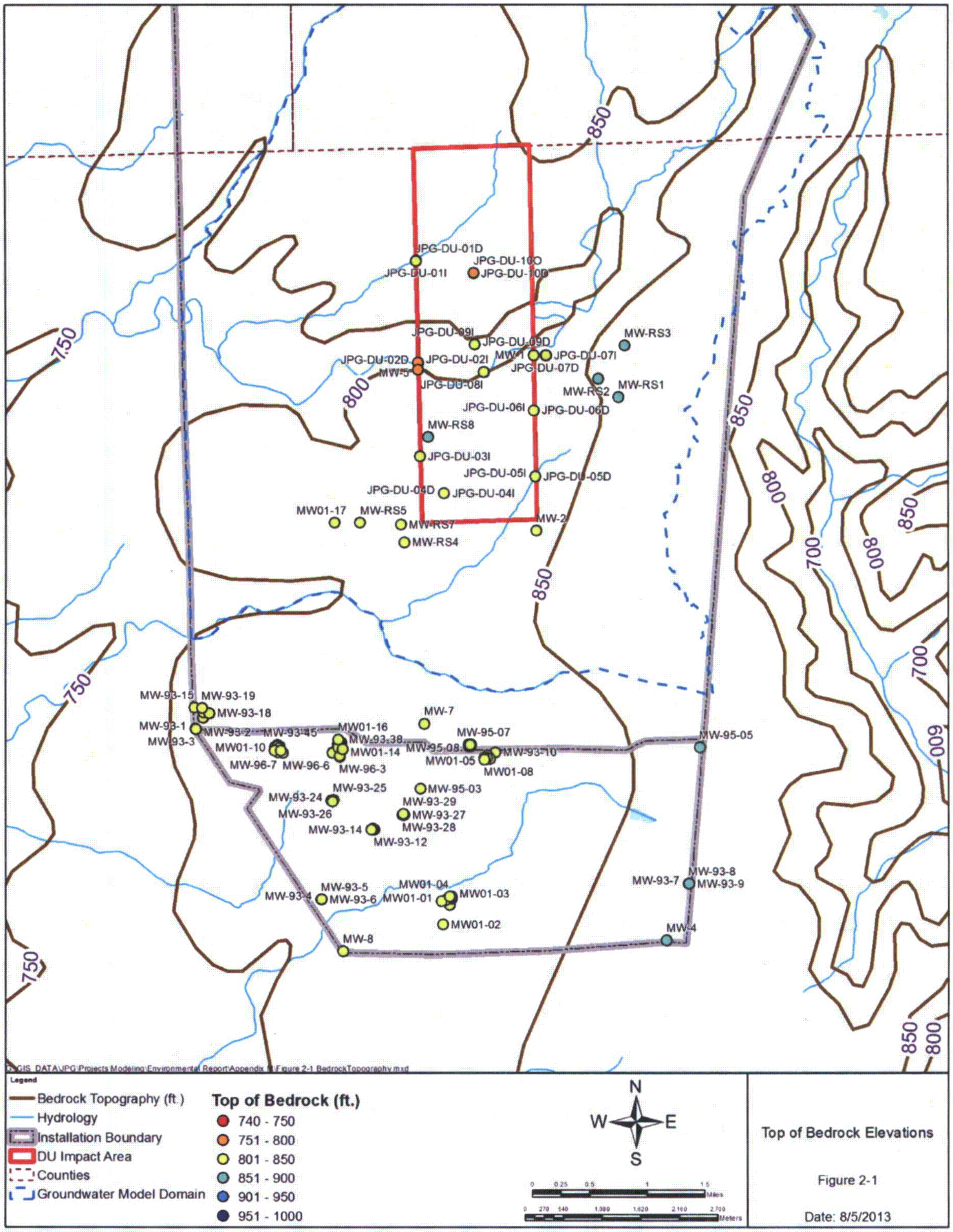
Legend
Bedrock Topography (ft.)
Hydrology
Installation Boundary
DU Impact Area
Counties
Groundwater Model Domain
Top of Bedrock (ft.)
740 - 750
751 - 800
801 - 850
851 - 900
901 - 950
951 - 1000
N
W
E
S
Miles
Meters
Top of Bedrock Elevations
Figure 2-1
Date: 8/5/2013

above the groundwater table and above the elevation of Big Creek. Wells were located on fracture traces and using geophysical techniques to selectively test areas where karst development would be greatest. However, results of the well drilling, field observations and an analysis of published reports and previous studies demonstrate that karst activity within and immediately surrounding the DU Impact Area is limited in depth and lateral extent, confined to the shallow bedrock (generally less than 50 ft BGS), and more prevalent in and adjacent to stream valleys:

- Of all of the new wells installed, only a single very minor solution feature was observed in each of the borings at the JPG-DU-02 well pair location (along Big Creek) during the well installation. The solution feature was located at a depth of 23 to 23.5 ft BGS. The absence of karst/weathered conditions in 19 borings cored in 10 locations that were expected to be preferentially developed demonstrates that karst weathering is not a predominant feature onsite.
- Karst development and the presence of a karst controlled groundwater flow network appears to be limited to within the narrow erosional plain along Big Creek and offsite along lower sections of Middle Fork Creek. Observations by Science Applications International Corporation (SAIC) soil scientists and geologists indicate no sinkholes or closed depressions in the elevated areas above this plain. Sheldon (1997) reported on extensive field reconnaissance work completed from January 1994 to April 1997 in and surrounding the DU Impact Area, in which caves, sinkholes, and karst features were recorded and catalogued. Sheldon's only reported, observed, and documented cave locations within the DU Impact Area were only along Big Creek (Sheldon 1997).
- The observations of karst features and weathering onsite concur with the following statements by Herring (2004), "...the majority of sinkholes or depressions occur along the larger stream valleys (especially Big Creek)...," "...water well records...indicate a few feet of crevices, broken limestone, or mud seams within the limestone bedrock, generally at depths less than 50 feet below land surface...," and "...The Silurian carbonates...show limited karst development in Jefferson County. These rocks contain thinner limestones and more layers of shale, conditions that significantly limit karst development."

2.3.3 Water Levels

Water level data were collected periodically from wells installed at JPG. Results from these point measurements indicate the water level depths in overburden (Table 2-4) range in depths from less than 2 ft to nearly 40 ft BGS and average 11 ft BGS. Water levels in the shallow bedrock from wells that are paired with overburden wells are generally a few feet lower, but follow the same general patterns, indicating a downward gradient and hydraulic connection between the overburden and shallow bedrock. Water levels in deep bedrock wells are generally much lower than those in the shallow/intermediate bedrock, show very slow recovery following sampling or attempted slug testing indicating limited communication between the shallow/intermediate and deep bedrock, and have limited flow within the deep bedrock (at least at the locations of the installed monitoring wells).

Continuous recorders were installed in 15 monitoring wells within and adjacent to the DU Impact Area (Figure 2-2). Note not all wells were equipped with continuous recorders. Three general types of responses are noted:

- Overburden wells and intermediate wells located in upland areas away from creeks generally show seasonal fluctuations that range from a few feet to as much as 9 ft. A gradual decline in water levels occurred within these wells from late spring 2008 through the summer of 2008 during a period of below normal precipitation, followed by recovery to similar or in some cases higher water levels that preceded the decline. Monitoring wells showing this type response include JPG-DU-01I, -03I, -06O, -06I, -09O, -09I, and MW-2.

Table 2-4. Depths to Groundwater in Overburden Wells Jefferson Proving Ground, Madison, Indiana

Station ID	Event/Date(s)				
	Quarterly Aug 07	Quarterly Nov 07	Site Wide Jan 08	Quarterly Feb 08	Quarterly Feb 09
	8/16/2007	11/15/07-11/16/07	1/23/2008	2/12/2008	2/2/2009
	DTW	DTW	DTW	DTW	DTW
JPG-DU-03O	—	—	6.26	5.21	7.88
JPG-DU-04O	—	—	11.03	9.95	12.91
JPG-DU-06O	—	—	5.69	4.72	8.26
JPG-DU-09O	12.55	12.13	11.29	11.59	13.57
JPG-DU-10O	38.74	39.75	38.14	37.66	39.02
MW-6	21.54	9.91	6.34	7.02	5.84
MW-10	9.51	8.73	2.62	1.79	2.98
MW-RS1	—	—	2.23	2.34	2.73
MW-RS3	10.89	11.14	6.92	6.59	7.57
MW-RS4	—	4.84	5.7	3.61	3.21
MW-RS5	—	9.38	5.61	4.95	3.34
MW-RS6	10.61	10.21	6.93	6.11	8.79
MW-RS7	—	10.14	7	6.05	8.55
MW-RS8	12.25	13.19	4.36	3.46	5.24
Min	9.51	4.84	2.23	1.79	2.73
Average	16.58	12.94	8.58	7.93	9.28
Max	38.74	39.75	38.14	37.66	39.02

Min	1.79
Average	11.06
Max	39.75

Note: DTW = depth to water in feet below ground surface.

- Shallow/intermediate bedrock wells near creeks exhibiting similar response to changes in stream stage, indicating hydraulic connection between the shallow bedrock and adjacent creeks. Monitoring wells showing this type response include JPG-DU-02I adjacent to Big Creek at the western boundary of the DU Impact Area and JPG-DU-05I adjacent to Middle Fork Creek at the eastern boundary of the DU Impact Area. One other monitoring well with a continuous recorder, JPG-DU-03I, was located adjacent to a tributary to Big Creek, but did not show the same hydraulic connection to creek stage.
- Deep bedrock wells and some shallow/intermediate bedrock wells exhibit very slow recovery to sampling events or attempts to slug test the wells. These wells indicate the very low permeability within the bedrock at their respective locations. Monitoring wells showing this type of response include JPG-DU-04D, -06D, -08I, -09D, MW-9, and MW-11.

Plots illustrating water level data collected from wells containing continuous recorders are included as Attachment 1 to this appendix. A brief description of each is also included.

Water level data from overburden and shallow/intermediate bedrock wells indicate flow directions roughly follow surface topography. Given the number of wells and spacing between wells, contour maps based upon observed water level data were not created. However, observations pertaining to flow directions and gradients can be made from the measured data. The direction of groundwater flow is roughly the same as the surface water drainage, which is to the west-southwest over most of the installation. The variability in the depth to groundwater in bedrock wells may reflect the occurrence of fractures in bedrock. SEC Donahue (1992) noted that in the vicinity of incised surface drainages, the potentiometric surface slopes toward the streams at roughly the same gradient as the surface topography.

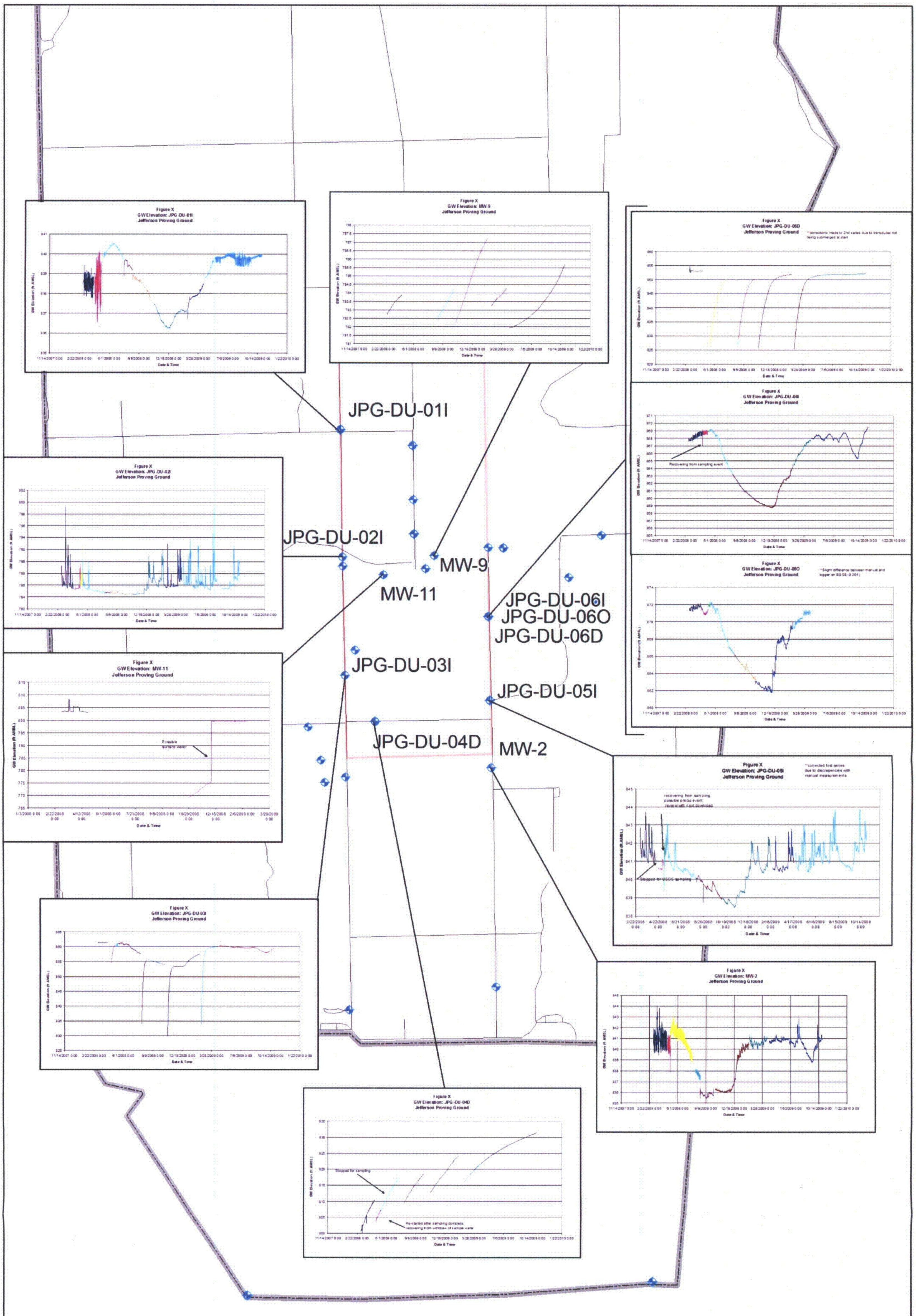

PROJECT NAME:

Jefferson Proving Ground - Groundwater Modeling

DRAWING TITLE:

Figure 2-2: Locations of Wells with Continuous Recorders and Collected Data

Therefore, on a local scale, the bedrock groundwater tends to discharge to surface streams. Data from the site characterization wells, range study wells, and ERM wells support this observation.

2.3.4 Hydraulic Conductivity

Slug tests were performed on the wells in the vicinity of the DU Impact Area and the analysis is presented in SAIC (2010). Tables 2-5 (overburden) and 2-6 (shallow bedrock) (SAIC 2010) summarize the hydraulic conductivity results for each of the wells tested.

Table 2-5. Overburden Slug Test Results
Jefferson Proving Ground, Madison, Indiana

Well	Hydraulic Conductivity		Notes
	(gpd/ft^{2})	(ft/d)	
JPG-DU-03O	2.4	0.32	
JPG-DU-04O	4.1	0.55	
JPG-DU-06O	5.3	0.71	
JPG-DU-09O	0.01	1.30E-03	
JPG-DU-10O	NA	NA	Very slow recovery
MW-10	NA	NA	Very slow recovery

Table 2-6. Shallow Bedrock Slug Test Results
Jefferson Proving Ground, Madison, Indiana

Well	Hydraulic Conductivity		Notes
	(gpd/ft^{2})	(ft/d)	
JPG-DU-01I	0.15	0.02	
JPG-DU-02I	18.55	2.48	Solution void
JPG-DU-03I	NA	NA	Very slow recovery
JPG-DU-04I	10.40	1.39	
JPG-DU-05I	0.08	0.01	
JPG-DU-06I	4.27	0.57	
JPG-DU-07I	NA	NA	No recovery
JPG-DU-08I	NA	NA	No recovery
JPG-DU-09I	NA	NA	Very slow recovery
MW-2	0.56	0.08	
MW-3	0.40	0.05	
MW-5	0.26	0.04	
MW-7	3.00	0.40	
MW-RS-2	10.20	1.36	

The hydraulic conductivity in the overburden and shallow bedrock is highly variable. Both zones included several wells where slug testing was not performed due to very slow water level recovery. The respective hydraulic conductivity in these cases is estimated to be at the low end of published literature values. Calculated hydraulic conductivities summarized below for both the overburden and shallow bedrock can be thought of as at the higher range of representative values at JPG, but representative of the transmissible portions of each hydrostratigraphic zone.

The range in hydraulic conductivity values in overburden wells is from 0.0013 to 0.71 feet per day (ft/day) (0.01 to 5.3 gal/day/ft^2) with a geometric mean for all overburden wells of 0.11 ft/day (0.85 gal/day/ft^2). The geometric mean for the overburden wells with JPG-DU-090 removed is 0.5 ft/day (3.74 gal/day/ft^2). The published range for till is approximately 1.3 to 1.3×10^{-6} ft/day (10 to 0.00001 gal/day/ft^2) (Freeze and Cherry 1979), putting the JPG average overburden hydraulic conductivity estimate in the upper range.

Hydraulic conductivity measured in overburden materials during the Final Phase II Remedial Investigation (RI) south of the firing line included the following results:

- Slug tests results ranging from 0.031 to 0.24 ft/day
- Matrix hydraulic conductivity ranging from 9.6×10^{-5} to 2.8×10^{-4} ft/day
- Small-scale fractures: 1.6×10^{-3} ft/day
- Large-scale fractures: 0.06 ft/day.

The geometric mean hydraulic conductivity value for shallow bedrock wells, including JPG-DU-021 where a 6-in solution void is present, is 0.18 ft/day (1.33 gal/day/ft^2). Without JPG-DU-021, the geometric mean is slightly lower at 0.13 ft/day (0.99 gal/day/ft^2). The published range for limestone and dolomite is approximately 1.3 to 0.003 ft/day (10 to 0.02 gal/day/ft^2) (Freeze and Cherry 1979), putting the JPG hydraulic conductivity value on the upper end of the published range for limestone and dolomite and at the low end of solution enhanced, or karst limestone. Factoring in the several wells that could not be tested would drop the shallow bedrock hydraulic conductivity.

Deeper bedrock permeability is clearly lower than overburden or shallow bedrock, although remains unquantified due to the incomplete recovery of wells following development or incomplete recovery following installation of the data logger transducer/slug the night before testing. The above traits have led to a qualitative estimate of permeability for the deep bedrock on the order of 0.003 ft/day (0.02 gal/day/ft^2), which is at the low end of published values for limestone (Freeze and Cherry 1979).

In terms of the CSM, slug testing has quantified the permeability of overburden and shallow bedrock with values relatively similar for both hydrostratigraphic zones. Results suggest on a local scale that the overburden can transmit groundwater horizontally, possibly in discrete coarser-grained zones in the till, and that the till is likely in hydraulic communication with shallow bedrock. Slug test results confirm portions of each medium will essentially not transmit groundwater or transmit it very slowly. Water will reside for long periods of time in these low-permeability areas. The response of shallow bedrock well JPG-DU-021 to slug testing and the resultant hydraulic conductivity value estimate indicates that the shallow limestone may be more permeable on an average, large-scale basis than the overlying till, especially where the till is thin and rock is most susceptible to dissolution over time and subsequent enhanced fracture permeability.

Based on observed very slow recovery in deeper bedrock wells (following development, sampling, etc.) and the inability to conclusively slug test these wells relative to the hydraulic conductivity values for overburden and shallow bedrock, there is a pronounced reduction in average rock permeability below an average depth of 29 to 33 ft into the bedrock. The deeper limestone bedrock may be three or more orders of magnitude lower in hydraulic conductivity than either the overburden or the shallow, solution enhanced bedrock. The lack of secondary porosity features at depth is the likely explanation for the pronounced decrease in permeability with depth in the DU Impact Area. There is little to no transmission of groundwater within this deeper rock.

In addition, data were taken based on wells south of the firing line from the RI performed at the site. The hydraulic conductivity of the till ranges from 0.079 to 0.24 ft/day in the area south of the firing line, based on slug tests in wells (Rust E&I 1998; MWH 2002). Small-scale fractures and sand lenses within the till contribute to the higher hydraulic conductivity measured by the slug tests.

Slug and pump tests were completed on 51 wells located south of the firing line screened in the bedrock aquifer. The hydraulic conductivity of the bedrock aquifer computed from slug tests ranges from 0.048 to 1.66 ft/day (MWH 2002). The pumping test results indicate hydraulic conductivities ranging from 0.40 to 17.3 ft/day (MWH 2002) in the bedrock.

2.3.5 Geotechnical Properties

The published range of porosity in glacial till is 12 to 41 percent with an average value of 26 percent (Kresic 2007). The published range of porosity in loess is 44 to 57 percent with an average value of 49 percent (Kresic 2007). Published bulk density of overburden materials is 1.92 grams per cubic centimeter (g/cm^3) (Telford et al. 1990).

The published range of porosity in dolomite is 1 to 32 percent with an average value of 7 percent (Kresic 2007). For limestone, the published range in porosity is 0 to 65 percent with an average value of 8 percent. Specific yield in carbonate bedrock is reported at 1 to 5 percent (USATHAMA 1988). Bulk density of limestone ranges from 1.92 to 2.90 g/cm^3; dolomite bulk density ranges from 2.28 to 2.90 g/cm^3 (Telford et al. 1990).

Grain size analysis of the 26 loess soil samples indicates the 3 shallow loess soils have very similar grain size distributions consistent with the field-determined silty clay and sandy loam soil descriptions made at the time of sampling. The three loess soil types are very similar, containing approximately 29 to 33 percent clay, 45 to 52 percent silt, 18 to 23 percent sand, and 1 percent or less gravel. Figure 2-3 shows the relative percent difference in grain sizes for the three soils. This textural composition is consistent with a silty clay to clayey silt loam.

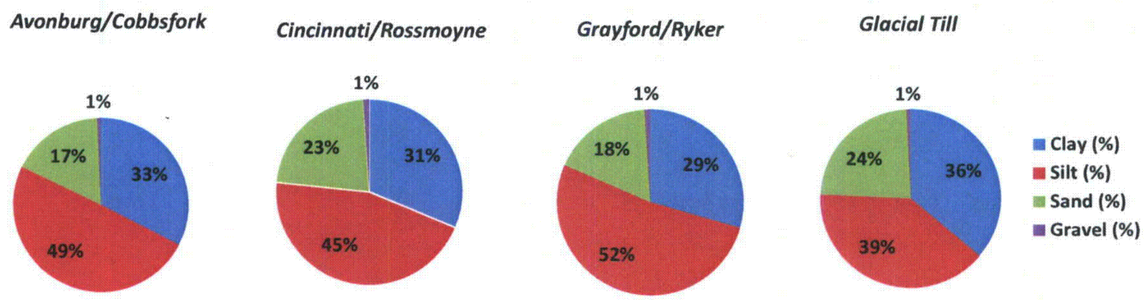

Figure 2-3. Particle Size Comparison of JPG Soil Types

2.3.6 Groundwater Use

The groundwater under JPG generally is of poor quality and is not used for drinking purposes or for other purposes in any significant capacity. The drinking water at JPG is obtained from the city of Madison Municipal Supply Systems and the Canaan Deposits in the Ohio River Valley, approximately 5 mi (8 km) from JPG (MWH 2002). Seven test holes drilled into the carbonate bedrock during initial development of the installation were unable to locate groundwater in sufficient quantities to support facility operations.

2.3.7 Water Budget

The water budget analysis (SAIC 2008) determined for an average precipitation year of 47 in, 56 percent (26.3 in) is lost to evapotranspiration, 8 percent (3.8 in) becomes groundwater recharge, and the remaining 36 percent (16.9 in) is runoff. Weather data collected at Madison, Indiana (1976 to 2007) and from FWS located northeast of the DU Impact Area on JPG were used to determine evapotranspiration rates. During this period, annual precipitation ranged from 33.24 to 60.93 in and actual evapotranspiration ranged from 17.2 to 29.7 in/y (SAIC 2008). Groundwater recharge rates were determined from base flow studies conducted for the neighboring Brush Creek and the larger Muscatatuck River (to which Big Creek and all JPG streams are tributaries). For comparison, published estimates indicate groundwater recharge at 4 to 8 in/y for southern Indiana (Bechert and Heckard 1966). Brush Creek in particular demonstrates the extremely flashy nature that is observed within the JPG streams; Brush Creek is similar in size and hydrology to the JPG streams. Large runoff volumes are observed quickly following a precipitation event followed by a rapid fall off to base flow conditions. The SAIC (2008) water budget assumes most of groundwater reemerges as base-flow into streams. Therefore, percolation losses to deep groundwater (deep bedrock) are insignificant.

2.4 ANALYTICAL DATA SUMMARY

Environmental media (groundwater, surface water, sediment, and soils [Figure 2-4]) are regularly monitored to ensure DU remaining within the DU Impact Area does not pose a radiological exposure risk to human health or the environment (SAIC 2013). Surface water and sediment samples are co-located to the extent possible. Results by media indicate low levels of total uranium activity at JPG and are not indicative of significant trends or migration in any media. The October 2012 Environmental Radiation Monitoring Program (SAIC 2013) for the fall sampling event and historical data are summarized below and presented in greater detail in the main report and Appendix F:

- Groundwater quality (11 monitoring wells)
  - October 2012 total uranium ranged from 0.19 ± 0.09 picocuries per liter (pCi/L) with an average concentration of 1.4 ± 1.0 pCi/L.
  - Historical assessment from 202 discrete samples collected from 2004 through October 2012 showed average total uranium concentration of 1.4 pCi/L, the standard deviation is 1.2 pCi/L, and the maximum detected concentration is 5.7 ± 0.6 pCi/L.
- Surface water quality (eight locations)
  - October 2012 total uranium ranged from 0.24 ± 0.09 pCi/L to 1.8 ± 0.3 pCi/L with an average concentration of 0.65 ± 0.46 pCi/L.
  - Historical assessment from 145 discrete samples collected from 2004 through October 2012 showed average total uranium concentration of 0.88 pCi/L, the standard deviation is 2.4 pCi/L, and the maximum detected concentration is 19 ± 2 pCi/L.
- Sediment (eight locations)
  - October 2012 total uranium ranged from 0.38 ± 0.08 to 1.0 ± 0.1 pCi/g with an average concentration of 0.77 ± 0.36 pCi/g. One sediment sample result from Big Creek within the DU Impact Area could have equaled a U-238:U-234 activity ratio of 3.0, indicating the possible presence of DU in the sample.
  - Historical assessment from 151 discrete samples collected from 2004 through October 2012 showed average total uranium concentration of 0.97 pCi/g, the standard deviation is 0.49 pCi/g, and the maximum detected concentration is 2.4 ± 0.4 pCi/g.
- Soils (four locations)
  - October 2012 total uranium ranged from 0.80 ± 0.12 to 1.4 ± 0.2 pCi/g with an average concentration of 1.2 ± 0.4 pCi/g.
  - Historical assessment from 91 discrete samples collected from 2004 through October 2012 showed average total uranium concentration of 1.5 pCi/g, the standard deviation is 0.3 pCi/g, and the maximum detected concentration is 2.2 ± 0.5 pCi/g.

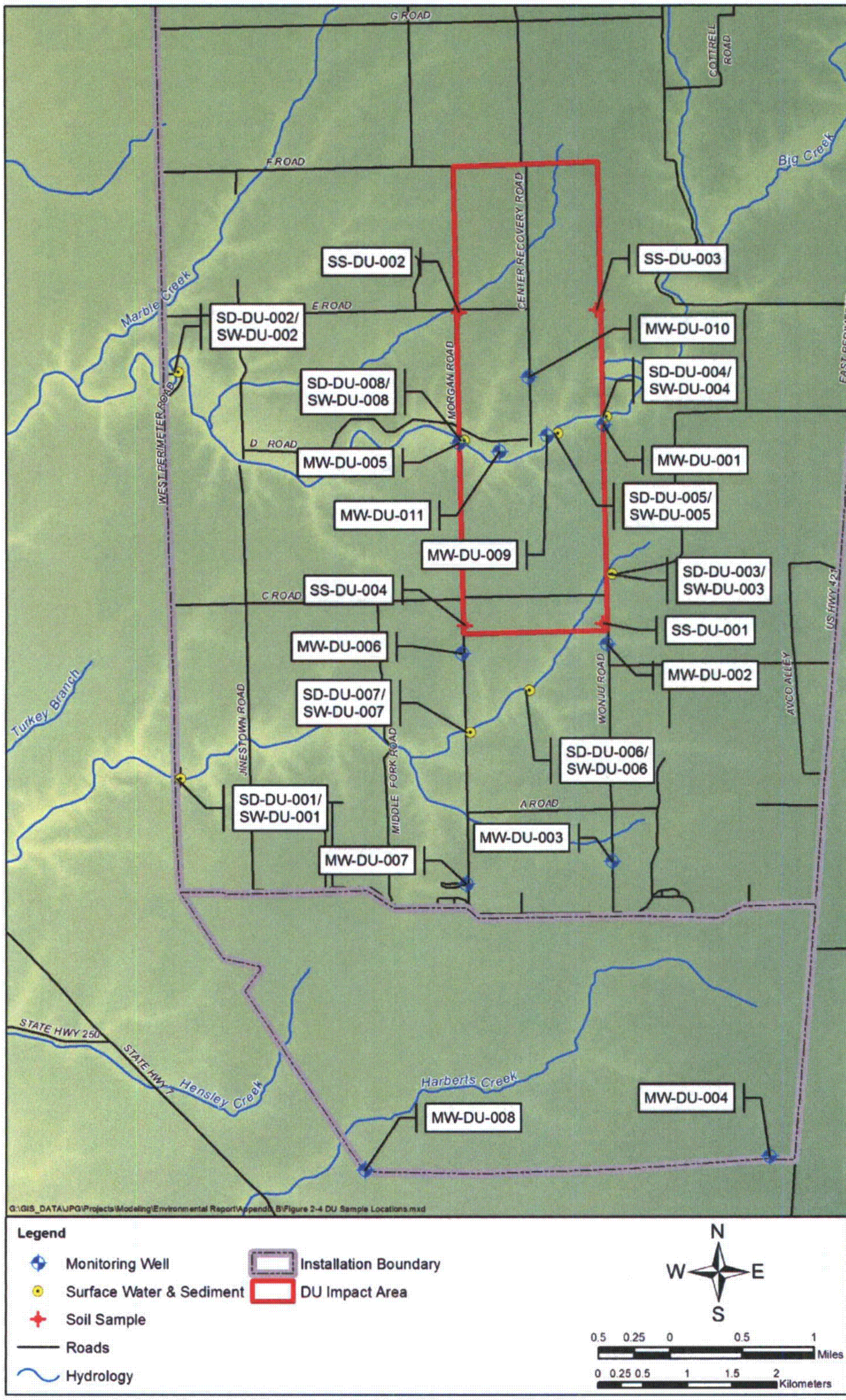

Environmental Radiation Monitoring Locations

Figure 2-4

Date: 8/15/2013

In addition to biannual ERM monitoring, site investigation data have been collected to further define the nature and extent of DU in the environmental media within and adjacent to the DU Impact Area. Groundwater, surface water, and sediment samples were collected quarterly (April 2008, July 2008, October 2008, and February 2009). Surface water and sediment sampling locations were co-located to the extent possible; samples were collected from locations along Big Creek and Middle Fork Creek and are most pertinent to the surface water modeling effort. Figures 2-5 and 2-6 show the locations of sediment and surface water sampling, respectively, along Big Creek and Middle Fork Creek. Key findings from these data are summarized below and presented in greater detail in the main report and Appendix F:

- Groundwater (42 wells sampled quarterly; April 2008, July 2008, October 2008, and February 2009)
  - 189 total samples, 44 background, and 145 site wells; some wells were periodically dry and could not be sampled
  - 14 overburden wells, 20 shallow bedrock wells, and 8 deep bedrock wells
  - Background results ranged from 0.060 ± 0.058 to 6.4 ± 1.1 pCi/L (0.2 to 18 micrograms per liter [μg/L]) with means, depending on hydrostratigraphic unit, ranging from of 0.080 to 2.5 pCi/L (0.23 to 6.9 μg/L)
  - Site wells ranged from 0.027 ± 0.14 to 47 ± 7.7 pCi/L (0.075 to 131 μg/L) with means, depending on hydrostratigraphic zone, ranging from 0.77 to 2.9 pCi/L (2.1 to 8.1 μg/L); highest observed concentration southwest of the DU Impact Area in overburden MW-RS-7.
- Surface water (20 locations sampled quarterly; April 2008, July 2008, October 2008, and February 2009; plus 4 background locations; locations are on Big Creek and Middle Fork Creek)
  - 90 total samples including 13 background and 77 site locations; some locations were dry and could not be sampled
  - Background results ranged from 0.047 to 2.83 pCi/L, with a mean of 0.44 pCi/L
  - Big Creek results for unfiltered samples ranged from 0 pCi/ to 51 pCi/L (0 to 140 μg/L) with a mean of 2.0 pCi/L (5.6 μg/L); results for filtered samples ranged from 0.059 to 22 pCi/L (0.16 to 61 μg/L) with a mean of 1.6 pCi/L (4.5 μg/L); highest observed concentrations where runoff is expected to enter Big Creek from DU impact trench
  - Middle Fork Creek results for unfiltered samples ranged from -0.038 to 2.0 pCi/L (-0.1 to 5.6 μg/L) with a mean of 0.27 pCi/L (0.75 μg/L); filtered samples ranged from 0.032 to 0.65 pCi/L (0.09 to 1.8 μg/L) with a mean of 0.13 pCi/L (0.36 μg/L)
  - Northern Tributary results for unfiltered samples ranged from 0.047 to 0.64 pCi/L (0.13 to 1.7 μg/L) with a mean of 0.26 pCi/L (0.72 μg/L); filtered samples ranged from 0.057 to 0.56 pCi/L (0.16 to 1.6 μg/L) with a mean of 0.23 pCi/L (0.64 μg/L).
- Sediment (20 locations sampled quarterly; April 2008, July 2008, October 2008, and February 2009; plus 4 background locations; locations are on Big Creek and Middle Fork Creek)
  - 96 total samples, 16 background, and 80 site locations
  - Big Creek, Middle Fork Creek, and Northern Tributary results ranged from -0.0176 ± 0.27 (nondetect) to 7.4 ± 1.6 pCi/g with a mean of 1.27 pCi/g (3.3 milligrams per kilogram [mg/kg]); highest observed concentration where runoff is expected to enter Big Creek from the DU impact trench.

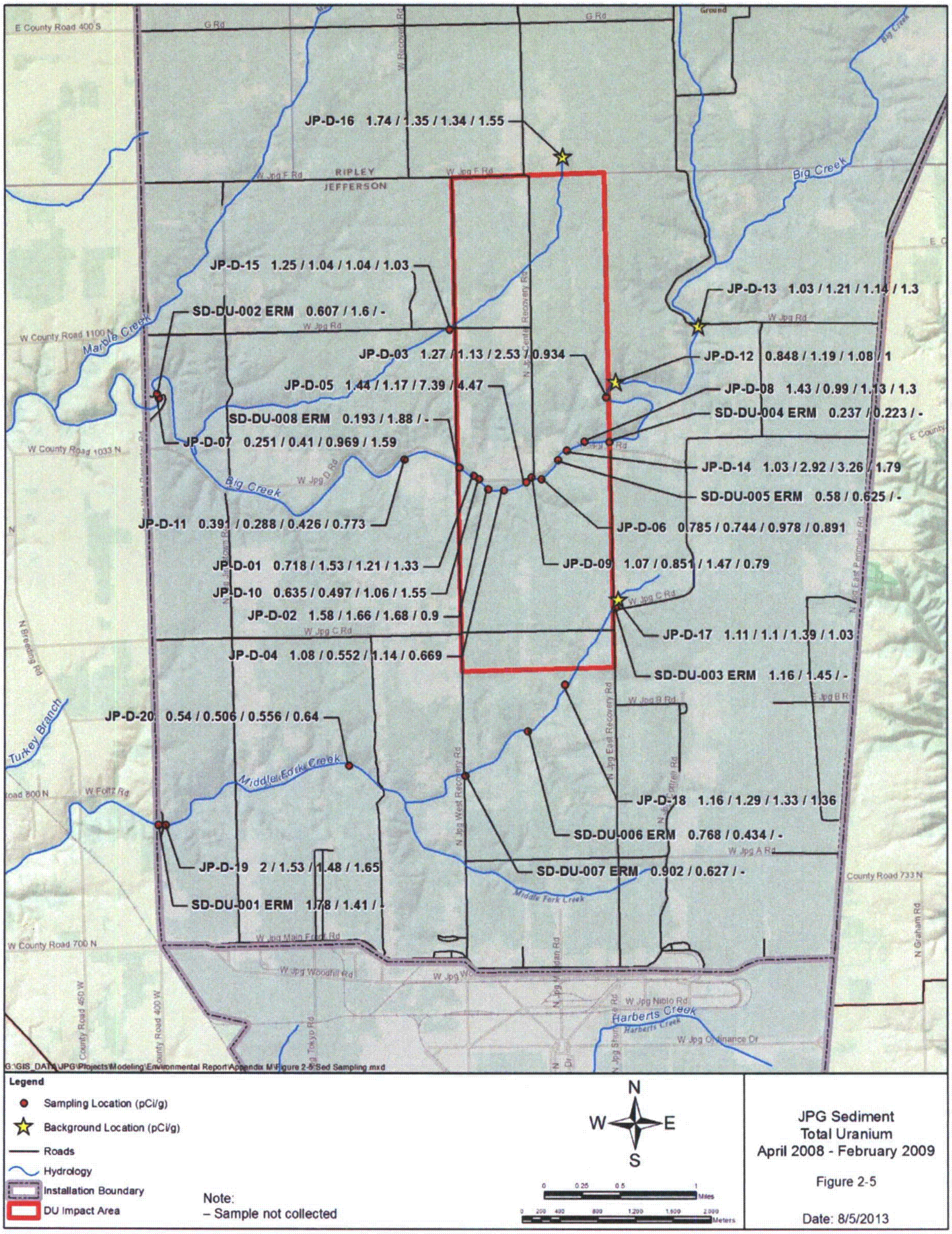

JPG Sediment
Total Uranium
April 2008 - February 2009

Figure 2-5

Date: 8/5/2013

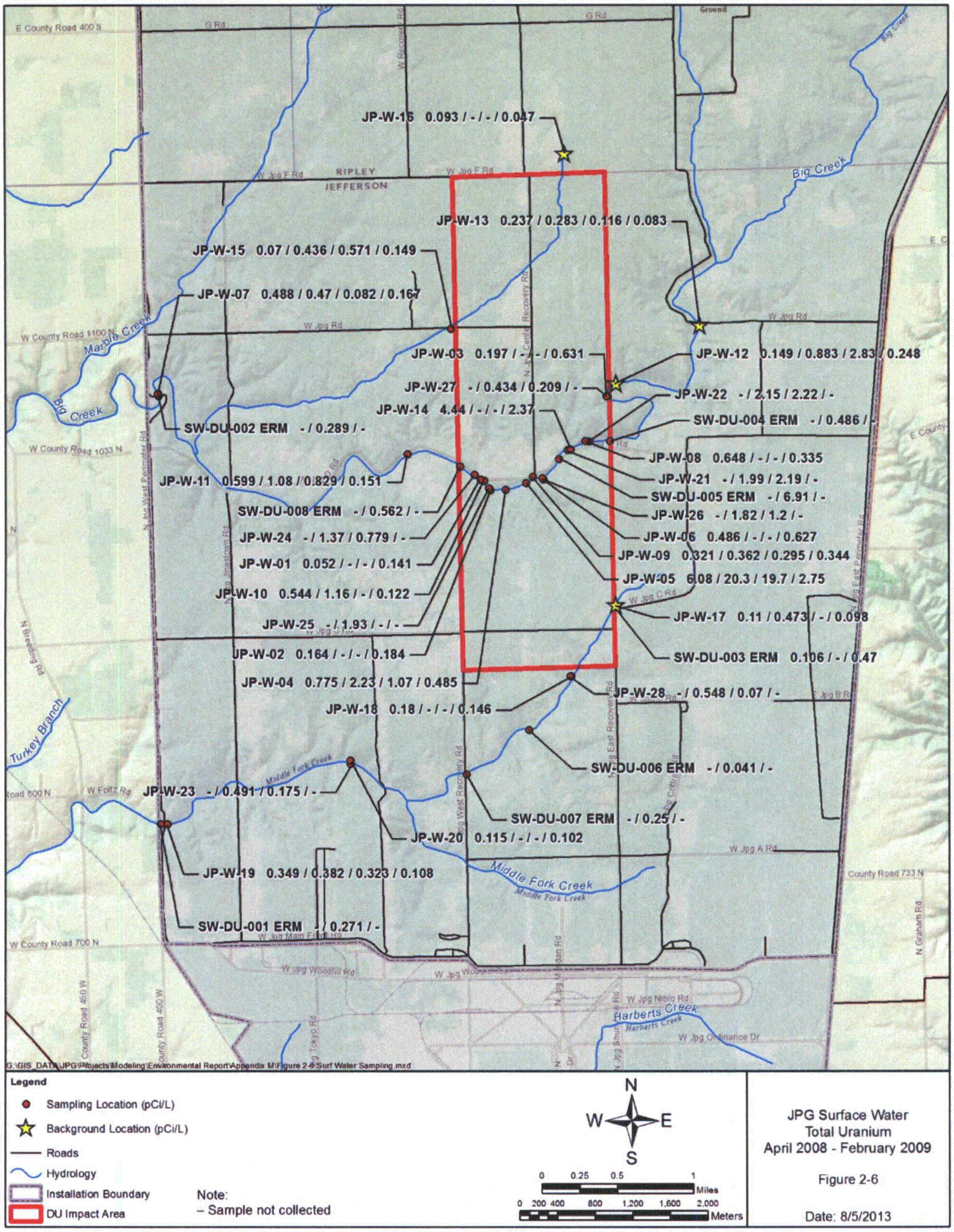

JPG Surface Water
Total Uranium
April 2008 - February 2009

Figure 2-6

Date: 8/5/2013

In addition to biannual ERM monitoring and quarterly sampling for groundwater, surface water, and sediment, site characterization data were collected to further define the nature and extent of DU in soil within and adjacent to the DU Impact Area. Soil samples were collected from 140 locations in October 2008, December 2009, and March 2012. Figures 2-7 and 2-8 show the locations of background soil sampling and sampling conducted within the DU Impact Area, respectively. Figure 2-9 shows the locations of soil samples collected from under penetrators to various depths. Figure 2-10 shows the locations of soil samples collected for use in the partition coefficient (K_d) study, which includes samples collected from the glacial till unit. Key findings from these data include:

- Soil (140 locations)
  - 596 soil samples (105 background and 491 characterization samples)
  - Sampling results from within impact trenches and above/below penetrators were elevated compared to background
    - Background results ranged from 0.16 ± 0.35 to 3.8 ± 1.1 pCi/g (0.45 to 10.4 mg/kg), with means of 651.3 (Avonburg/Cobbsfork), 1.4 (Cincinnati/Rossmoyne), and 1.7 (Grayford/Ryker) pCi/g (3.6, 3.9, and 4.7 mg/kg, respectively)
    - Total uranium concentrations in soil samples collected away from the trench and penetrators ranged from 0.030 ± 2.0 (nondetect) to 140 ± 10 pCi/g (0.08 to 389 mg/kg)
    - Samples from the glacial till ranged from 0.16 ± 0.13 to 2.2 ± 0.24 pCi/g (0.4 to 6.1 mg/kg)
    - Samples collected from within the trench area (Category 6) and samples collected from over or under penetrators ranged from -3.2 ± 2.28 to 40,693 ± 3,580 pCi/g (-9 to 113,000 mg/kg)
    - Within trench results ranged from 0.32 to 142 pCi/g (-9 to 394 mg/kg), with a mean of 8.5 pCi/g (25 mg/kg)
    - Above/below penetrators ranged from -1.5 to 40,694 pCi/g (-4.2 to 113,000 mg/kg), with means of 6,831 (Avonburg/Cobbsfork), 3,956 (Cincinnati/Rossmoyne), and 3,620 (Grayford/Ryker) pCi/g (18,975, 10,989, and 10,055 mg/kg, respectively)
    - Soil sampling results indicate elevated uranium concentrations above background levels detected up to 4.5 ft BGS.

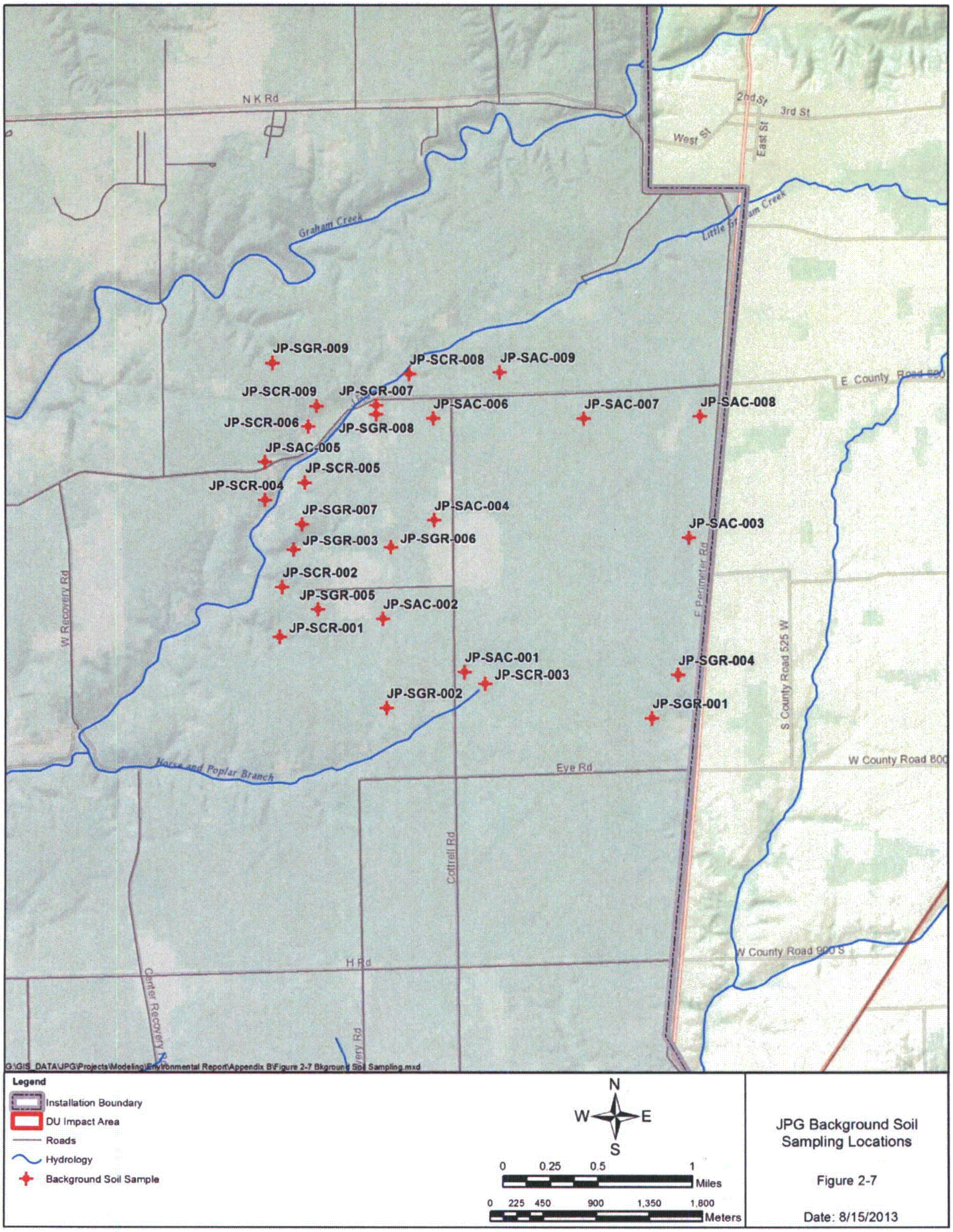

JPG Background Soil Sampling Locations

Figure 2-7

Date: 8/15/2013

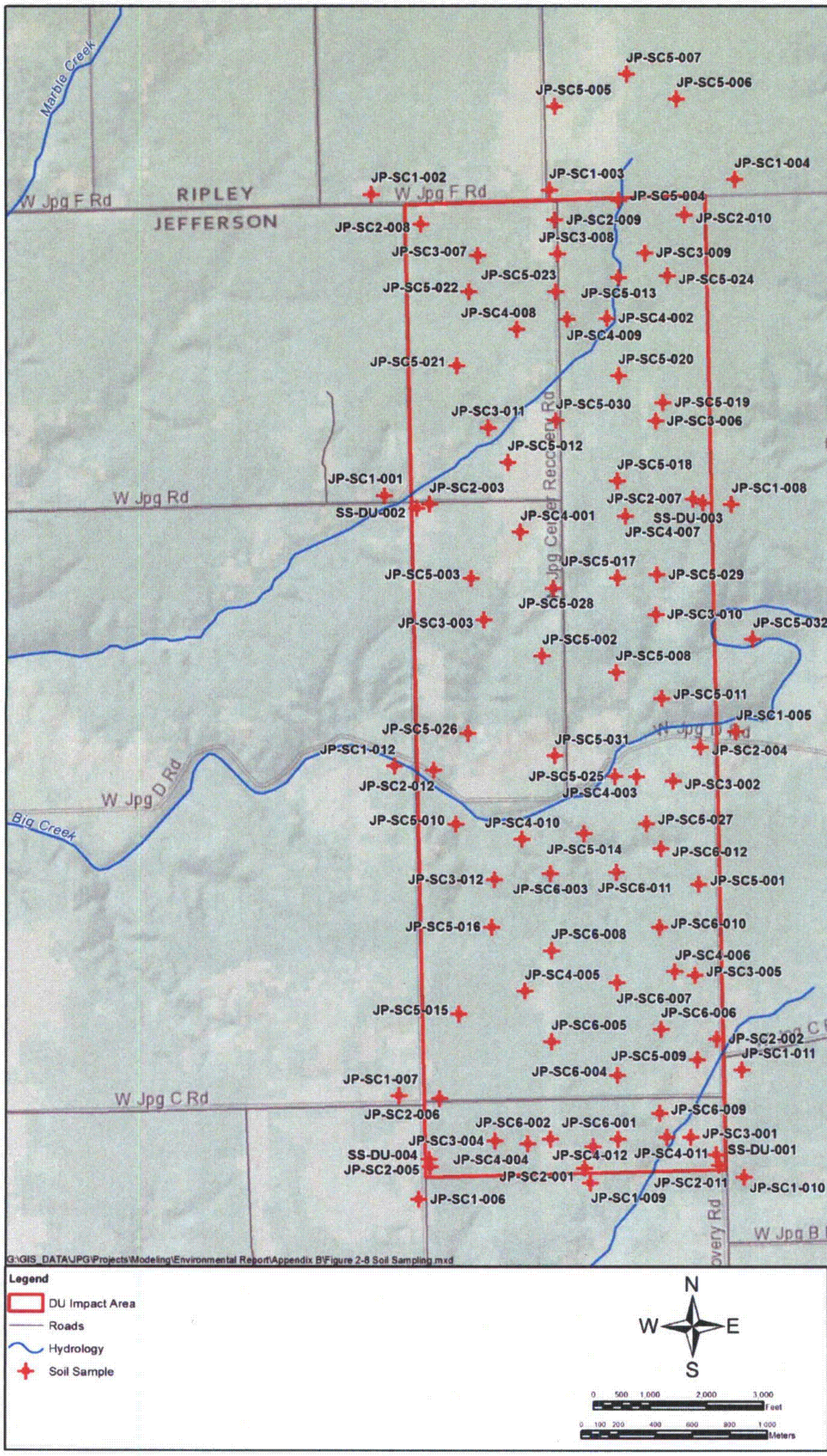

JPG Soil Sampling Locations Within and Around the DU Impact Area

Figure 2-8

Date: 8/15/2013

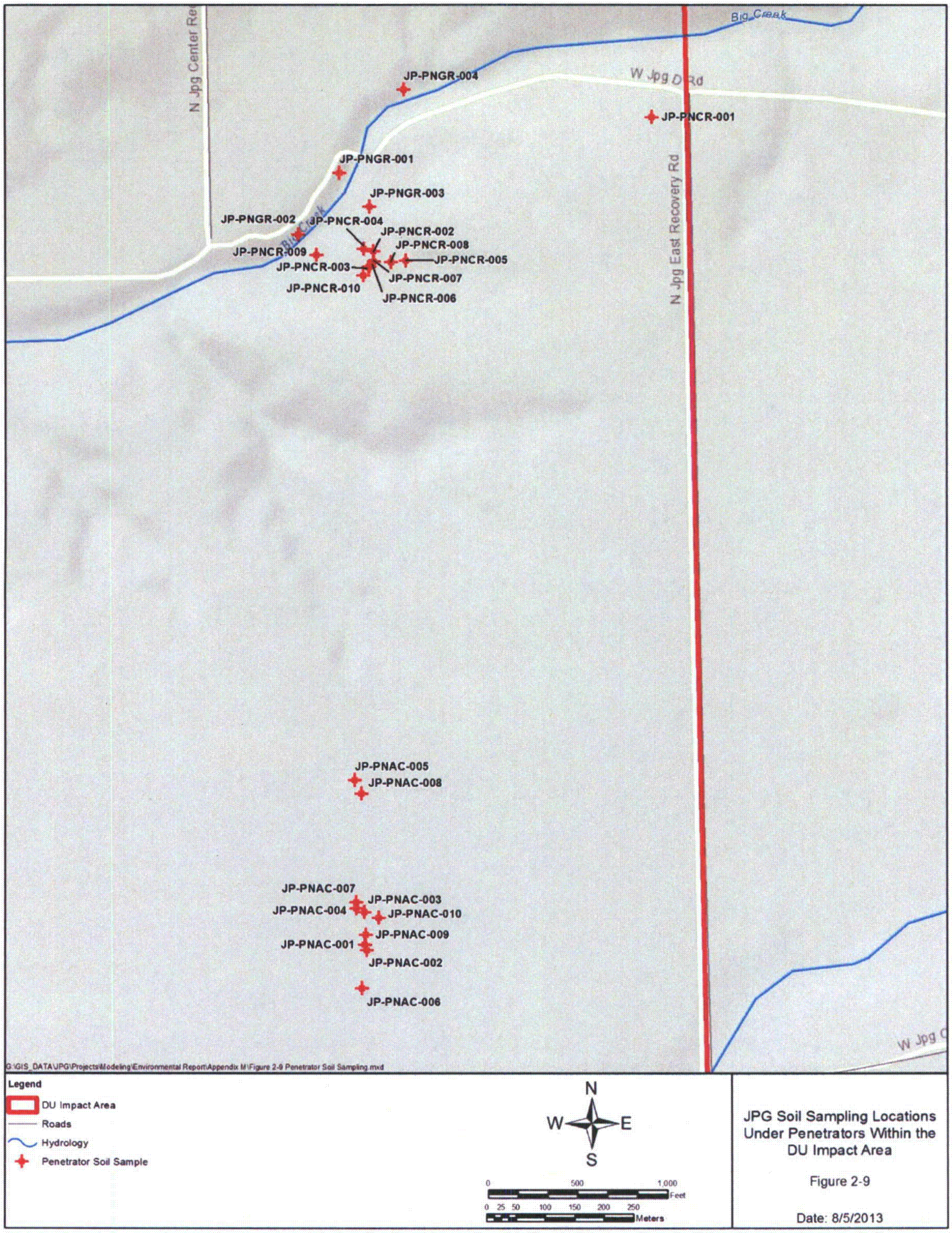

JPG Soil Sampling Locations Under Penetrators Within the DU Impact Area

Figure 2-9

Date: 8/5/2013

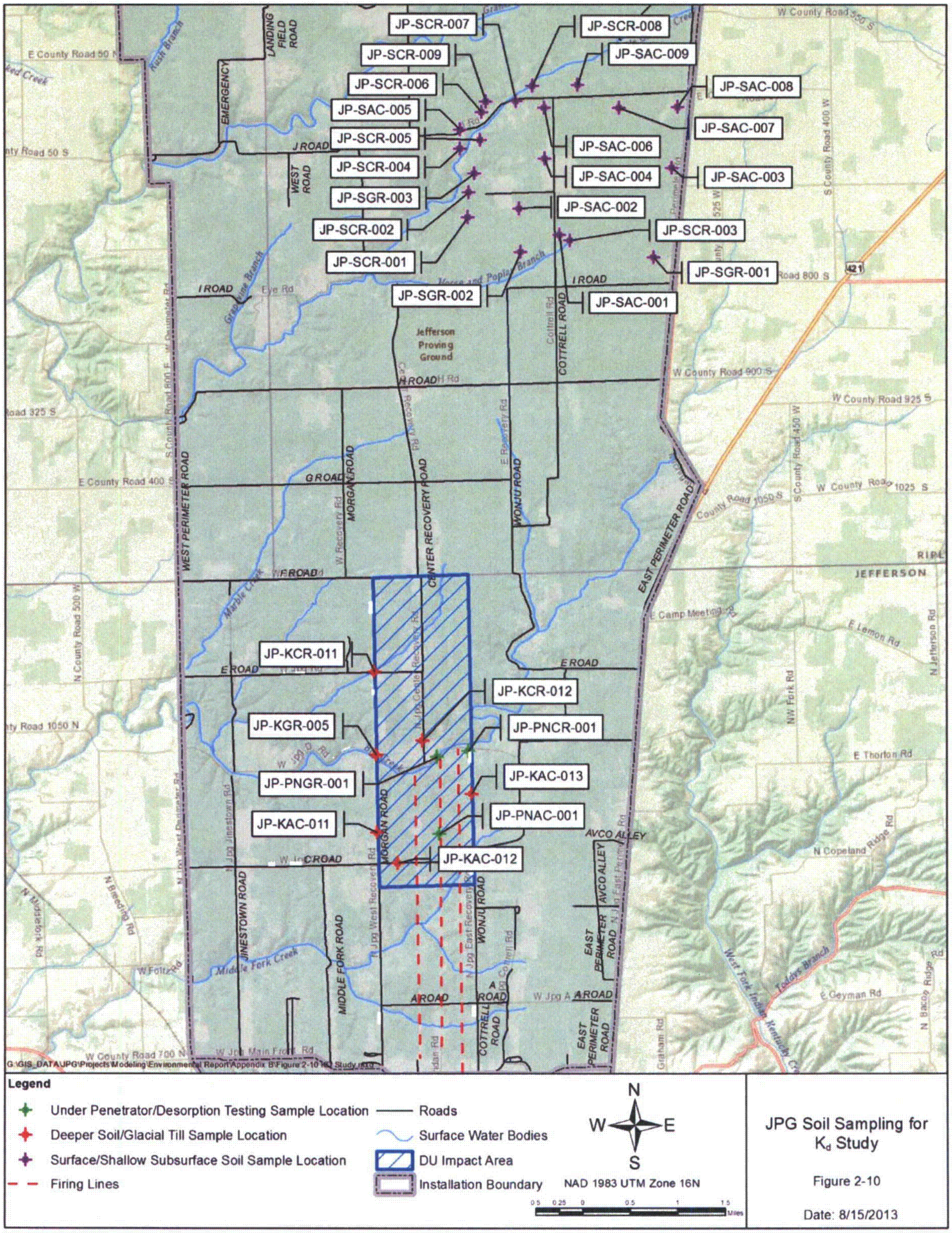

JPG Soil Sampling for K_d Study

Figure 2-10

Date: 8/15/2013

THIS PAGE WAS INTENTIONALLY LEFT BLANK

3. CONCEPTUAL SITE MODEL

A CSM is a description of a site and its environment that is based on existing knowledge. It describes sources; complete, potentially complete, and incomplete transport mechanisms and exposure pathways; current or reasonable proposed use of property; and potential receptors. The CSM serves as a planning instrument, a modeling and data interpretation aid, and a communication device. A central concept to understanding the site-specific problem at the DU Impact Area (U.S. Army 2002) is that doses to humans and ecosystem receptors can come from any number of exposure pathways beginning when the munitions are tested and lasting until the DU and corrosion/weathering products are removed from the system. Thus, the dose to humans from DU must be assessed for a variety of pathways, and for a relatively long time due to slow transport through the soils (U.S. Army 2002).

The CSM for the DU Impact Area is based on the DU penetrators that have been deposited on, or immediately below, the ground surface and/or within the surface water (streams). Once the DU has been deposited within the soil or surface water, it is available for transport through the environment by several different processes. DU in the soil or surface water can be subject to physical movement by erosion, flooding/high water conditions, and dust movement by wind or fire and leaching. Processes of erosion could cause migration and transport of DU penetrators or fragments (during floods and high runoff events) along the ground surface and along surface water drainageways. DU corrosion products from the penetrators and related secondary byproducts (e.g., uranium carbonates) in the soil and surface runoff could be transported to groundwater and surface water. These DU corrosion products and related byproducts could be absorbed by plants and incorporated within the plant matter. The simplest and most direct exposure pathway to wildlife and humans would be from direct contact with the penetrators and/or fragments and incidental ingestion of DU or DU impacted soils. Impacted surface water and groundwater could migrate to drinking water sources. The drinking and surface water could be ingested by humans, livestock, and wildlife. Meat and/or animal products from animals ingesting DU impacted media (i.e., vegetation, soil, water) could be ingested by humans. Humans could have contact with, and incidental ingestion of, impacted surface water during recreational activities such as fishing and hunting.

DU penetrators were test fired at JPG from 1984 through 1994 along three firing lines at soft cloth targets placed at 1,000-m intervals from gun positions extending up to 4,000 m down range. The area where penetrators impacted the ground is referred to as the DU Impact Area. Most penetrators (89 percent) were fired along 500 Center, resulting in the formation of a trench roughly 1,900 m long, 20 to 30 m wide, and 1 m deep. Twice per year during this period, penetrators were recovered by JPG personnel to ensure the facility remained within permit requirements. Of the 100,000 kg of penetrators fired, approximately 26,500 kg were recovered, leaving approximately 73,500 kg in the DU Impact Area and vicinity.

The DU Impact Area lies within the Muscatatuck Plateau physiographic region and is characterized by broad uplands covered by glacial till with entrenched valleys (Gray 2001). The glacial deposits overlie Paleozoic bedrock consisting of interbedded limestone, dolomite, and shale, and overburden thicknesses based on previously installed monitoring wells range from 10 to greater than 65 ft thick (SAIC 2002). According to Franzmeier et al. (2004), the glacial till is Pre-Wisconsinan age and thought to be Illinoian age or older and is covered with a thick (>6 ft thick) mantle of Wisconsinan age loess (wind deposited silt). The soil region that encompasses the DU Impact Area is described as "moderately thick loess over weathered loamy glacial till" (USDA NRCS 1999).

The DU Impact Area is incised by two streams (i.e., Middle Fork Creek and Big Creek and associated tributaries). The surface relief generally is a result of erosion and down cutting associated with the streams and surface water flow to the streams. The surface water drainage is characterized as exhibiting a dendritic pattern that discharges to the streams. The vegetative cover consists of wooded areas containing deciduous trees and open spaces populated with grasses, sedges, and other herbaceous plants. The FWS uses controlled burns (management of vegetation by fire) lasting less than 24 hours to manage some of the grassland areas. A wide variety of wildlife inhabits the area, including terrestrial crayfish and other burrowing animals that may cause localized bioturbation of the soil.

The entire DU Impact Area has undergone anthropogenic disturbance of various types and magnitude. Prior to the establishment of JPG, the majority of the land was agricultural and the soils were disturbed in the act of tilling the lands. Following the establishment of JPG, disturbances ranged from installation and maintenance of the infrastructure (e.g., utility trenching, construction of buildings/structures, and road building) to testing operations in impact fields (i.e., disturbance by detonation) for a great number and variety of military ordnance between 1941 and 1994.

3.1 CHARACTERISTICS OF URANIUM AND DEPLETED URANIUM

As stated earlier, approximately 220,462 lb (100,000 kg) of DU projectiles were fired at soft cloth targets with approximately 58,423 lb (26,500 kg) of the projectiles and fragments being recovered from impact areas on or near the ground surface. These retrieval efforts were generally conducted on a semiannual basis to ensure that the total 100,000-kg license limit was not exceeded. About 161,700 lb (73,500 kg) of DU is believed to remain in the DU Impact Area (SEG 1995 and 1996). The following sections describe characteristics of uranium and DU.

3.1.1 Uranium

Uranium is a naturally occurring metal that can be found throughout the environment in rocks, soil, water, plants, and animals. Natural uranium has three primary isotopes (forms): U-234, U-235, and U-238. U-235 and U-238 are the two most abundant isotopes in terms of mass. U-234 is formed during the natural radioactive decay of U-238. Naturally occurring uranium consists of approximately 99.27 percent U-238, approximately 0.72 percent U-235, and approximately 0.0055 percent U-234 (Royal Society 2001). Humans and wildlife are exposed to natural uranium on a daily basis both in soil and in their food and water (Royal Society 2002). As a result, humans ingest approximately 2 micrograms (μg) of natural uranium each day in food and fluids. A similar quantity is excreted each day in the feces and urine (DOE 2000). This presents a uranium balance in which uranium is always present in the tissues.

The range of intake and losses has been observed to vary over several orders of magnitude, depending upon the uranium concentration in foods and in the water supply (DOE 2000). This condition also may occur in wildlife. As a result of this potential exposure, it is possible that uranium may be detected in tissue samples from humans or wildlife.

3.1.2 Depleted Uranium

DU is defined by NRC as "...uranium with a percentage of U-235 lower than the 0.7 percent (by mass) contained in natural uranium." DU is created as a byproduct of the uranium enrichment process. However, because of its high density, DU can have other uses, such as radiation shielding. DU also is used by the military for tank armor, armor-piercing projectiles, and counterweights in missiles and aircraft.

Although the percent by weight of U-235 in DU can vary significantly, DOD DU generally contains approximately 0.2 percent of U-235 by mass, with the remainder of the mass being U-238 with a very small type amount of U-234. The difference in U-235 content (by mass) can be used to distinguish natural uranium from DU (DOE 2000). The percent by mass of U-235 for each type of uranium is provided in Table 3-1.

Table 3-1. Percent U-235 by Mass in Different Types of Uranium
Jefferson Proving Ground, Madison, Indiana

Type of Uranium	Percent U-235 by Mass
Natural Uranium	0.72
Depleted Uranium (DU)	Approximately 0.2

The decay of each atom of uranium gives off radiation that can be detected by laboratory and field instruments. Although each isotope of uranium (U-238, U-235, and U-234) decays at its own characteristic rate, U-234 and U-238 are generally present in about the same activity concentration in natural uranium (i.e., are in secular equilibrium) with the activity concentration of U-235 being about 2.3 percent of the total activity. The contributions for each isotope of uranium in a natural uranium mixture are provided in Table 3-2.

Table 3-2. Amount of Isotope Present by Activity in Natural Uranium
Jefferson Proving Ground, Madison, Indiana

Isotope	Percent
U-238	47.3
U-235	2.3
U-234	50.4

Source: U.S. Army 1995

Since the radiation from the radioactive decay of uranium isotopes is relatively easy to detect, the levels of activity in a sample can be used to determine the relative amounts of the individual isotopes in the sample. When uranium is enriched, the level of U-235 is increased in the product. As the mass of the U-234 atom is both very close to and lower than the mass of the U-235 atom, the levels of U-234 also are increased in low enriched uranium (LEU) resulting in lower residual U-234 mass in DU. Given that the enrichment process results in the preferential removal of U-234 and U-235, DU exhibits roughly 60 percent of the alpha radiation as naturally occurring uranium (U.S. Army 1995). The contributions for each isotope of uranium in DU are provided in Table 3-3.

Table 3-3. Relative Isotopic Activity in DU
Jefferson Proving Ground, Madison, Indiana

Isotope	Percent
U-238	84.7
U-235	1.1
U-234	14.2

Source: WISE 2006

Because natural uranium and DU are identical except for their isotopic composition (percentage of U-234, U-235, and U-238), their chemical characteristics are the same. Thus, their biochemical action is also the same (Royal Society 2001 and 2002).

3.1.3 Radioactivity

The radioactive decay of DU results in the emission of alpha particles along with beta particles and gamma photons. Alpha particles taken internally deposit relatively large amounts of energy in comparatively small volumes of tissue and are, therefore, more biologically harmful than beta particles or gamma rays if taken into the body. By contrast, alpha particles that are located outside the body cannot penetrate the outer dead layer of the skin and do not, therefore, constitute an external hazard. In large quantities, beta particles located outside the body can damage skin cells and underlying tissues as well as tissues of the eyes. Nonetheless, given the decay rates of uranium series radionuclides, uranium isotopes and their daughter products do not represent a significant external hazard. Similarly, although gamma photons are capable of penetrating internal organs, the very long decay rates of uranium and actinium decay series radionuclides, together with other characteristics such as energy and percent abundance, serve to minimize the gamma hazards associated with uranium.

3.2 TRANSPORT MECHANISMS

Figure 3-1 is a graphical representation of the CSM, including DU sources, release mechanisms, exposure mediums, potential exposure pathways, and potential receptors at JPG. The transport mechanisms are described in further detail below.

The type of release affects the type and amount of DU released into the environment and the potential for exposure of humans and wildlife. In general, soft target testing of DU penetrators, which took place between 1984 and 1994, was not accompanied by significant concentrations of airborne particulate. Rather, DU residuals at JPG generally consisted of penetrators or portions thereof. As such, the potential for subsequent inhalation of re-suspended particulate from contaminated soil or dust is very limited.

DU that had been distributed on or immediately below the ground surface and/or within the surface water (streams) of the DU Impact Area may be transported throughout the environment by several different processes. DU in the soil or surface water can be subject to physical movement by erosion (during floods and high runoff events), and these processes may cause migration and transport of DU penetrators along the ground surface and along the surface water drainageways. Migration and transport of intact DU penetrators and/or fragments thereof are less likely to occur relative to the migration of DU corrosion products in that DU deposited on or near the soil surface in the DU Impact Area was selectively retrieved by semiannual penetrator collection efforts. In addition, corrosion of the DU in the surface water or soil could enable soluble forms of DU to be absorbed by plants and incorporated within the plant matter and subsequently taken up by exposed personnel and wildlife. Although vegetation may be burned as part of a management effort or unintended fires (e.g., from lightning), the levels of DU carried in smoke associated with natural vegetation (such as the controlled burns at JPG) is not likely significant (Williams et al. 1998, U.S. Army 2001, Ridge 2007). Leached DU from the penetrators and/or fragments in the surface water potentially could be transported to groundwater and surface water, which in turn could migrate to drinking water sources and be ingested by humans, livestock, and wildlife.

3.2.1 Groundwater Pathway

Based on the observations from the wells installed during 2007 and the available logs for the existing wells, the subsurface materials can be categorized into three hydrostratigraphic layers consisting of the following: overburden, shallow bedrock zone, and deep bedrock zone. A description of the zones is provided below.

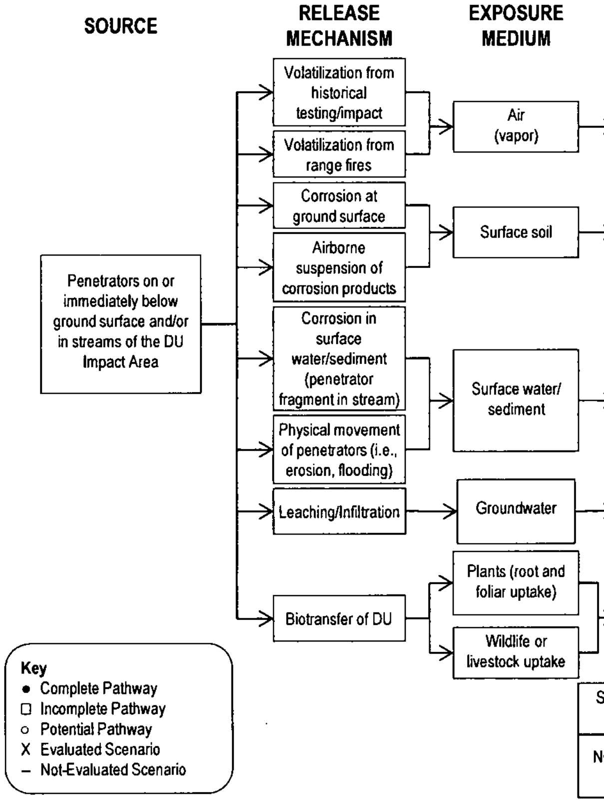

HUMAN RECEPTORS

Exposure Medium	Exposure Route	Exposure Scenarios with Institutional Controls in Place												Exposure Scenarios with Loss of Institutional Controls							
		Onsite Recreationist	Onsite Hunter	Onsite Fisherman	Offsite Resident Farmer	Offsite Boundary Recreationist	Offsite Boundary Recreationist (Hunter)	Offsite Boundary Recreationist (Fisherman)	Offsite Part-Time Resident	Offsite Part- Time Resident, Mod. 1	Offsite Industrial Worker	City Resident	Downwind Resident Farmer	Resident Farmer, Without Irrigation[a]	Resident Farmer, With Irrigation[a,b]	Onsite Hunter	Onsite Fisherman	Domestic[a]	Part-Time Domestic[a]	Onsite Industrial Worker	Onsite Sportsman/ Recreationalist
Air (vapor)	Inhalation	□	□	□	□	□	□	□	□	□	□	□	□	□	□	□	□	□	□	□	□
Surface soil	Ingestion	●	●	□	●	□	●	●	□	□	□	□	●	●	●	●	●	●	●	●	●
Surface soil	Inhalation (dust)	●	●	●	●	●	●	●	●	●	●	●	●	●	●	●	●	●	●	●	●
Surface soil	External radiation	●	●	●	●	●	●	●	●	●	●	□	●	●	●	●	●	●	●	●	●
Surface water/ sediment	Ingestion	□	□	□	●	●	○	○	●	●	●	●	□	□	□	●	●	○	□	□	●
Surface water/ sediment	External radiation	●	●	●	●	●	●	●	●	●	●	●	●	●	●	●	●	●	●	●	●
Groundwater	Ingestion	□	□	□	□	□	□	□	□	□	□	□	□	●	●	□	□	●	□	□	□
Groundwater	External radiation	□	□	□	□	□	□	□	□	□	□	□	□	●	●	□	□	●	□	□	□
Plants (root and foliar uptake); Wildlife or livestock uptake	Ingestion	□	●	○	●	●	●	●	□	●	□	□	●	●	●	●	●	●	●	□	●
	Scenarios Evaluated in Dose Assessment	–	–	–	X	–	–	–	–	–	–	–	–	–	X	–	–	–	–	X	X

NOTE: Scenarios that were not evaluated in the Dose Assessment, including those with potential pathways, were bounded by other scenarios that were evaluated (reference dose assessment section).

Figure 3-1. Revised Conceptual Site Model of DU Transport Through the Environment at and in Close Proximity to the DU Impact Area

3.2.1.1 Overburden

The overburden consists of the unconsolidated materials or overburden present above the bedrock. As determined from the well installation and well logs, the depth of the overburden materials range from 0.65 to 72.5 ft, with an average depth to bedrock of 20.8 ft. The overburden materials consist of glacial tills and loess. A soil verification study (SVS) was completed and the results of the study are provided in Section 2 of the Well Location Selection Report (SAIC 2007) in which the soils present within the DU Impact Area are described in detail.

The soil in the study area is composed of mostly fine-grained materials, which appear to have a low permeability. At five well locations, sufficiently permeable materials were observed that would provide sufficient well yield to provide a suitable groundwater monitoring and sampling point. The majority of the existing monitoring wells that were completed in the overburden have been observed or documented in previous reports to have low well yields.

3.2.1.2 Shallow Bedrock Zone

The shallow bedrock zone consists of the top 40 to 60 ft of the carbonate bedrock. Generally, the bedrock encountered consists of nearly horizontally bedded limestone, shaley interbedded limestone, dolostone, and shaley interbedded dolostone. Observations from the well installations and from the logs for the existing monitoring wells show there is limited secondary porosity consisting of weathering near the bedrock surface, fractures, and very limited solution features. In addition, there was very little evidence of weathering along observed fracture surfaces. The amount and severity of the fractures generally decreased with depth. The only void of significance that was observed during the recent well installation was approximately 6 inches in size at a depth of 23 ft BGS in the boreholes for both JPG-DU-02I and JPG-DU-02D.

3.2.1.3 Deep Bedrock Zone

The deep bedrock zone consists of the bedrock below the permeability observed in the shallow bedrock zone, below 40 to 60 ft BGS. Within the deep zone the fractures observed were extremely limited and fresh (e.g., practically nonexistent weathering). No evidence of solution features were observed within the deep zone. The minimum rock core recoveries for all of the core holes was 93.1 percent and all but two were greater than 95 percent recovery (95 percent recovery means 9.5 ft core are recovered for 10 ft of coring or only 0.5 ft of core are lost in 10 ft of core). In the deep zone, the measured and calculated Rock Quality Designation (RQD) was excellent (or very high rock quality), indicating competent bedrock with little fracturing or weathering. RQD refers to the percentage of rock core recovered from a borehole incorporating only solid pieces of core 10 or more cm in length. RQD of 90 to 100 percent is referred to as excellent (or very high rock quality). Additional details concerning the RQD analysis are included in the main body of this report (Section 6). The deep bedrock wells were constructed with screen intervals located within the interval that appeared to have the highest potential for permeability. After several months, a number of the deep bedrock wells were still recovering from pumping that occurred during the well development activities.

3.2.1.4 Karst Development

Karst features have been observed at JPG and specifically within the DU Impact Area consisting of surface expressions of sinkholes, caves along Big Creek, and weathered jointing (fracturing) of bedrock observed at outcrops along Big Creek. Wells were located on fracture traces and using geophysical techniques to selectively test areas where karst development would be greatest. However, as a result of the well drilling, field observations and an analysis of published reports and previous studies demonstrate that karst activity within and immediately surrounding the DU Impact Area is limited in depth and lateral extent.

As a result of these observations, the CSM limits the location of shallow karst features (caves and sinkholes) to a narrow plain along Big Creek. Caves and solution features appear to most commonly occur above the groundwater table and above the elevation of Big Creek, limited to depths of less than 50 ft below the land surface.

3.2.1.5 Recharge and Groundwater Flow

Recharge to the aquifer is limited by the low permeability overburden (soil) materials present within the study area, very tight bedrock (horizontal bedding, shaley interbedding, fresh, unweathered) observed during the 2007 well installation, and further limited by collection of surface water/infiltration/interflow by the limited shallow karst/cave system, which is at or above the water table, and discharges through open channel flow to the surface water. The majority of the limited groundwater flow within and from the DU Impact Area is expected to occur within the overburden and shallow bedrock zone, whereas the deeper bedrock zone is tight and groundwater flows are expected to be extremely limited. In addition, based on the available data, groundwater elevations within the overburden and the shallow bedrock zones generally mimic the surface topography, and groundwater flow directions are generally toward the local surface water drainages.

3.2.2 Surface Water Pathway

Based on the limited recharge to the aquifer and reduced or low permeability with depth, the surface water pathway represents the most significant potential migration pathway from the DU Impact Area. The hydrographs from nearby USGS stream gauges and results from stream gauges onsite indicate that surface runoff after a precipitation event spikes rapidly and dissipates quickly. This may indicate the majority of sediment migration from the DU Impact Area could occur during short durations during peak runoff conditions when considerable flows in the streams would potentially carry particulates, either sediments with DU attached or DU particles, and deposit them downstream when flow velocities dissipate.

3.2.3 Biotransfer Pathways

Plants are generally poor accumulators of uranium and concentrations of uranium in plants are several orders of magnitude lower than those in the soil in which they grow (Royal Society 2002). However, despite the generally low transfer of uranium from soil to plants, certain plant species (i.e., microbial species such as fungi, yeasts, algae, and other unicellular bacteria (Hu, Norman, and Faison 1996, reported in Royal Society 2002), black spruce and some forest plants (Thomas 2000, reported in Royal Society 2002), sugar beets and sunflowers (Erikkson and Evans 1983 and Dushenkov et al. 1997, reported in Royal Society 2002), and Indian mustard (Edenspace 2004) have been shown to exhibit high uptake of uranium. Nonvascular plants (mosses and lichens) generally accumulate higher concentrations than vascular plants (Cramp et al. 1990, reported in Royal Society 2002).

Ingestion of microbial and plant species with accumulation of DU presents a route by which higher trophic levels of wildlife can be exposed. Some accumulation of uranium has been observed in animals. Measurements of uranium in tissues of animals grazing in uranium-contaminated areas have been reported to be higher than those in control areas. Few measurements of uranium in wild animals have been made, but those compiled do not report significant accumulation in tissues (e.g., Clulow et al. 1998), although they are measurable and often elevated in whole animal samples at contaminated sites (Royal Society 2001). Ingestion of animal species with accumulation of DU presents a route by which higher trophic levels of wildlife can be exposed.

Ingestion of contaminated soil could be an important exposure pathway for animals as animals typically eat more soil than humans (i.e., incidentally when licking fur or pelts or as part of their diet). Wildlife may be exposed indirectly to DU by ingestion of plants that have taken up DU or where DU has been deposited on the leaves by wind dispersion.

3.3 EXPOSURE PATHWAYS

Humans at JPG may be exposed to DU from direct contact or incidental ingestion of penetrators and/or fragments from impacted surface water during recreational activities such as hunting. However, as indicated in the Deer Tissue Sampling Report (SAIC 2006b), the level of uranium detected within the tissues of harvested deer for the DU Impact Area, near the DU Impact Area, and background areas showed only background levels of uranium within the deer tissue and no DU. As fishing is not permitted in JPG streams and the nearest fishing is several miles north of the DU Impact Area in Old Timbers Lake during only part of a calendar year (on Mondays, Fridays, and second and fourth Saturdays of the month during the public use period from mid-April to November), humans are not exposed to DU from direct contact while fishing. Possible exposure pathways for humans include ingestion of food (i.e., meat and/or animal products from animals that have ingested DU impacted soil, water, or biota), water, or soil containing DU; inhalation of dust containing DU; or external radiation from the presence of DU.

Insoluble uranium from DU or natural sources that has been inhaled may deposit in the lungs and associated lymph nodes and may remain in the lungs for years. Soluble uranium, once inhaled, may be transported to the gastrointestinal tract. In addition, uranium may be deposited in the intestinal tract of humans or wildlife from ingestion (Royal Society 2001). Once inside the intestinal tract, accumulation may occur in bones, livers, or kidneys. To a lesser degree, the uranium may accumulate in the muscle. Uptake from the stomach gut to the blood is low (0.2 to 5 percent) and most ingested uranium is excreted, where it could be re-ingested or recycled via the soil into forage. Uptake factors of uranium from the gut to the blood for ruminants (i.e., deer, cattle, or goats) may vary depending upon environmental conditions, but are approximately five times greater than that of humans (Royal Society 2002, see also Deer Tissue Sampling Report [SAIC 2006b]).

4. VADOSE ZONE COLUMN MODEL

The transport of DU via the groundwater pathway includes vertical leaching or migration of DU from shallow soils where DU still resides, down through the unsaturated loess soils and upper reaches of till to the underlying groundwater in the lower portion of the till. Observed soil sampling results, which are presented in the main report and listed in Appendix F, indicate DU has been detected to a depth deeper than 4 ft BGS. It is not clear if DU detected at this depth represents migration over the roughly 30 years since penetrator testing began at the former proving ground in 1984 or if the detection represents sample contamination from near surface particles during the collection of the soil sample. The assessment of DU migration through the vadose zone through the use of observed data to date and forward looking numerical modeling is presented here, including, for the model: evaluation of the DU source term, code selection, model setup, and execution.

4.1 CURRENT DU ACTIVITY IN SOIL

Table 4-1 lists the average gamma activities, based on field measurements with a sodium iodide (NaI) detector in October 2008, per 6-in and 1-ft intervals between grade and a total depth of 4 ft beneath penetrators found in each principal soil series where DU penetrators reside. The highest average gamma activity observed in these measurements is in the top 6 in of soil, where DU corrosion products are most prevalent along with total organic carbon (TOC). Average gamma activities trail off markedly at depths of 1 to 2 ft BGS, with values at one to two orders of magnitude lower at depths of 3 to 4 ft BGS. The one exception is the average DU activity at 2 to 4 ft BGS for Grayford/Ryker soils. This soil series is the least prevalent soil type where penetrators are found and is therefore represented by only three samples. DU activity in this depth interval at two of the three locations was similar to the Avonburg/Cobbsfork and Cincinnati/Rossmoyne soils, on the order of 191 to 288 pCi/g. DU activity at the third sample location was 12,491 pCi/g, which influenced the higher apparent average DU activity for this soil series.

Table 4-1. DU Activity with Depth in Shallow Loess Soils Jefferson Proving Ground, Madison, Indiana

		Average DU Activity (pCi/g)			
Loess Soil Series	Sample Depth	0-0.5 (ft)	0.5-1.0 (ft)	1.0-2.0 (ft)	2.0-4.0 (ft)
Avonburg/Cobbsfork Soil Average DU Activity		14,488	1,663	368	120
Cincinnati/Rossmoyne Soil Average DU Activity		9,971	3,655	767	503
Grayford/Ryker Soil Average DU Activity		3,117	626	466	4,323

Note: DU activity determined in the field with a sodium iodide detector.

Review of the average gamma activity over depth indicates that the highest activity is in the uppermost 6 in of soil. This is a function of the accumulation of corrosion solids, but also likely reflects DU partitioning and possibly DU mineral precipitation due to widely fluctuating soil moisture, DU solubility so close to a uranium/DU source, and transitional reducing conditions (see Appendix D for K_d Study). The rapid decline in gamma activity over a short depth interval is a reflection of the poor mobility of DU in shallow oxidizing substrate or its susceptibility to reduction and precipitation. The pore water and soil geochemical factors, as discussed in the K_d Study, promote DU partitioning and potentially mineral precipitation/co-precipitation significantly over mobility, achieving near complete attenuation by a depth of 4 ft BGS after 30 years. The anomalously high DU activity in the one soil sample at a depth of 4 ft may reflect the role of near surface macropores in short circuiting porous media flow or possible inclusion of DU particles or corrosion product carried down to this depth during sampling efforts.

4.2 SOURCE TERM EVALUATION

The source term, as defined here, represents the rate of DU mass released over time for transport via the groundwater pathway. The source term depends on the location of the DU penetrators, the processes that affect the weathering (corrosion and dissolution) of penetrators, and the distribution coefficient (K_d) of DU to subsurface soils.

In most geologic formations, U^{+4} (IV), and U^{+6} (VI) are the most important oxidation states of uranium present. Uranium (VI) and (IV) species dominate in oxidizing and reducing environments, respectively. The fate and transport of uranium in soil and aqueous environments is largely controlled by its adsorption and desorption to/and from porous media into the dissolved phase. Available research (USEPA 1999) shows that pH and dissolved carbonate concentrations are the two most important factors influencing the adsorption behavior of uranium.

DU is created as a byproduct of the uranium enrichment process. Although metallic uranium is essentially immobile, corrosion reactions of DU can yield oxidized products that can dissolve, adsorb to the soil matrix, and complex with natural organic matter (Chen and Yiacoumi 2002). Geochemical reaction codes and surface complexation models have been used to investigate mobility of uranium within various co-existing media (e.g., soil, surface water, and groundwater) generally at small scales. For large sites such as the JPG groundwater model, a feasible approach is to use the K_d, defined as the ratio of adsorbed concentration to dissolved concentration to represent sorption and dissolution and mobility of DU.

4.2.1 Penetrator Distribution

The distribution of penetrators remaining within the DU Impact Area is uncertain. Penetrators were test fired from 1984 through 1994. During this period, penetrators were recovered twice each year to ensure the total DU mass remained below permitted levels.

SAIC reviewed available literature, conducted field surveys, and developed methodology to estimate the spatial distribution of penetrators remaining within and near the DU Impact Area. An estimated total of 162,000 lb (73,500 kg) of DU remains unrecovered within the DU Impact Area (Section 1 of Decommissioning Plan). Most of the penetrator mass occurs in near surface soils, within and adjacent to DU Impact Area trenches formed from penetrator test firing.

4.2.2 DU Corrosion and Dissolution Rates

The rate of uranium released from penetrators to the environment is dependent upon the penetrator corrosion rate and the subsequent dissolution of the corrosion products. Uranium metal is unstable when in contact with oxygen and water. The uranium is oxidized, and in the presence of water the oxides are hydrated to form minerals such as schoepite ($UO_3 \cdot nH_2O$). The corrosion rate and subsequent dissolution of the corrosion products were estimated from similar studies published in the literature and from laboratory studies conducted on penetrators recovered from the DU Impact Area and available in literature on a per penetrator basis.

As shown in Table 4-2, which is taken from a more detailed description provided in Appendix C, the most likely estimate of the penetrator corrosion rate is 0.25 grams of DU per square centimeter (cm^2) each year under assumed oxidizing conditions. The dissolution rate of the corrosion products is estimated at 0.15 grams of DU per cm^2 of the corroded penetrator. The calculated time to complete corrosion and dissolution of the penetrator is 107 years and peak loss of mass is 56.8 grams per year in years 18 through 24. Figure 4-1 shows the calculated time-dependent source of uranium into the soil based on these

Table 4-2. Most Likely Estimate Values for Corrosion and Dissolution Rates
Jefferson Proving Ground, Madison, Indiana

Parameter	Most Likely Estimate Value	Notes
DU Corrosion Rate	0.25 g/cm^2-y	Calculated per unit surface area of remaining DU metal
Dissolution Rate	0.15 g/cm^2-y	Calculated per unit surface area of corroded penetrator (outer surface)

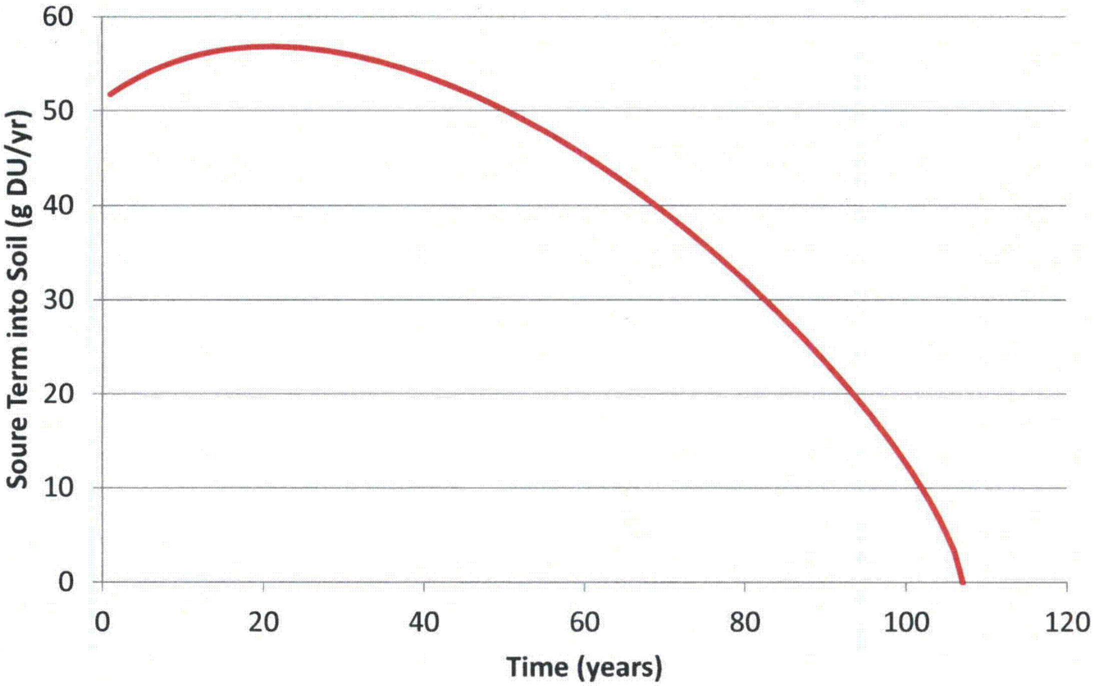

Figure 4-1. Estimated DU Mass Release Into Soil From Penetrator Corrosion/Dissolution

values. The figure displays the mass of DU entering the soil per year per penetrator and the estimated range in rates.

The estimated mass of DU entering the soil per year per penetrator was developed assuming a 50/50 mixture of 105-millimeter (mm) and 120-mm projectiles were fired at JPG with an average penetrator mass of 4.4 kg. However, different penetrator models of varied mass and surface area were test fired at JPG. Therefore, they will exhibit slightly different dissolution rates than the estimated rates shown above. It is assumed that dissolution rate from such penetrators is proportional to their mass and surface area.

One last note regarding the estimated rates of penetrator corrosion and subsequent dissolution; DU penetrators were test fired from 18 March 1984 to 2 May 1994. The most likely estimated rate shown in Figure 4-1 indicates the rate of DU mass release to soil should be near the maximum rate if assumptions regarding development of the rates (oxidizing conditions) are valid. As noted in Section 2, greater than 55 percent of the soils in the DU Impact Area are somewhat poorly drained and exhibit redoximorphic features (soil mottling) that indicate a reducing environment exists in the shallow (<3 ft) subsurface for some period of time (late winter to spring) during the year. The rates presented here do not take into account this effect. Therefore, the values presented here represent the upper end of corrosion and dissolution rates. The rates (DU mass released to soil over time) used to calibrate DU transport in the JPG model are expected to be lower (less mass each year) and occur over a longer period of time as a result of the periodic seasonal reducing conditions.

4.2.3 Laboratory Derived K_d Values

The K_d was measured at JPG to characterize how DU may adsorb to or desorb from site soils during fate and transport. Two basic tests (sorption and desorption) were used to estimate the site-specific K_d and desorption potential, respectively, for DU. Appendix D contains the results of the K_d Study, briefly summarized below.

Sorption tests were performed for site soils and glacial till. Rain water collected at the site was spiked with uranium at known concentrations and mixed with representative soils collected from background locations to determine what fraction of uranium would adsorb to the soils. Similarly, groundwater spiked with uranium at known concentrations was mixed with glacial till samples to determine uranium sorption to glacial till in the saturated zone. Desorption tests consisted of passing rain water collected at the site through impacted soil samples (collected beneath penetrators) to determine the fraction of uranium that could desorb from impacted soils as rain water comes in contact with the soils. Results from the tests are summarized in Table 4-3. In summary, sorption tests showed the lowest K_d (lowest fraction of uranium portioning onto the till) for groundwater in glacial tills. Sorption tests for soils at the surface showed high K_d (uranium strongly sorbed to soils). Desorption tests indicated a higher fraction of uranium will partition to rain water in contact with highly impacted soils beneath or near the penetrators. Figure 4-2 illustrates the determination of the loess-glacial till interface and the approximate zones where the different K_ds are applicable.

The laboratory results show a wide range in potential K_d for uranium at JPG, which is consistent with reported K_d in the literature for uranium. Near surface soils are expected to have a relatively high K_d for uranium due to the low alkalinity and acidic soils and the typically low alkaline, oxidizing precipitation that infiltrates these soils. Twenty-six soil samples collected at the surface for K_d testing had an average pH of 5.5 and ranged from pH 4.4 to 7.6. Eight soil/glacial till samples collected from depths of 6 to 13 ft had higher alkalinity with an average pH of 8.6 and ranged from pH 7.4 to 10.4, owing to the carbonate content assimilated from the underlying regional carbonate terrane.

Table 4-3. Summary of DU Batch Testing Results
Jefferson Proving Ground, Madison, Indiana

Soil Type	Number of Tests	Minimum Value	Maximum Value	Average Value
K_d (mL/g): Rainwater Sorption for Loess Soil Types				
Avonburg/Cobbsfork	10	1,058	3,831	2,290
Cincinnati/Rossmoyne	10	57	4,470	2,132
Grayford/Ryker	4	1,073	1,421	1,208
K_d (mL/g): Groundwater Sorption for Glacial Till				
Avonburg/Cobbsfork	3	0.93	1.03	0.97
Cincinnati/Rossmoyne	1	11.7	11.7	11.7
Grayford/Ryker	2	16	20	18
R_d (mL/g): Desorption by Loess Soil Type				
Avonburg/Cobbsfork	1	189	189	189
Cincinnati/Rossmoyne	1	591	591	591
Grayford/Ryker	1	507	507	507

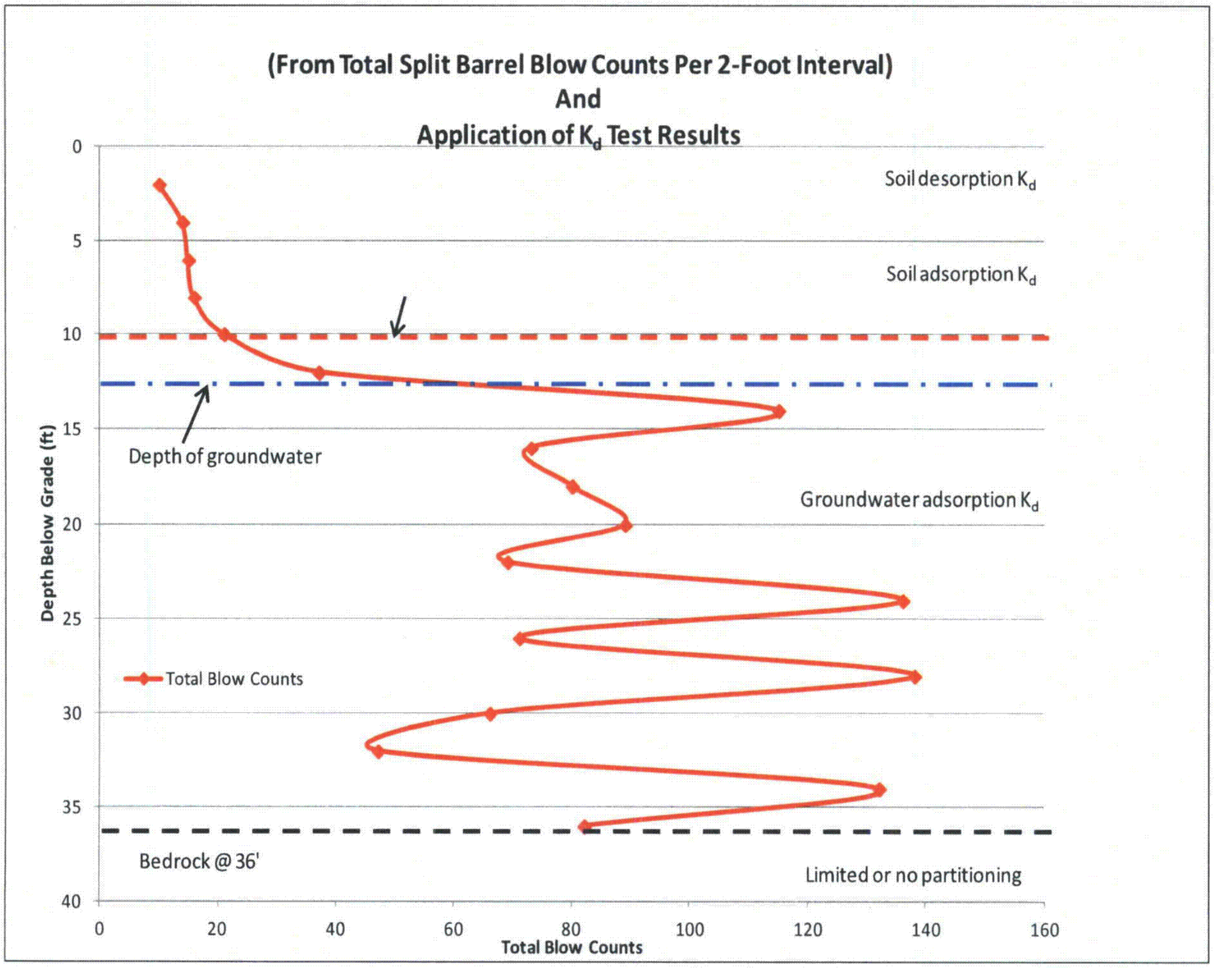

Figure 4-2. Example Soil Density Profile Through Loess Soil and Glacial Till at Well Location JP-DU-06

The weighted average K_d values for each type of test group: loess soil sorption, loess soil desorption-dissolution, and glacial till sorption is presented in Section 9 of Appendix D and summarized here. Given the small representation of the Holton soil type in the DU Impact Area (1.7 percent) with limited potential to contain penetrators, this soil group was excluded from the soil area component of the weighted average. Respective weighted average K_d values and associated standard deviations for the three types of tests were as follows:

- Loess soil sorption: weighted average 2,116 milliliters per gram (mL/g); standard deviation 410 mL/g
- Loess soil desorption-dissolution: weighted average 354 mL/g; standard deviation 204 mL/g
- Glacial till sorption: weighted average 6.4 mL/g; standard deviation 7.5 mL/g.

4.3 MODEL SELECTION AND DESCRIPTION

The FEHM model (FEHM, version 3.06) developed and validated by Los Alamos National Laboratory, was selected to estimate the potential for migration of DU through variably saturated soil to the groundwater table. The model assumes DU penetrators are corroded at the surface and these corrosion products release DU into the subsurface vadose zone via infiltrating precipitation.

The FEHM model was selected given its ability to simulate DU transport through the vadose zone, its recognition in the industry as a well-documented, verified, and validated code, and our team's experience in utilizing the code for similar fate and transport assessments.

4.4 MODEL DESIGN

A representative column model was developed to examine the movement of DU within the vadose zone. The column was first set up with representative parameters and allowed to come to equilibrium producing a partially saturated column similar to that expected at the JPG site. A constant concentration of DU in aqueous concentration was applied at the surface of the column model. The relative ratio of the predicted aqueous concentration at different depths within the column model, including the water table, is determined by comparing model predictions at depths of interest against the initial source concentration. Using this approach, output from a few simulations can be used to predict DU concentrations at the water table from observed soil concentrations at or near the surface. The model assumes simple linear sorption and employs site-specific values of K_d for soils. Geochemical modeling of reactions was not performed.

An initial source of 100 milligrams per liter (mg/L) of DU dissolved in porewater was placed at the top of the column (ground surface) and allowed to migrate vertically for a 1,000-year simulation period. The source was held constant at 100 mg/L at the ground surface for the 1,000-year duration of the modeling. The selected DU concentration of 100 mg/L is not tied to an assumed or measured pore water concentration; it was selected for convenience to permit scaling of results to different initial conditions that may be observed at different locations across the DU Impact Area. This is a common convention applied when conducting transport predictions through a soil column utilizing constant recharge and linear sorption. For example, should model predictions indicate a 50 percent reduction in pore water concentration at the water table, one can induce a 50 percent reduction for all starting pore concentrations within the current column model configuration.

Using this approach, the potential for DU migration through the soil column to groundwater and associated travel times were examined for three different depths associated with minimum, average, and maximum depths of groundwater table in the vicinity of the DU Impact Area.

4.4.1 Model Domain and Discretization

Since substantial uncertainty exists regarding the exact location of penetrators and heterogeneity occurs within the site geology, a representative column was developed to approximate the conditions observed at the site. Overburden wells in the vicinity of the DU Impact Area were examined to determine minimum, average, and maximum depths to groundwater as shown in Table 2-4. Based on these results, a 6.56 × 6.56 × 40-ft deep column was developed. Results of the column model were examined at the following depths: 2 ft, to look at the concentration at the shallowest recorded water table depth, 11 ft for the average depth to groundwater, and 40 ft for the maximum depth to the water table within the DU Impact Area. The model was discretized into 5 nodes by 5 nodes in the x-y plane and 81 nodes in the z (vertical) direction for 2,025 total nodes (see Figure 4-3).

4.4.2 Boundary Conditions

In order to solve the equations necessary for simulating water movement in the subsurface, boundary conditions must be applied to tie the model to real world situations. For this problem, three different boundary conditions were applied to the flow model for this purpose.

The top of the model is the area in contact with recharge from precipitation. During the 1,000 year simulated model run, this boundary is set up with a constant flux equivalent to the average recharge of 4 in/y (see Section 2.3.7). The remaining boundary conditions for the flow problem involve using no-flow

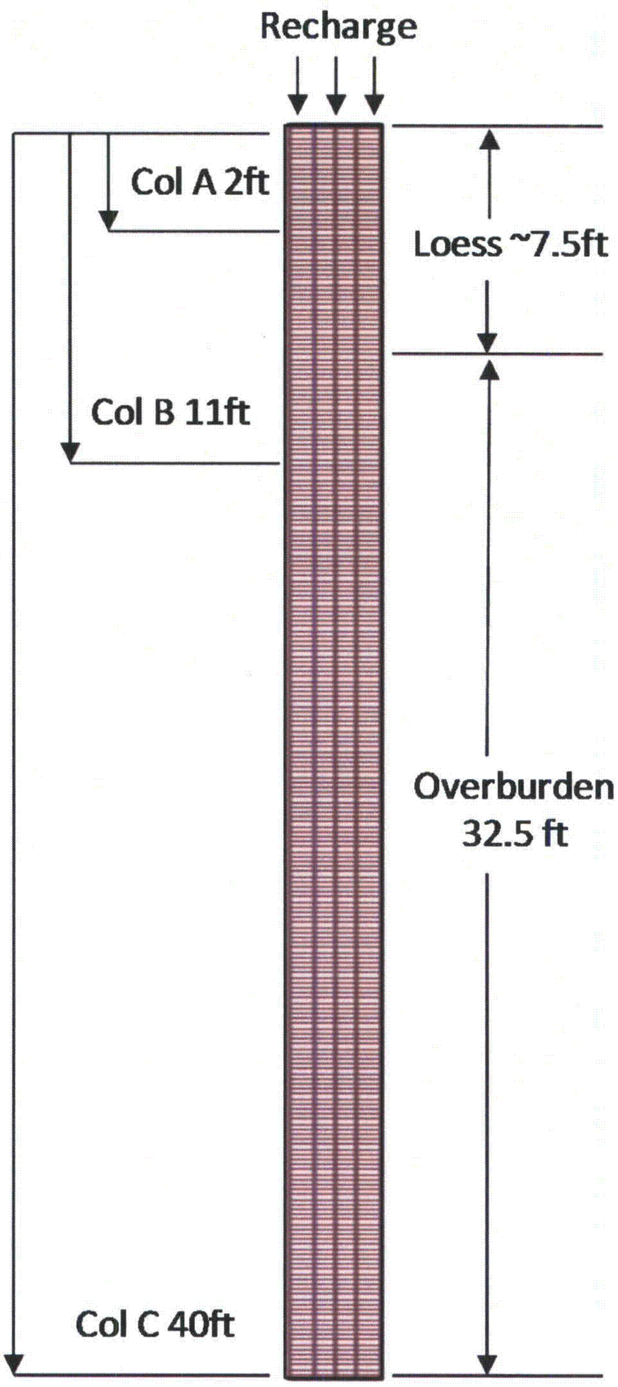

Figure 4-3. Schematic of Vadose Zone Column Model

conditions on the sides of the column, causing movement to be one-dimensional in a downward direction. The water table is simulated at the bottom of the column model. Therefore, a third type of boundary condition is imposed yielding a saturation of water of 1 and 0.1 megapascals (MPa) reference pressure to represent the water table. One boundary condition is applied to assess DU transport through the column model. A constant source concentration of 100 mg/L is imposed at the top of the column for the full simulation period.

4.4.3 Layer Properties

Table 4-4 describes the parameters used for the base case of the vadose zone column model., In the base case, the distribution ratio determined for the Avonburg/Cobbsfork soils from desorption testing (189 liters per kilogram [L/kg]) was used. The Avonburg/Cobbsfork soils represent the largest fraction (55 percent) of the soils at or near the surface within the DU Impact Area. Distribution ratios (R_d) determined from desorption testing are assumed analogous or representative of the K_d for DU in rainwater passing through impacted soils adjacent to and beneath DU penetrators. The R_ds are much lower than the K_ds determined for loess as described in Appendix D.

Table 4-4. FEHM Input Parameters
Jefferson Proving Ground, Madison, Indiana

FEHM Input Parameters	Value	Remarks
Column Width	6.56 ft	Total
Nodal Spacing (horizontal)	1.64 ft	Square
Column Height	40 ft	Ground surface to maximum depth to groundwater table
Nodal Spacing (vertical)	0.5 ft	
Reference Pressure	0.1 MPa	Zero datum
Reference Temperature	20 °C	
Maximum Saturation	100%	Fully saturated
Matrix Residual Saturation	20%	Carsel & Parrish (1988)
Boundary Condition (top of model)	4 in/y	From site-specific water budget calculations
Boundary Condition (bottom of model)	Saturation = 1	Vadose zone model
Van Genuchten Model Parameters	Inverse air entry head: 3.28 ft^{-1} Power in formula: 1.23	Parameters for the Silty clay loam Carsel & Parrish (1988)
Porosity	0.45	Kresic (2007)
Bulk Density	1.46 g/cm^3	Telford et al. (1990)
Distribution Coefficient (K_d)	189 L/kg	Minimum desorption K_d results
Decay/Half-Life	no decay	Assumed no decay for conservative estimate
Hydraulic Conductivity	Kx= Ky= 39.4 m/y Kz= 3.94 m/y	Aquifer testing (SAIC 2010)
Total Simulation Time for Flow Simulation	1.0E+09 days	Solve for steady-state flow field
Total Simulation Time for Transport Simulation	1,000 years	After flow field reaches steady-state

The spatial and vertical distribution of penetrators within the DU Impact Area is uncertain; use of the Avonburg/Cobbsfork R_d was selected because it does represent the largest fraction of soils at the surface, including the majority of the DU impact trench and is also the lowest R_d determined. Therefore, this base case is conservative (likely overestimates DU transport) in that it utilizes the lowest analogous K_d value determined for the impacted loess soils beneath penetrators and the base case also applies a continuous source at the surface of the model for the entire simulation. Inclusion of loess K_ds would result in the use of larger values for K_d within the transport model simulations.

The rest of the parameters used in the base case scenario are representative of average site conditions. A brief description of the parameters and important range of the parameters evaluated in sensitivity/uncertainty simulations are presented below. A more detailed description of the parameters can be found in Section 2.

4.5 MODELING RESULTS OF THE BASE CASE SIMULATION

The FEHM simulation results after 1,000 years of transport using the minimum distribution ratio determined from desorption tests (189 L/kg) indicate DU migration is predicted to be less than 40 ft BGS at the DU Impact Area, as shown in Figure 4-4. The FEHM model predicted DU contaminant at 2 ft (shallow water table), 11 ft (average water table), and 40 ft (maximum water table) are listed in Table 4-5 and shown in Attachment 2.

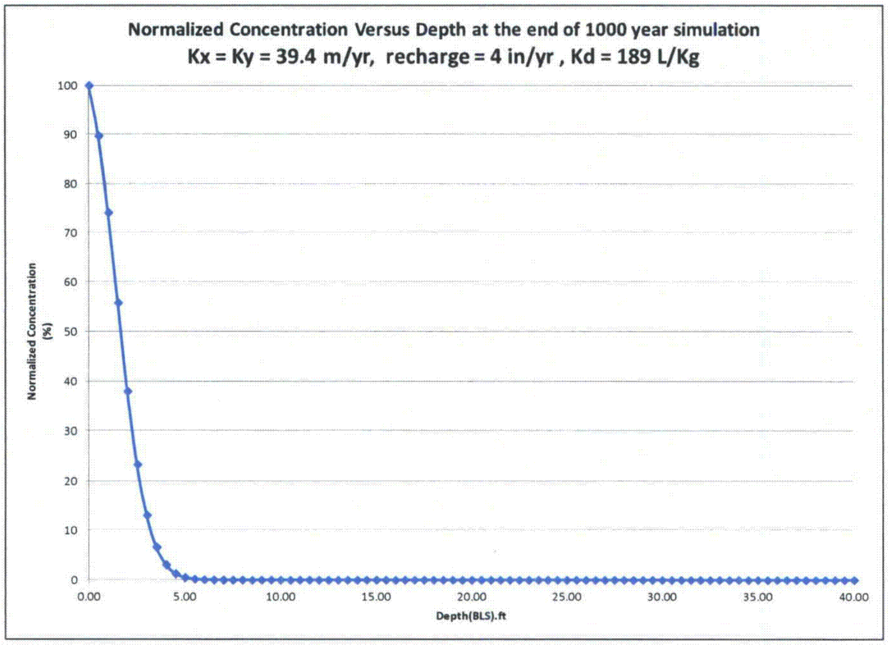

Figure 4-4. Base Case Results Showing Predicted Concentrations with Depth

Table 4-5. FEHM Model Predicted Percentage of Source Concentration at End of 1,000 Years Jefferson Proving Ground, Madison, Indiana

Type of Uranium	2 ft BGS	11 ft BGS	40 ft BGS
Percentage of source concentration	37.9	5.19 × 10^{-8}	DU will not migrate to this depth
Source held constant for simulated 1,000 years at ground surface)			

The FEHM model results indicate less than 40 ft of constituent migration using a constant source concentration at ground surface for the entire simulation period. With the conservative distribution ratio (189 L/kg) of DU contaminant in soil column, model results indicate DU never approached the depth of 40 ft in 1,000 years, due primarily to the observed low permeability of vadose zone materials, relatively low average recharge rate of 4 in/y, and the conservative distribution ratio utilized. As noted above, this distribution ratio is conservative (low) relative to the sorption coefficients determined for the loess soils, which are nearly an order of magnitude higher than the value used in the column modeling.

Column model results also show the maximum constituent concentrations at the end of the simulated 1,000 years were 37.9 and 3.19 × 10^{-8} percent of the source concentration at 2 and 11 ft BGS, respectively. Applying these results to the maximum observed soil contamination beneath a penetrator (40,694 pCi/g or 113,040 mg/kg), yields a predicted maximum concentration of less than 1.0 μg/L at 11 ft. This value represents the predicted leachate concentration from the soil column; the concentration will reduce further through mixing with underlying groundwater. Therefore, migration to the average groundwater depth does not represent a critical pathway for the base case scenario. Migration to depths of 2 ft beneath ground surface does produce elevated model-predicted leachate concentrations when using the maximum observed soil contamination levels as the starting concentration.

As described in the Decommissioning Plan (U.S. Army 2013), dose calculations utilized the weighted average sorption coefficients for the materials present within a representative soil column within the DU Impact Area (refer to Section 9 of Appendix E for calculation of the weighted average values). In the dose calculations, the primary and secondary contaminated zones represent the upper 3.3 ft (1 m) of the soil column and utilized a weighted average of 354 mL/g from the loess soil desorption-dissolution test results and the loess soil sorption weighted average of 2,116 mL/g beneath from 3.3 ft to 7.5 ft (the average depth to the loess/till contact in the DU Impact Area). The remainder of the soil column utilized the weight average of 6.4 mL/g determined from the glacial till sorption test results. Using these values in the soil column model results in less DU transport through the soil column. Column model results also show the maximum constituent concentrations at the end of the simulated 1,000-year period were 13.2 and 1.39×10^{-12} percent of the source concentration at 2 and 11 feet BGS, respectively, when using the weighted average sorption coefficients.

Model base case simulation results were compared against the maximum observed depth (4.5 ft) of DU migration. Applying a continuous source at the surface did not yield migration to 4.5-ft depth in 1,000-year simulation period, even with the lowest measured site-specific K_d value. Reproduction of 4.5 ft of migration in a 30-year period would require a K_d value of about 4 L/kg. The site-specific K_ds or R_ds determined for JPG soils at or near the surface are significantly greater indicating the value of 4 L/kg is not representative of conditions (transport through the soil column) within the DU Impact Area. Given the K_d values determined for the site, other factors may be contributing to the DU migration in the soil. One possibility consists of preferential pathways in the shallow subsurface soils due to biological (roots, burrows, etc.) or anthropogenic (munitions testing) conditions that permit slightly greater vertical migration than predicted in the base case scenario. Another possible explanation is that a particle or particles of DU fragments or corrosion product could have been carried down during sampling, which has been cited in previous studies as an explanation for observed anomalies in sampling data (Parkhurst et al. 2012).

The observed characterization data and column modeling results indicate leaching through the vadose zone to groundwater does not appear to be a significant migration pathway. Shallow groundwater near the creeks exhibits similar water levels and responses to storm events, which demonstrates a hydraulic connection (short travel path and travel time to the creeks). Model results do suggest the possible migration in shallow soils (generally a few feet beneath a penetrator). Model results do not indicate migration to the average depth of groundwater at the site. Predicted concentrations are less than 1.0 µg/L in the leachate concentration at the average depth to groundwater (11 ft).

4.6 SENSITIVITY ANALYSIS

The following six sensitivity analyses were conducted to assess the potential for leaching DU through the soil column to groundwater at the JPG site:

1. To assess the upper end of published hydraulic conductivity of loess soil type, the hydraulic conductivities were increased to 445 meters per year (m/y) (Kx = Ky) and 44.5 m/y (Kz).
2. To assess the sensitivity of hydraulic conductivity beyond upper range of published value, the hydraulic conductivities were increased to 4,450 m/y (Kx = Ky) and 445 m/y (Kz).
3. To assess the potential for leaching DU through the soil column at the lower end of published range of hydraulic conductivity for soil types at JPG, a run was completed mainly to

demonstrate the extent of migration at the lower end of representative hydraulic conductivity values.

4. Higher recharges were used to assess the potential for leaching DU to groundwater under increased recharge conditions.
5. A desorption value representative of 591 L/kg was used to assess the potential for leaching DU to groundwater in soils along drainages where Cincinnati-Rossmoyne soil types dominate. Since the soils are thinner here, predicted results were evaluated in the upper few feet of shallow soil.
6. A baseline simulation was conducted based on parameters in upper 7.5 ft underlain by till using laboratory K_d results for till (K_d = 1 L/kg) beneath Avonburg-Cobbsfork.

The results of the sensitivity analyses are summarized in Table 4-6. For details of the sensitivity analyses please refer to Attachment 3. The constituent concentrations at 2 ft BGS ranged from 89.7 percent for the 12 in/y recharge to 3.9 percent for a sorption (K_d) of 591 L/kg. The constituent concentrations at 11 ft BGS ranged from 8.66×10^{-3} percent for the 12 in/y recharge to never approached within the simulated 1,000-year test period for a sorption (K_d) of 591 L/kg. Similarly, the constituent concentrations at 40 ft BGS ranged from 1.96×10^{-4} percent for sorption of till (K_d = 1 L/kg) from 8 to 40 ft BGS (sensitivity analysis 6) to never approached within the simulated 1,000-year test period for all other sensitivity analyses.

4.7 UNCERTAINTIES IN MODELING SIMULATIONS

The largest uncertainties in the predictions for DU migration through the soil column for the JPG site are:

- DU contaminant distribution is assumed to be uniform throughout the column area. There exists a tremendous amount of uncertainty of the exact locations of individual penetrators and the respective geology. The investigation data also showed that the penetrators were not uniformly distributed (most clustered near impact trenches).
- The K_d value for near surface soils and loess above the glacial till was specified at the lowest site-specific value determined from desorption testing (i.e., maximizes migration rates).
- The model does not account for time-varying or transient conditions (e.g., seasonal high water table conditions that result in near surface reducing conditions, which in turn result in reduction and precipitation of DU in the soil matrix).
- Transport through preferential pathways is not accounted for in the modeling. Preferential pathways typically represent a small fraction of the soil volume and must intersect or occur in close proximity to penetrators for migration via preferential pathways.
- The source concentration was held constant for the 1,000-year duration of the modeling.

These assumptions result in a conservative overestimation of the DU concentration and mass in the subsurface and overestimation of the potential for migration.

Table 4-6. Summary of Sensitivity Analysis for FEHM Column Modeling Jefferson Proving Ground, Madison, Indiana

Sensitivity Run	Summary Description	Purpose/Objective	Sensitivity Model Result
1	Baseline properties except for hydraulic conductivity; increase hydraulic conductivity to 445 m/y (upper end of published value for loess soil types, also greater than upper end of slug test results for over burden/"till" materials; all other properties remain same	Assess potential for leaching through soil column to groundwater at upper end of published hydraulic conductivity.	With the observed minimum desorption distribution K_d value (189 L/kg) of DU contaminant in soil column, it is shown that the constituent never approached the depth of 40 ft in 1,000 years. It is also shown that the maximum constituent concentrations at the end of 1,000 years were 36.5% and 3.18×10^{-8} % at 2 and 11 ft BGS, respectively.
2	Baseline properties except for hydraulic conductivity; increase upper end of hydraulic conductivity by a factor of 10 over run # 1 above (hydraulic conductivity = 4450) m/y	Assess sensitivity of hydraulic conductivity beyond upper range of published value.	With the observed sorption (189 L/kg) of DU contaminant in soil column, it is shown that the constituent never approached the depth of 40 ft in 1,000 years. It is also shown that the maximum constituent concentrations at the end of 1,000 years were 35.2% and 9.60×10^{-9} % at 2 and 11 ft BGS, respectively.
3	Baseline properties except for hydraulic conductivity; reduce hydraulic conductivity to lower end of published hydraulic conductivity for loess/soil types to 2.2 m/y	Assess potential for leaching through soil column at lower end of published range of hydraulic conductivity for soil types at JPG. This run is mainly to demonstrate extent of migration at the lower end of representative hydraulic conductivity values.	With the observed sorption (189 L/kg) of DU contaminant in soil column, it is shown the constituent never approached the depth of 40 ft in 1,000 years. It is also shown that the maximum constituent concentrations at the end of 1,000 years were 38.6% and 7.89×10^{-8} % at 2 and 11 ft BGS, respectively.
4	Baseline properties except for recharge; increase recharge to 12 in/y	Assess potential for leaching to groundwater under increased recharge conditions	With the observed sorption (189 L/kg) of DU contaminant in soil column, it is shown that the constituent never approached the depth of 40 ft in 1,000 years. It is also shown that the maximum constituent concentrations at the end of 1,000 years were 89.7% and 8.66×10^{-3} % at 2 and 11 ft BGS, respectively.
5	Baseline properties except use K_d of 591 L/kg to represent Cincinnati-Rossmoyne for column	Assess the potential for leaching to groundwater in soils along drainages where Cincinnati-Rossmoyne soil types dominate. Since the soils are thinner here, the emphasis will be on the predicted results in the upper few feet.	With the sorption of 591 L/kg of DU contaminant in soil column, it is shown that the constituent never approached the depth of 11 ft in 1,000 years. It is also shown that the maximum constituent concentrations at the end of 1,000 years were 3.9% at 2 ft BGS.
6	Baseline properties for upper 7.5 ft, K_d 189, hydraulic conductivity = 39.4 m/y etc.; below 7.5 ft, use till properties as K_d = 1 L/kg to represent K_d for till beneath Avonburg-Cobbsfork soils. Hydraulic conductivity = 48.7 m/y was used for the till.	Assess potential leaching groundwater with baseline parameters in upper 7.5 ft underlain by till using laboratory K_d results for till beneath Avonburg-Cobbsfork.	With the sorption of 189 L/kg for upper 7.5 ft and 1 L/kg for the lower 32.5 ft of DU contaminant in soil column, it is shown that the maximum constituent concentrations at the end of 1,000 years were 37.9%, 1.5×10^{-3} %, and 1.96×10^{-4} % of source concentration at 2, 11, and 40 ft BGS, respectively.

5. GROUNDWATER FLOW MODEL

The soil to groundwater pathway discussion and results of the forward-looking FEHM model presented in Section 4 demonstrated limited potential migration of DU to groundwater, generally confined to within a few feet of land surface, very similar to empirical data trends for the last 30 years. The co-location of penetrators and shallow depth to groundwater are generally located within or near the creek valleys draining the DU Impact Area. Observed data indicate flow in these areas are generally to the streams, except in instances of high stream flow, where gradients may be reversed (locally near the streams) for the short periods of high flow (high stage) in response to precipitation events. In areas where the water table is deeper, observed data also indicate flow to the creeks. Therefore, groundwater from beneath the DU Impact Area is expected to discharge to the creeks within the former JPG boundaries. Observed site characterization data, including sampling results from various media indicate limited DU migration through the soil to groundwater.

The groundwater modeling at JPG comprises subsurface simulations designed to determine the potential for migration of DU within groundwater. Site-specific hydrogeologic properties and stratigraphy as described in the CSM setup are incorporated into a numerical framework in order to make predictions over time. The numerical model was then calibrated to a set of observed water level targets to numerically represent the subsurface flow at JPG. Transport simulation of DU within the groundwater beneath the DU Impact Area has not been performed at this time because observed site data are not indicative of a current impact, and predictive modeling results for migration through the soil column do not indicate impacts to groundwater. The model is constructed and capable of completing DU transport simulations should this be deemed necessary in the future.

5.1 MODEL DESIGN

The groundwater flow modeling approach is described in this section. Information on the development of the model with model domain selection, boundary condition estimates, and layer properties are described. Model calibration and sensitivity analysis results are then presented.

5.1.1 Model Selection and Description

The stratigraphy observed during well installation at JPG indicated the presence of fractures and secondary porosity in the shallow bedrock at the site, suggesting a code capable of simulating groundwater flow through fractures and secondary porosity features may be required. Simulation of flow and transport under these require additional characterization data (e.g., fracture distribution and characteristics), some of which are available. However, given the results from the column modeling and the observations of the shallow bedrock groundwater zone, initial efforts focused on simulating flow as an equivalent porous media.

The finite-difference numerical flow and transport simulator MODFLOW-SURFACT™ (HydroGeoLogic 1996) was used to perform the groundwater modeling for JPG. The model is a porous media code with capabilities to simulate dual porosity (if needed) to represent site conditions. Due to steeply incised stream banks at the site, MODFLOW-SURFACT (Version 4) was chosen over MODFLOW-2000 due to its ability to handle variably saturated model cells, alleviating MODFLOW-2000's convergence issues when dry cells are present.

5.1.2 Model Domain and Discretization

The area of interest for the groundwater modeling is the area around the DU Impact Area, where the DU source (DU penetrators and corrosion products) exists. Site maps and hydrologic features were examined to determine a model domain that would use as many natural boundary conditions as possible. The groundwater model domain is shown in Figure 5-1.

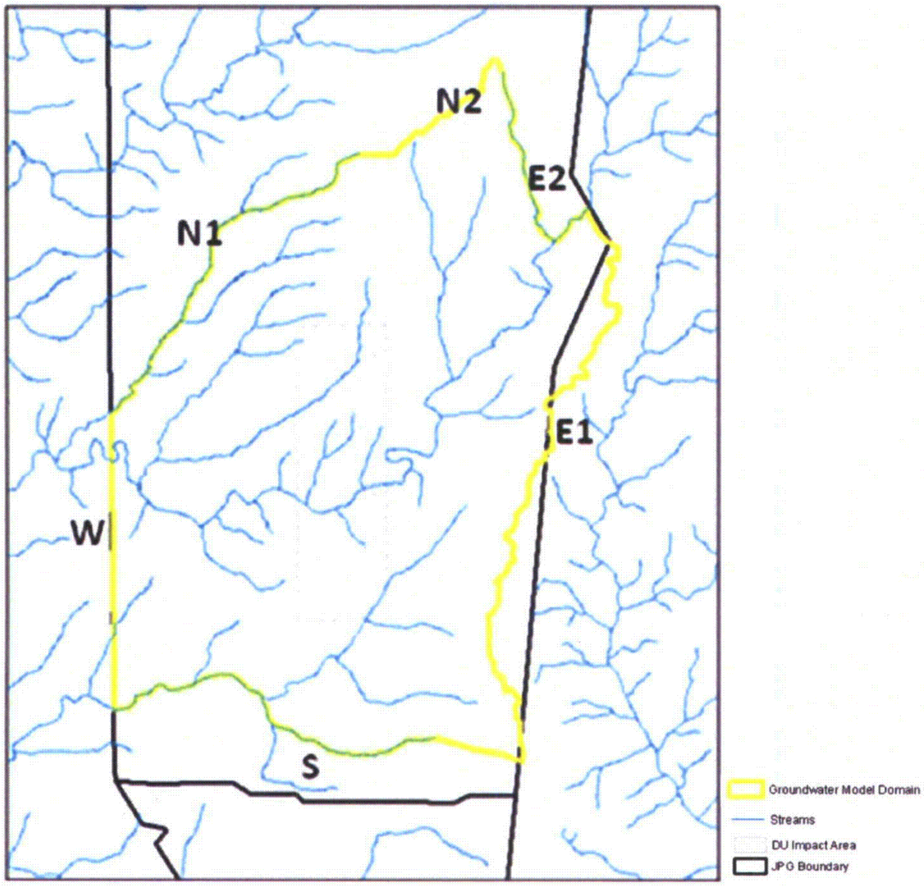

Figure 5-1. Groundwater Model Domain

The main portions of the north and south model boundaries are formed by creeks. The northern creek is an unnamed tributary to Big Creek while the southern boundary is formed by a tributary to Middle Fork Creek and Middle Fork Creek itself. Additionally, a portion of the eastern boundary follows another tributary to Big Creek. The remainder of the eastern boundary follows along the watershed sub-basin flow divides. Flow divides are typically used in groundwater models as they effectively act as no-flow boundaries where water enters into the model domain only from recharge and not from lateral flow into the model area from the adjacent basin. The western boundary of the model falls along the former JPG boundary and allows for assessment of potential groundwater migration off the former JPG. As this western boundary does not fall on a natural hydrogeologic boundary, a General Head Boundary (GHB) was chosen as a way to minimize the model size and computational requirements associated with extending the model to further down gradient natural boundaries.

The groundwater model consists of the two units that transmit water, the overburden and the shallow bedrock zone as seen in Figure 5-2. Evaluation of hydrographs and attempts to slug test (SAIC 2010) the deep bedrock wells indicated there is very limited or no connection between the deep and shallow bedrock zones. Therefore, a no-flow boundary is set at the base of the model (at the base of the shallow bedrock). This configuration forces all groundwater flow leaving the model domain to discharge to surface water bodies (creeks) or exit along the western model boundary. The overburden was modeled as a single model layer. However, based on observed site conditions, the shallow bedrock unit divided into two model layers (Layers 2 and 3).

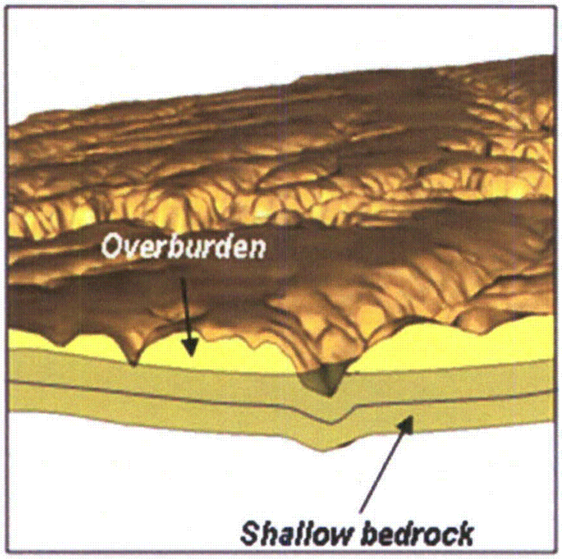

Figure 5-2. Water Bearing Units in Groundwater Flow Model

The numerical model was discretized using a finite difference grid. Grid dimensions were initially set at 100 by 100 ft using 420 rows, 320 columns, and 3 layers. Due to the irregularity of the domain, a large number of blocks are outside the model domain, resulting in 227,556 active cells.

5.1.3 Boundary Conditions

The boundaries are the locations that define the physical extent of the model. External boundary conditions (conditions on exterior boundaries of the model) describe the relationship between the modeled area and the surrounding area (e.g., to account for flow into the model from an adjacent nonmodeled area). Calculations are completed inside the domain, and the boundary supplies the interface with the model calculations and the known or presumed field conditions. Additionally, internal boundary conditions (within the interior of the model domain) exist within the model domain to account for entering or exiting streams.

5.1.3.1 External Boundary Conditions

Conditions are necessary at the top and bottom of the model as well as along the sides of each model layer. As the JPG model has varying boundary conditions based on layer number, after the discussion of the top and bottom boundaries, the layers will be presented separately. External boundary conditions include the following:

- The top and bottom boundary conditions are:
  - ***Top of Model***—The top of the model was set at ground surface, above the water table to account for the unconfined nature of the aquifer. In areas where shallow bedrock surfaces, inactive zones were instituted in Layer 1 of the model to account for the layer not being present. Recharge is applied to the uppermost active layer within the model.
  - ***Bottom of Model***—The bottom of the model was set as a no-flow boundary based on the previously presented hydrograph information. Flow within the deep bedrock is considered so low that the condition is considered realistic for the physical setting.

- Layer 1 Boundary Conditions (Figure 5-3):

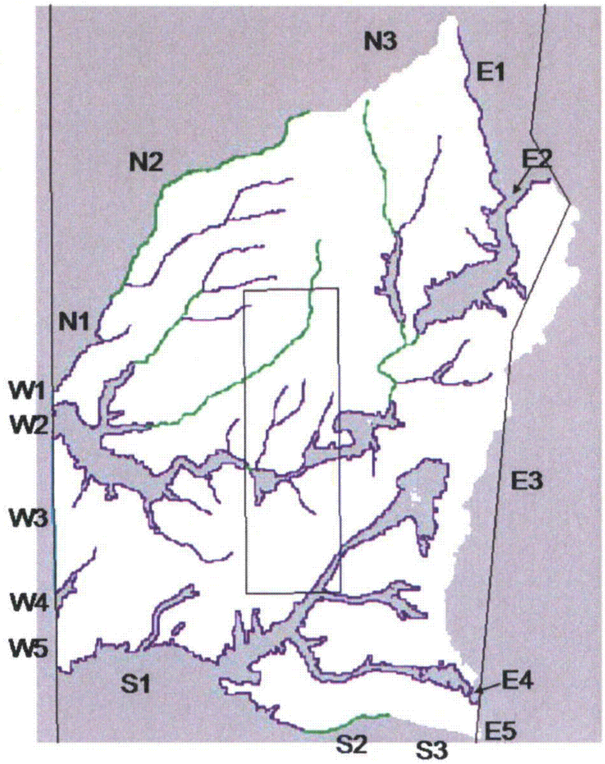

Figure 5-3. Layer 1 Boundary Conditions

- ***Northern Boundary***—Though the majority of the northern boundary lies along an unnamed tributary to Big Creek, a portion of this stream flows within the bedrock (Layer 2) of the model. Therefore, as described above, inactive cells exist in these areas (shown in gray). Drain cells (shown in purple) were used along these boundaries to allow for seepage out of the zone as depicted as N1 in the figure with the drain elevation set as the bottom elevation of the cell. The remainder of the stream (N2 – shown in green) is set as a river boundary condition that is set to the average river stage for the grid block. Based on field observations, an average width of 20 ft was assumed. The remainder of the northern boundary (N3) was considered no-flow as it follows the sub-basin divide. No groundwater flow into or out of the model is assumed at the flow divide.
- ***Eastern Boundary***—The majority of the eastern boundary (E3 and E5) was set as no-flow as it follows the sub-basin divide. One exception is a small portion of the boundary that follows an intermittent tributary of Big Creek (E1). Due to this intermittency, this portion of the boundary was set as a drain boundary condition that only allows for water to flow out of the model domain, with the drain elevation set as the average stream bottom elevation within the 100-ft grid block. The width of the drain was assumed to be 10 ft. Lastly, the portions marked as E2 and E4 are areas set as seepage faces due to bedrock surfacing in these areas.
- ***Southern Boundary***—Similar to the northern boundary, the southern boundary lies primarily along Middle Fork Creek, though a large portion of this creek flows within the bedrock layer. The areas depicted as S1 (purple) shows the seepage face nodes associated with this phenomena. The area shown as S2 (green) represents the stream segment that

flows within the overburden and is set as a river boundary condition. The river stage of Middle Fork Creek is set based on the average stage of the stream within the 100-ft grid block, with a width assumed to be 10 ft. Lastly, the area shown as S3 follows the sub-basin boundary and is considered a no-flow condition.

- *Western Boundary*—The majority of the western boundary, W1, W3, and W5 are set as a GHB based on the observed creek stage where Big Creek and Middle Fork Creek join together, the distance between the western model boundary and creek confluence, and the hydraulic conductivity associated with the overburden. The remaining zones (W2 and W4) are associated with the seepage faces along stream channels where the channels have cut down through the overburden to bedrock.

- Layer 2 Boundary Conditions (Figure 5-4):

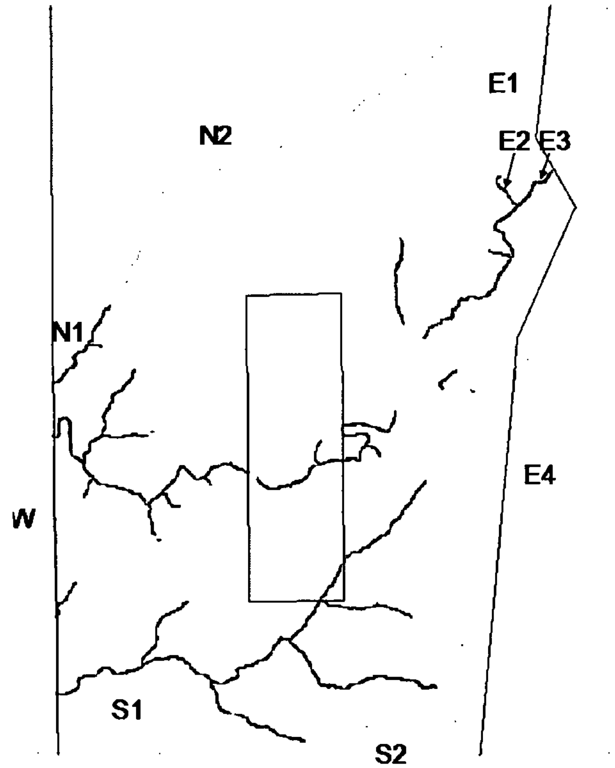

Figure 5-4. Layer 2 Boundary Conditions

- *Northern Boundary*—The location represented as N1 is the area set to a river condition to account for the portion of the unnamed Big Creek tributary that flows within the shallow bedrock. Similar to the Layer 1 northern boundary condition, the stage set as the average stage of the stream within the 100-ft grid block. The width of the river is assumed to be 20 ft. The area labeled N2 is set as a no-flow condition. This condition is used at the sub-basin divide as stated previously, but also is used in the areas directly below the streams. In the CSM description, flow in the shallow bedrock is assumed to discharge to the streams. Therefore, flow in these cell blocks should be directed vertically upwards, not allowing flow to move laterally through the boundary.

- *Eastern Boundary*—The area labeled E1 represents the no-flow condition associated with an area directly below a stream. Zones E2 and E3 represent the portions of streams that flow within the shallow bedrock. E2 is set as a drain based on the intermittent nature of the stream whereas E3 is set as a river based on its perennial nature. The stage for E2 is based on the average stream bottom within the grid block and assumes a width of 10 ft. E3 sets the stream stage based on the average stage within the grid block and assumes a width of 20 ft. Lastly, E4 is a no-flow condition based on the sub-basin divide.

- ***Southern Boundary***—This boundary is divided up into two sections, a river condition (S1) and a no-flow condition (S2). S1 is the portion of Middle Fork Creek that flows within the shallow bedrock. The stage is set based on the average stream stage within each 100-ft grid block and assumes a width of 10 ft. The S2 condition exists at both the sub-basin divide as well as the locations underneath the creeks.
- ***Western Boundary***—Similar to the western boundary for Layer 1, a GHB was used based on river confluences located to the west of the model.

- Layer 3 Boundary Conditions:
  - ***Northern, Eastern, and Southern Boundaries***—All but the western model boundaries are set as no-flow conditions at sub-basin flow divides or in the areas directly below the streams.
  - ***Western Boundary***—Similar to the western boundary for Layers 1 and 2, a GHB was used based on river confluences located to the west of the model. Stream stage and distance was approximated for the model runs.

5.1.3.2 Internal Boundary Conditions

Perennial and intermittent streams, including Big Creek and Middle Fork Creek exist within the model domain. Water level data indicate the streams have a large effect on the groundwater, and that shallow groundwater near the streams is in hydraulic connection with the streams. Two different types of boundary conditions were used based on the nature of the streams. Those that typically flow year-round were designated as river boundary conditions (i.e., allow simulated flow into and out of the groundwater model domain), while those that flow intermittently were set as drain boundary conditions (i.e., only allows flow out of the model domain).

Figures 5-3 and 5-4 show the setup within the model using green for river conditions versus purple for drain conditions for Layers 1 and 2 respectively. The locations of these rivers (Layer 1 or 2) were determined based on the bedrock surface. In some areas, streams flow within the overburden (Layer 1) while in others the streams have incised through the overburden and flow primarily on the bedrock surface (Layer 2). No internal boundary conditions are present in Layer 3.

For the river conditions, stream stage was set using the average stage over the length of the stream within each 100-ft grid block. Stream width on Big Creek and its tributaries was set at a width of 20 ft based on the relatively wide river beds associated with these stretches. Middle Fork Creek is typically much narrower; therefore, an average width of 10 ft was used in the model.

In the areas set as drain boundary conditions, an average drain elevation was used based on the stream within each 100-ft grid block. The conditions used on Big Creek and its tributaries assumed a width of 10 ft; a value of 5 ft was used for Middle Fork Creek drain cells.

5.1.4 Layer Elevations

The CSM was built using site-specific and reference information. The 100- by 100-ft grid was then applied to this model and nodal elevations were taken for land surface (top of Layer 1), top of shallow bedrock (bottom of Layer 1, top of Layer 2), and for bottom of shallow bedrock (bottom of Layer 3). The interface between Layers 2 and 3 was determined by dividing the total thickness of shallow bedrock in half. Areas where Layer 1 is not present were set as inactive zones. Minimum, maximum, and average elevations for the different horizons can be seen in Table 5-1. Average or representative parameters (e.g., hydraulic conductivity) are assigned to each layer, then adjusted during model calibration. The range of various input parameters has been described in the preceding sections of this report. Therefore, only the final calibrated values will be presented (see Section 5.2).

Table 5-1. Layer Elevation Summary
Jefferson Proving Ground, Madison, Indiana

Layer	Minimum Elevation (ft)	Maximum Elevation (ft)	Average Elevation (ft)
Top of Overburden (L1)	794.81	906.44	865.25
Top of Bedrock (L2)	756.83	873.23	830.35
Bottom of Bedrock (L3)	726.92	832.92	790.36

5.2 FLOW CALIBRATION

Groundwater flow calibration is the process of adjusting model input parameters within observed or published values to match a set of conditions (calibration targets). For JPG, groundwater flow calibration was completed under assumed steady state conditions, which can be thought of as long-term average conditions. Calibration targets under steady state conditions consist of long-term average water levels, a water budget error of less than 1 percent, and a qualitative match with observed or expected flow conditions. Key assumptions pertaining to the groundwater model include:

- Measured site data are representative of conditions within the groundwater model domain for the period of simulation
- Fractures are interconnected such that the assumption of equivalent porous media applies at the scale of the model grid blocks (cells)
- Shallow bedrock hydraulic conductivity decreases with depth (fracture density and secondary porosity features within the bedrock decrease with depth)
- The interaction of groundwater between the shallow and deep bedrock is negligible and the boundary between the two can be simulated as a no-flow boundary
- Topographic divides mimic shallow groundwater flow divides, and thus represent no-flow boundaries.

5.2.1 Groundwater Calibration Targets

Observed groundwater elevation data, both point measurements and continuous recorder data were examined for selection of calibration targets. Ideally, the target dataset would consist of a complete round of measurements representing near average conditions. The period of record onsite in the DU Impact Area covers a short period of time and includes a significant decline in water levels in the spring through late summer of 2008 followed by recovery in water levels. This short period of time and observed variability makes determination of water level data representative of long-term average conditions difficult. Data from February 2009 were selected as calibration targets because water levels appeared close to average conditions and a complete round of water level data was available.

Longer term groundwater level data are available from the USGS for a well located about 2 mi west of the main gate at the former JPG (USGS 2013). The well is completed in the carbonate bedrock with first open interval at 36 ft BGS and a total well depth of 200 ft. Daily water level measurements are available from this well from October 1984 through May 2013. Water levels fluctuate from about 3 to 10 ft BGS with an average depth to groundwater of 6 ft BGS for the period of record. In the USGS data, water levels measured in February 2009 were 6.9 ft BGS, close but slightly deeper than average groundwater levels.

Therefore, the calibration target dataset from February 2009 site measured data are also believed to be close to average conditions, possibly below average water level conditions. Based on the USGS data, the February 2009 dataset could be about a foot below average water level conditions, assuming trends and conditions observed in the USGS data can be applied to conditions observed at the DU Impact Area.

Not all wells were used in the calibration target dataset. Some wells were located close to the streams and based on the grid spacing within the model, were located directly on boundary condition cells. Therefore they were removed. The remaining calibration targets are shown in Table 5-2.

Table 5-2. February 2009 Calibration Targets
Jefferson Proving Ground, Madison, Indiana

Overburden Well Calibration Targets		Shallow Bedrock Well Calibration Targets	
Well	Target Water Level (ft)	Well	Target Water Level (ft)
JPG-DU-03O	854.22	JPG-DU-01I	833.94
JPG-DU-04O	851.2	JPG-DU-02I	784.18
JPG-DU-06O	864.3	JPG-DU-04I	851.11
JPG-DU-09O	833.06	JPG-DU-06I	859.94
MW-6	852.6	MW-RS-2	868
MW-RS-3	871.62	MW-1	841.81
MW-RS-4	855	MW-2	837.91
MW-RS-5	848.08	MW-5	783.55
MW-RS-6	849.45	MW-11	802.2
MW-RS-7	850.87	--	--
MW-RS-8	859.79	--	--

Model calibration was performed by adjusting hydraulic conductivity and recharge within the range of observed site data. Where specific hydraulic conductivity measurements were known from site-specific testing, these values were placed in the model. Through a series of calibration runs varying the two parameters, a final grid of conductivity values (for all three layers) as well as for recharge was determined that gave the best fit to the data.

The modeled domain covers an area much larger than the DU Impact Area, where most of the site-specific data on parameter values exists. In areas outside the DU Impact Area where limited site-specific data are available (e.g., overburden thickness, shallow bedrock thickness, conductivity and recharge), some variations were seen in the calibrated parameters due to uncertainties in site-specific parameter values.

5.2.2 Hydraulic Conductivity

The calibrated hydraulic conductivity distribution for the overburden layer (Layer 1) is shown in Figure 5-5. The conductivity varies from 0.7 ft/day to 6 ft/day based on calibration to the target water levels. Much of the model domain is set to a value of 1 ft/day, which is at the high end of the hydraulic conductivity determined for the overburden from testing (both within the DU Impact Area and south of the firing line). Based on the grid spacing of 100 by 100 ft, it was not always possible to capture the conductivity values from slug testing, as they are considered to be "near well" values and do not typically reflect areas as large as the model grid blocks or cells. However, whenever possible (such as with JPG-DU-04O and -06O), the data were incorporated.

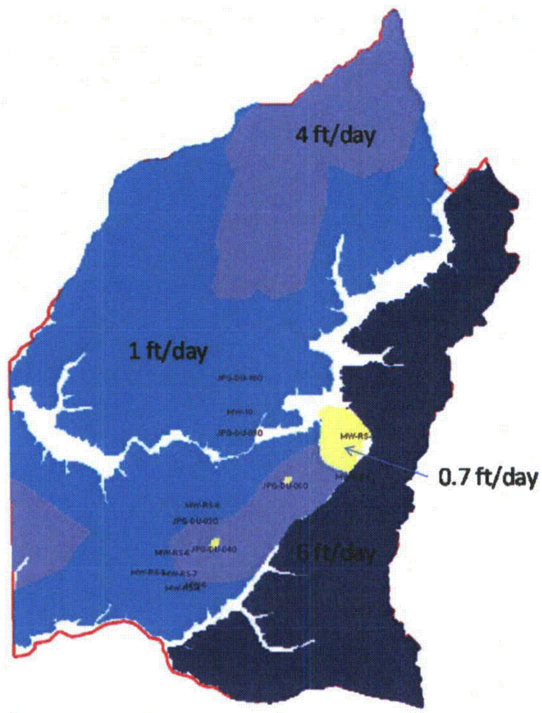

Figure 5-5. Layer 1 Hydraulic Conductivity Distribution

The areas outside the DU Impact Area have larger uncertainties associated with them than areas within due to limited site-specific data. As a result, the area along the eastern boundary (and to some extent the northern boundary), experienced high water tables that created ponding within the model. To reduce this affect, the hydraulic conductivity was increased to allow more water movement out of the zones. Values of hydraulic conductivity, and recharge were chosen that minimized the amount of ponding at the surface and still met the calibration criteria. Overburden thickness, depth to groundwater, and hydraulic conductivity has not been measured in these areas.

The hydraulic conductivity for Layer 2 is presented in Figure 5-6. A value of 2 ft/day was used for the majority of the model, simulating a more highly conductive zone in the upper portion of the shallow bedrock where fracturing and a higher degree of weathering exist. Three smaller zones were included within the model having a conductivity value of 0.07 ft/day. These zones had slug tests that showed little or no recovery or showed no signs of weathering in bore logs. Similar to Layer 1, not all slug test values were specified at the location of measurement (including no/slow recovery) due to the coarse grid used in the model.

The hydraulic conductivity for Layer 3 is shown in Figure 5-7. A value of 0.707 ft/day was used for the majority of the model domain, based on the average value of conductivity for shallow bedrock. For consistency, the same three low conductivity zones in Layer 2 were incorporated into Layer 3.

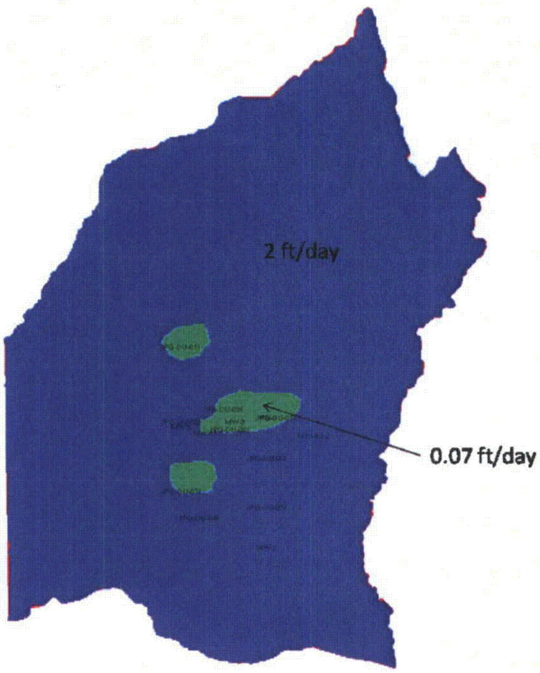

Figure 5-6. Layer 2 Hydraulic Conductivity Distribution

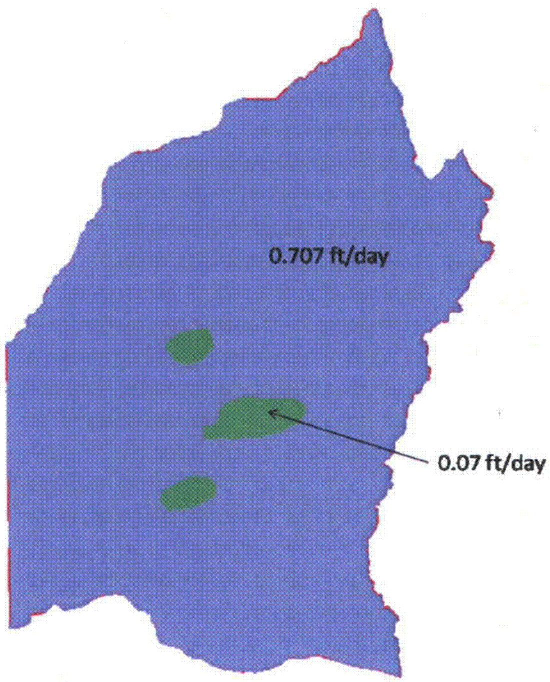

Figure 5-7. Layer 3 Hydraulic Conductivity Distribution

5.2.3 *Recharge*

The calibrated recharge rate for a majority of the model domain was 3 in/y as seen in Figure 5-8. This value is at the low end of the expected range for the site and may reflect the influence of slightly lower than average water levels in the February 2009 data set. Calibrated hydraulic conductivities are at the high end of the range in observed values. However, at the scale of the model (100- by 100-ft cell spacing), the calibrated hydraulic conductivity values may be under predicted and contribute to the lower calibrated recharge values. Areas along the streams were either removed (boundary condition cells) or reduced to a value of 1.2 in/y to accommodate the groundwater/surface water environment where rainfall quickly becomes surface water flow rather than migrating and remaining within the underlying groundwater.

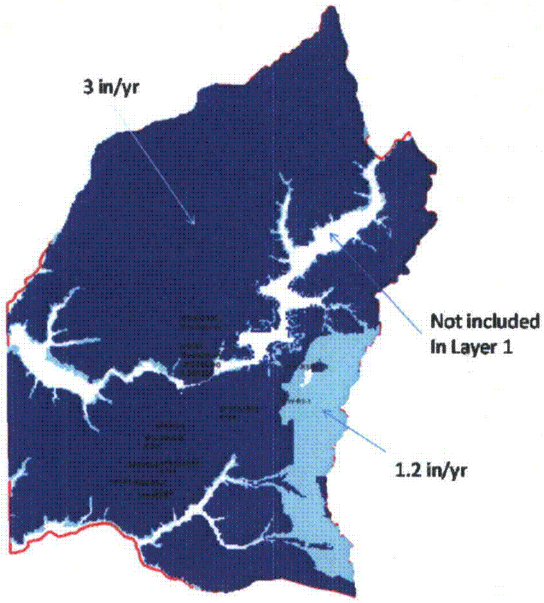

Figure 5-8. Model Recharge Distribution

5.2.4 *Calibration Results*

Flow model calibration results show groundwater flow generally to the southwest with steep gradients existing in the vicinity of the streams, consistent with observed conditions (Figure 5-9). Comparison of observed water levels (February 2009 calibration targets) against modeled targets showed an absolute residual mean of 3.3 ft with a standard deviation of 4.1 ft. Plotting observed water levels versus simulated water levels (Table 5-3 and Figure 5-10) generated a line with slope of almost exactly 1 and an r-squared of 0.97 (note that "perfect calibration would have all data fall on a line with slope of 1 and r-squared of 1).

Review of the model water budget shows a budget error much less than one percent with calculated water flow into the model essentially the same as the calculated water flow out of the model. Nearly all of the water that enters the groundwater discharges to the streams with less than 0.5 percent exiting the model domain through the model boundary. The amount of groundwater discharging to streams (sum for all streams across the model area) is calculated at 5.5 cubic feet per second (cfs) under the simulated steady state flow conditions. Examining groundwater flow beneath the main DU Impact Area trench on 500 Center line of fire shows discharges to both Big Creek (0.09 cfs) and Middle Fork Creek (0.05 cfs).

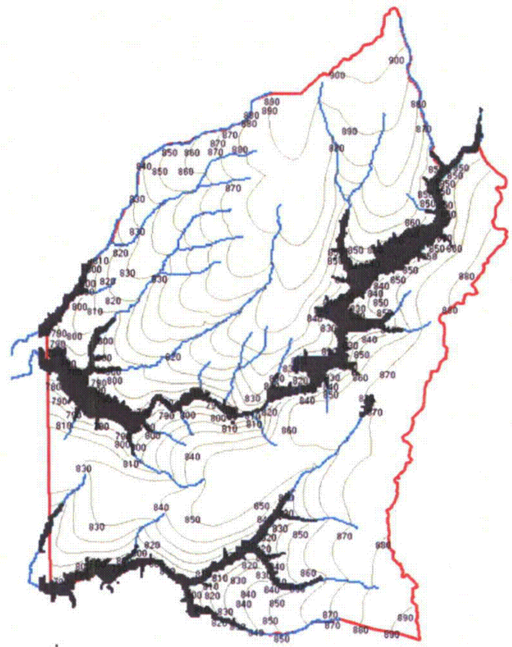

Figure 5-9. Modeled Groundwater Elevations in Layer 1

Table 5-3. Calibration Statistics
Jefferson Proving Ground, Madison, Indiana

Well	Layer	Observed	Computed	Residual
JPG-DU-03O	1	854.22	855.304	-1.08402
JPG-DU-04O	1	851.2	856.0196	-4.81961
JPG-DU-06O	1	864.3	861.3662	2.93385
JPG-DU-09O	1	833.06	833.3603	-0.30029
MW-6	1	852.6	850.204	2.39601
MW-RS-3	1	871.62	868.9605	2.659492
MW-RS-4	1	855	848.4247	6.575279
MW-RS-5	1	848.08	842.7465	5.333538
MW-RS-6	1	849.45	848.5888	0.861188
MW-RS-7	1	850.87	851.3176	-0.44759
MW-RS-8	1	859.79	851.3051	8.484871
JPG-DU-01I	2	833.94	837.3873	-3.44733
JPG-DU-02I	2	784.18	787.1603	-2.98027
JPG-DU-04I	2	851.11	855.9864	-4.87635
JPG-DU-06I	2	859.94	861.3143	-1.37434
MW-11	2	802.2	803.509	-1.30901
MW-2	2	837.91	840.201	-2.29103
MW-5	2	783.55	791.6238	-8.0738
MW-RS-2	2	868	867.7902	0.209831
MW-1	2	841.81	846.5005	-4.69046

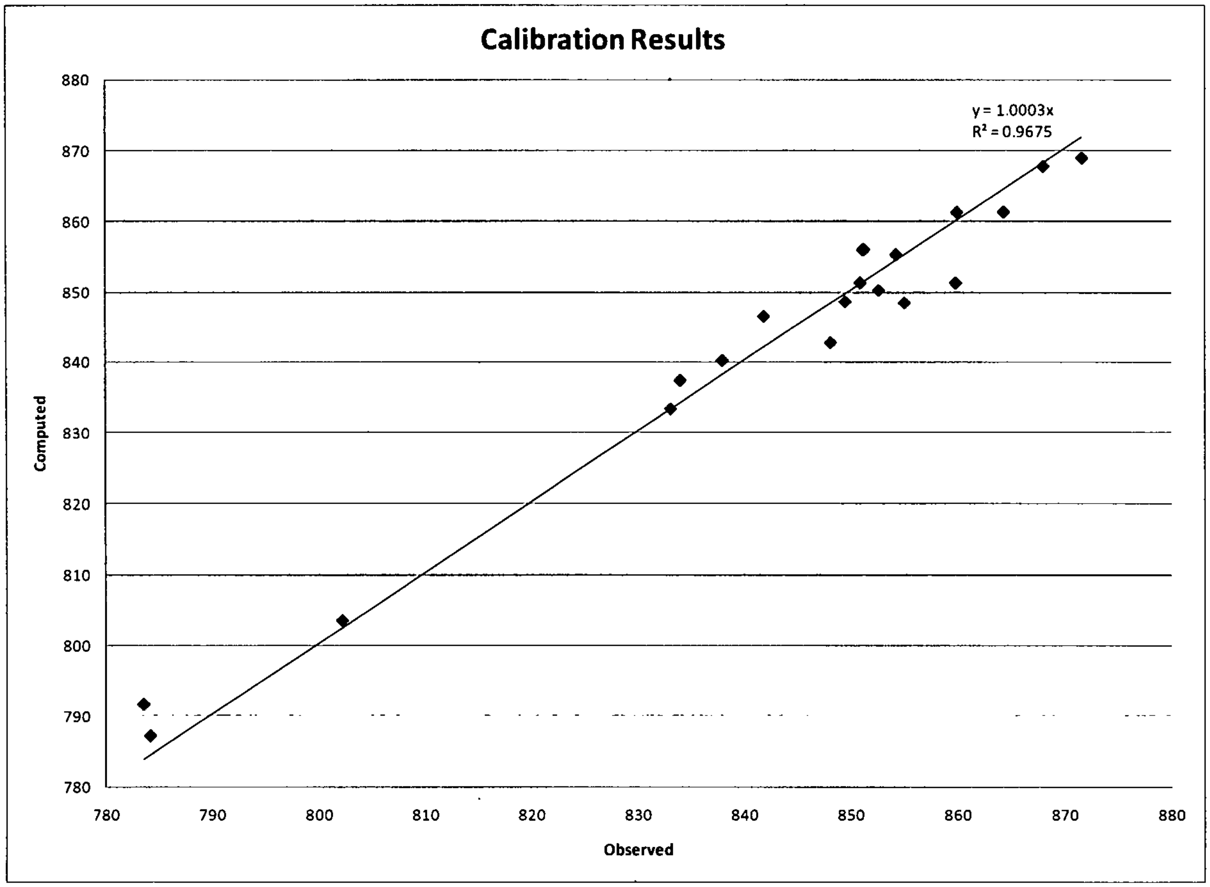

Figure 5-10. Observed Versus Modeled Water Levels

5.3 MODEL UNCERTAINTY AND SENSITIVITY ANALYSIS

Uncertainty in model calibration or predictive scenarios arises from variability within model input parameters and boundary conditions used to define the model domain. In groundwater flow modeling, hydraulic conductivity and recharge typically have the greatest influence on model predictions. The distribution of hydraulic conductivity within the model domain is approximated from a limited number of observations, which vary over several orders of magnitude. Groundwater recharge is difficult to measure and also varies spatially depending upon land cover and near surface soils. Other parameters that typically impart uncertainty into model results include stream bed conductance (used to quantify the amount of groundwater-surface water interactions), the no-flow lower model boundary within the carbonate bedrock, and the assumption of steady-state flow conditions to name a few. Based upon the available information, the groundwater pathway for DU transport is negligible, and therefore, a rigorous evaluation of model uncertainty was not completed.

A sensitivity analysis (Attachment 3) was conducted for the horizontal hydraulic conductivity (Kx = Ky), the vertical hydraulic conductivity (Kz), and the recharge rate. The calibrated values for Kh, Kz, and recharge were multiplied by 0.1, 0.50, 1.0, 2, and 10 to ascertain the effects on the model flow solution.

Results are presented in Attachment 3 in the form of graphs of sum of squared residuals (SSR), a measure of the overall error in model calibration) versus parameter multiplier for each parameter. The most sensitive parameters are those with the greatest change in the SSR when the parameter value is adjusted away from the provisionally calibrated value, which is designated by a parameter multiplier of 1.0 in Attachment 3.

Within the multiplier range considered, the sensitivity analysis reveals that model calibration is sensitive to horizontal conductivity and recharge of zone 1. The model is only slightly sensitive to vertical hydraulic conductivity (Kz). The SSR curves are, in general, at a minimum at the base (1.0) multiplier value, indicating that further significant improvement of model calibration cannot be achieved by adjusting parameter values individually.

6. GROUNDWATER MODELING SUMMARY AND CONCLUSIONS

The groundwater pathway was evaluated through modeling using FEHM to simulate groundwater flow and potential for DU transport through the soil column to groundwater. The groundwater flow system beneath JPG was modeled using MODFLOW-SURFACT. Modeling results indicate limited potential for DU migration via the groundwater pathway. Observed uranium sampling results in the environmental media at JPG show limited migration of DU in shallow soils and essentially no evidence of DU migration to groundwater away from surface water bodies. Low uranium concentrations observed near creeks may be the result of creek-groundwater interactions or shallow migration in soils near the creeks and are not necessarily indicative of migration via the groundwater pathway.

6.1 SOIL TO GROUNDWATER RESULTS

Model predictions using FEHM indicate very limited migration to groundwater within 1,000 years based on observed site conditions and conservative input parameters like source DU concentration and (lowest) distribution coefficients (desorption K_d) determined from site-specific testing.

- Migration to groundwater may occur where the water table is shallow (~2 to 4 ft BGS). Shallow groundwater typically occurs in areas near streams.
- Migration to groundwater does not occur through the overburden at average depths to groundwater (11 ft BGS), nor at the depths typical of overburden near the bulk of remaining penetrators (30 to 40 ft BGS).

6.2 GROUNDWATER FLOW RESULTS

The groundwater flow model was developed and calibrated to February 2009 measured water levels. The groundwater contribution to streams within the model domain is 5.5 cfs distributed across all of the streams in the model domain.

- The volume of groundwater discharge to Big Creek from the area beneath the DU Impact Area trench is 0.09 cfs.
- The volume of groundwater discharge to Middle Fork Creek from the area beneath the DU Impact Area trench is 0.05 cfs.

Nearly all (99.5 percent) groundwater exiting the model domain does so by discharge to streams; 0.5 percent of groundwater exiting the model domain does so at the western model boundary.

THIS PAGE WAS INTENTIONALLY LEFT BLANK

7. REFERENCES

Bechert, C.H. and J.M. Heckard. 1966. In Lindsey, A.A., ed, Natural features of Indiana: Indianapolis, Indiana Academy on Science, p. 100-115.

Carsel, R.F., and R.S. Parrish. 1988. Developing joint probability distributions of soil water retention characteristics. Water Resources Research, 24(5):755-770.

Chen, J.P., and S. Yiacoumi. 2002. Modeling Of Depleted Uranium Transport In Subsurface Systems, Water, Air, and Soil Pollution 140: 173–201. © 2002 Kluwer Academic Publishers. Printed in the Netherlands. Received 28 March 2001, accepted 22 January 2002.

Clulow F.V, N.K. Dave, T.P. Lim, and R. Avadhanula. 1998. Radionuclides (lead-210, polonium-210, thorium-230, and thorium-232) and thorium and uranium in water, sediments, and fish from lakes near the city of Elliot Lake, Ontario, Canada. Environmental Pollution 99(2), 199-213.

Cramp, T.J., Y.S. Cuff, A. Davis, and J.E. Morgan. 1990. (Reported in Royal Society 2002). Review of Data for Uranium, Nickel, and Cobalt. Report 2150-R1. Associated Nuclear Services, Epson.

DOE (U.S. Department of Energy). 2000. Guide of Good Practices for Occupational Radiological Protection in Uranium Facilities, DOE-STD-1136-2000, U.S. Department of Energy. August.

Dushenkov S., D. Vasudev, Y. Kapulnik, D. Gleba, D. Fleisher, K.C. Ting, and B. Ensley. 1997. (Reported in Royal Society 2002). Removal of Uranium from water using terrestrial plants. Environmental Science & Technology 31(12), pp. 3468-3474.

Edenspace (Edenspace Systems Corporation). 2004. Phytoremediation of Depleted Uranium in an Arid Environment.

Erikkson, A. and S. Evans. 1983. (Reported in Royal Society 2002). Uranium, thorium and radium in soils and crop s-calculations of transfer factors. Swedish Nuclear Fuel and Waste Management Co. (SKB). Stockholm, Sweden.

Franzmeier, D.P., G.C. Steinhardt, and D.G. Schulze. 2004. Indiana soil and landscape evaluation manual. Ay-323. Version 1.0. Purdue Univ. Coop. Extension Service, West Lafayette, Indiana 47907. 72p.

Freeze, R.L. and J.A. Cherry. 1979. Groundwater. Prentice-Hall, Inc., Englewood, New Jersey 07632.

Gray, H.H. 2001. Miscellaneous Map 69 modified from Gray, H.H. 2000. Physiographic Divisions of Indiana, Indiana Geological Survey Special Report 61, Plate 1.

Health Physics Society. Internet Website: http://hps.org/publicinformation/radterms/radfact116.html.

Herring, W.C. 2004. Karst Features and the Dissolution of Carbonate Rocks in Jefferson County. Division of Water, Resource Assessment Section. April.

Hu MZ-C, J.M. Norman, and B.D. Faison. 1996. (Reported in Royal Society 2002). Biosorption of uranium by *pseudomonas aeruginosa* strain CSU: characterization and comparison studies. Biotechnol Bioeng 51, 137-167.

HydroGeoLogic, Inc. 1996. MODFLOW-SURF (Version 1.2). The HydroGeoLogic Enhanced Version of the U.S. Geological Modular Groundwater Flow Model, Code Documentation Report. Copyright © 1996, by Hydrogeologic, Inc. All Rights Reserved.

Kresic, N. 2007. Quantitative Solutions in Hydrogeology and Groundwater Modeling, Second Edition. LAW Engineering and Environmental Services, Inc. © 1997 by CRC Press LLC. Lewis Publishers is an imprint of CRC Press.

Lattman, L.H. 1958. Technique of mapping geologic fracture traces and lineaments on aerial photographs: Photogrammetric Engineering, Vol. 84, p. 568-576.

MWH (Montgomery Watson Harza). 2002. Draft Final Remedial Investigation, JPG. Prepared for USACE Louisville District under Contract DACW27-97-D-0015, Task Order 008. March.

NRC (Nuclear Regulatory Commission). 1996. Press release dated May 13, 1996, NRC ADAMS accession number ML003705136.

Parkhurst, M.A., K.M. Krupka, K.J. Cantrell, J.A. Glissmeyer, S.P. Shelton, E.W. Morgan, and S. Mattigod. 2012. Final Report Review of Depleted Uranium Soil Contamination and Environmental Migration: Oxide Generation, Characteristics, and Dispersion. Prepared for the U.S. Army Institute of Public Health by Battelle Memorial Institute Pacific Northwest National Laboratory, July.

Ridge, Christanne. 2007. Prefiled Testimony of A. Christianne Ridge before the Atomic Safety and Licensing Board of the United States of America Nuclear Regulatory Commission, Docket No. 40 8838-MLA, pp. 17-18. August 17.

Royal Society. 2001. The Health Hazards of Depleted Uranium Munitions Part 1. May.

Royal Society. 2002. The Health Hazards of DU Munitions Part II. March.

Rust E&I (Rust Environment and Infrastructure). 1994. JPG South of the Firing Line Final Draft Remedial Investigation (Phase I). Prepared for USAEC, Aberdeen Proving Ground, Maryland. July.

Rust E&I. 1998. JPG South of the Firing Line Phase II Draft Remedial Investigation. Prepared for USAEC, Aberdeen Proving Ground, Maryland. August.

SEC Donahue, Inc. 1992. Letter Report of Site Specific Sampling and Analysis Program Results. Prepared for U.S. Army Toxic and Hazardous Materials Agency. August.

Scientific Ecology Group (SEG) 1995. Jefferson Proving Ground Depleted Uranium Impact Area Scoping Survey Report. Volume 1, Survey Report. March.

SEG. 1996. Jefferson Proving Ground Depleted Uranium Impact Area Characterization Survey Report. Volumes 1 and 2. Oak Ridge, Tennessee. February.

SAIC (Science Applications International Corporation). 1997. Base Realignment and Closure Cleanup Plan. Version 3. Prepared for the U.S. Army Environmental Center (USAEC) under Contract DACA31-94-D-0066, DO 0001. June.

SAIC. 2002. Environmental Report, JPG, Madison, Indiana. Prepared for the U.S. Army SBCCOM. June.

SAIC. 2006a. Fracture Trace Analysis. Submitted to U.S. Department of Army Installation Support Management Agency Aberdeen Proving Ground, Maryland. June.

SAIC. 2006b. Deer Tissue Sampling Report. Prepared for the U.S. Department of Army and U.S. Army Corps of Engineers under Contract W2912QR-04-D-0019, DO 017.

SAIC. 2007. Well Location Selections Report. Prepared for the U.S. Department of Army and U.S. Army Corps of Engineers under Contract W912QR-04-D-0019, DOs 0012 and 0017.

SAIC. 2008. Well Construction and Surface Water Data Report. Prepared for U.S. Department of Army and U.S. Army Corps of Engineers under Contract DACW62-03-D-0003; DO CY07.

SAIC. 2010. Slug Testing Report, Depleted Uranium Impact Area Site Characterization: Aquifer Testing for Hydraulic Conductivity, Jefferson Proving Ground, Madison, Indiana. Final. Prepared for U.S. Department of Army, Installation Support Management Activity, 5183 Blackhawk Road, Aberdeen Proving Ground, Maryland 21010-5424 and U.S. Army Corps of Engineers, Louisville District, 600 Dr. Martin Luther King, Jr. Place, Louisville, Kentucky 40202-2230. Submitted by Science Applications International Corporation (SAIC), 12100 Sunset Hills Road, Reston, Virginia 20190 under Contract No. DACW62-03-D-0003, Delivery Order No. CY07. August.

SAIC. 2013. Radiation Monitoring Report for License Sub-1435 Jefferson Proving Ground Summary of Results for the March-April 2012 Sampling Event, Final. Submitted to: U.S. Department of Army U.S. Army Garrison, Rock Island Arsenal, Rock Island, Illinois. January.

SEG. 1996. Jefferson Proving Ground Depleted Uranium Impact Area Characterization Survey Report, Vol. 1 and 2. Scientific Ecology Group, Inc., Radiological Engineering and Decommissioning Service, February.

Sheldon, R. 1997. Jefferson Proving Ground Karst Study. Report to Jefferson Proving Ground, unnumbered pages.

Telford, W.M, R.E. Sheriff, and L.P. Geldart. 1990. Applied Geophysics, Second Edition. © Cambridge University Press.

The Weather Channel. 2013. Temperature data obtained from http://www.weather.com/weather/wxclimatology/monthly/USIN0386.

Thomas, P.A. 2000. (reported in Royal Society 2002). Radionuclides in the terrestrial ecosystems near a Canadian uranium mill – Part 1: Distribution and doses. Health Physics 78(6), 614-624.

USATHAMA (U.S. Army Toxic and Hazardous Materials Agency). 1988. Remedial Investigation at Jefferson Proving Ground, Technical Plan Data Item A005. Environmental Science and Engineering, Inc., Gainesville, Florida 32602. May.

U.S. Army. 1995. Health and Environmental Consequences of Depleted Uranium Use in the U.S. Army: Technical Report. June.

U.S. Army. 2000. Memorandum of Agreement between the U.S. Army, U.S. Air Force, and U.S. Fish and Wildlife Service.

U.S. Army. 2001. Controlled Burn Air Sampling Technical Report. Aberdeen Proving Ground. August.

U.S. Army. 2002. Decommissioning Plan for License Sub-1435, Jefferson Proving Ground, Madison, Indiana. June.

U.S. Army. 2013. Decommissioning Plan for Materials License SUB-1435, Depleted Uranium Impact Area, Jefferson Proving Ground, Madison, Indiana. August.

U.S. Census Bureau. 2010. U.S. Census Bureau, State and County Quickfacts. U.S. Census Bureau Website. http://quickfacts.census.gov/qfd/states/18000.html.

USACE (U.S. Army Corps of Engineers). 1995. Archives Search Report for Ordnance and Explosive Waste, Chemical Warfare Materials, Jefferson Proving Ground, Madison, Indiana; Volume 1 – Records Review and Interviews. Prepared by U.S. Army Corps of Engineers, St. Louis District. June.

USDA NRCS (U.S. Department of Agriculture Natural Resources Conservation Service). 1999. Soil Taxonomy: A basic system of soil classification for making and interpreting soil surveys. 2nd edition. USDA NRCS Handbook 436.

USDA NRCS. 2005. Soil Survey Geographic Database (SSURGO) for Jefferson County, Indiana – Interim Product, SV 2.7.

USEPA (U.S. Environmental Protection Agency). 1999. Understanding Variation in Partition Coefficient, K_d, Values, Volume II, Office of Air and Radiation, EPA 402-R-99-004B, Washington, DC: USEPA.

USGS (U.S. Geological Survey). 2010. Estimates of Groundwater Age from Till and Carbonate Bedrock Hydrogeologic Units at Jefferson Proving Ground, Southeastern Indiana, 2007–08. Scientific Investigations Report 2010–5178. By Paul M. Buszka, David C. Lampe, and Amanda L. Egler.

USGS. 2013. National Water Information System: Web Interface, water level data accessed at http://nwis.waterdata.usgs.gov/nwis/dv?referred_module=gw&site_no=384949085251901.

U.S. Public Law 100-526. 1988. Base Closure and Realignment Act of 1988. 24 October.

Williams, G.P., A.M. Hermes, A.J. Policastro, H.M. Hartmann, and D. Tomasko. 1998. Potential Health Impacts from Range Fires at Aberdeen Proving Ground, Maryland. Argonne National Laboratory, Argonne, IL. 84 pp.

ATTACHMENT 1 – WATER LEVEL HYDROGRAPHS AND CONTINUOUS RECORDER DATA FOR DU IMPACT AREA WELLS

THIS PAGE WAS INTENTIONALLY LEFT BLANK

ATTACHMENT 1 – WATER LEVEL HYDROGRAPHS AND CONTINUOUS RECORDER DATA FOR DU IMPACT AREA WELLS

A brief description of each hydrograph is included here followed by individual plots of the data collected from each well.

- JPG-DU-01I: Graph has some irregularities at the beginning and end, but the rest has usable information. The beginning cycling is caused by the well cap being left on accidentally. When the cap was removed, the data smoothed out. The irregularities seen at the end are caused by the vent becoming submerged.
- JPG-DU-02I: This well contains a visible void with a direct connection to the stream. These water level readings are accurate with similar fluctuations seen in stream gauge data.
- JPG-DU-03I: Well does take a long time to recover from purging during sampling; water levels do show seasonal variations, including drops in water levels from spring 2008 through summer 2008.
- JPG-DU-04D: Well does not recover from purging for sampling.
- JPG-DU-05I: Due to the proximity of the well to the stream, there is a strong correlation between precipitation events causing rise in the stream stage and in the well. Changes in water levels in the well have a slight delay when compared with stream gauge data.
- JPG-DU-06O: Semismooth graph showing seasonal variations.
- JPG-DU-06I: Semismooth graph showing seasonal variations.
- JPG-DU-06D: Water levels take a long time to recover from purging during sampling events.
- JPG-DU-8I: Well does not recover from purging for sampling.
- JPG-DU-09O: Graph has some irregularities at the beginning cycling is caused by the cap being left on accidentally. Water levels do indicate slightly longer recovery time following sampling efforts.
- JPG-DU-09I: Water levels show seasonal variation and indicate slightly longer recovery time following sampling efforts.
- JPG-DU-09D: Water levels take a long time to recover from purging during sampling events.
- MW-2: Graph has some irregularities at the beginning cycling, which is caused by the cap being left on accidentally. Seasonal variations apparent in the data.
- MW-9: Well does not recover from purging for sampling.
- MW-11: No useable data.

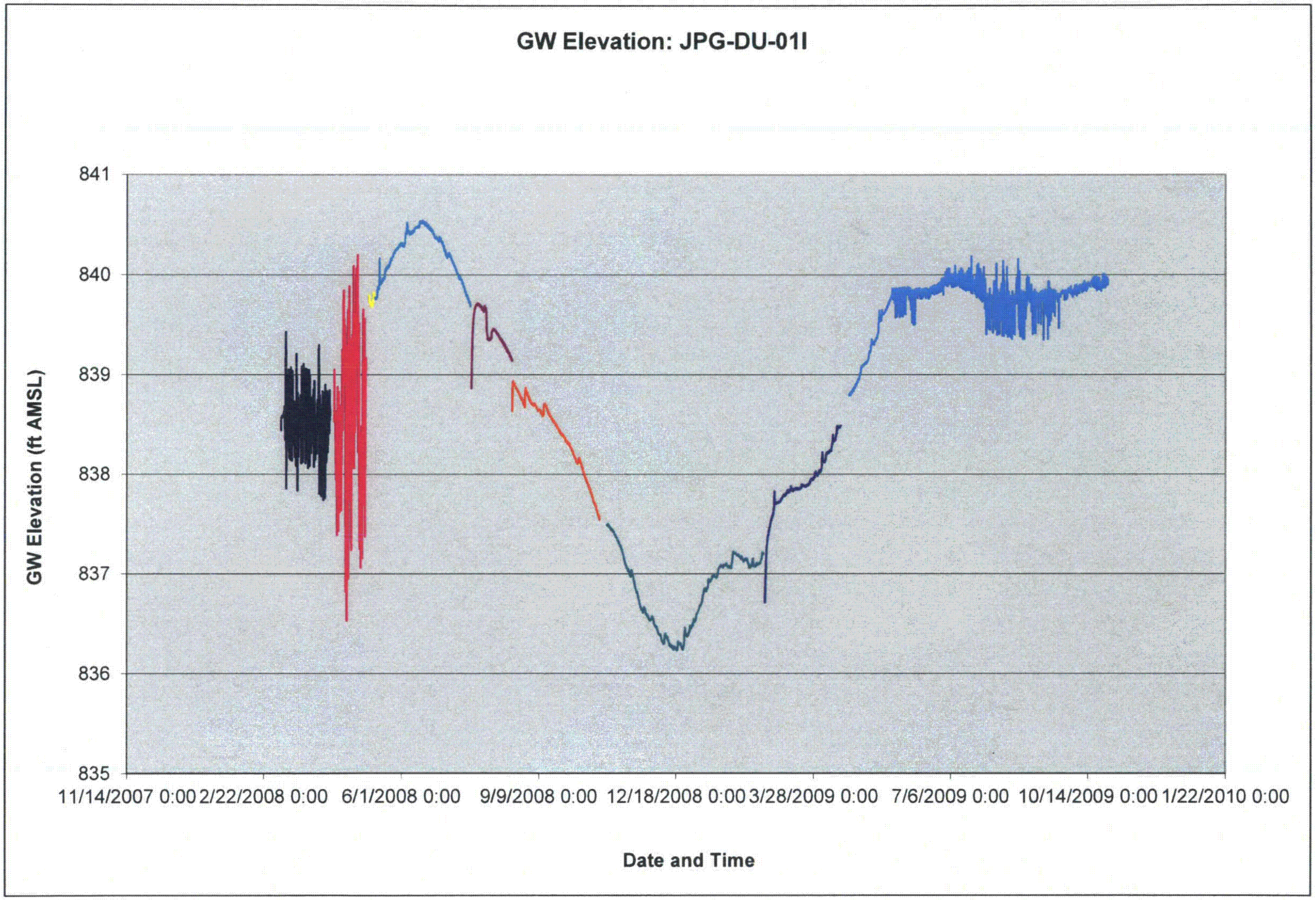
GW Elevation: JPG-DU-01I
GW Elevation (ft AMSL)
841
840
839
838
837
836
835
11/14/2007 0:00
2/22/2008 0:00
6/1/2008 0:00
9/9/2008 0:00
12/18/2008 0:00
3/28/2009 0:00
7/6/2009 0:00
10/14/2009 0:00
1/22/2010 0:00
Date and Time

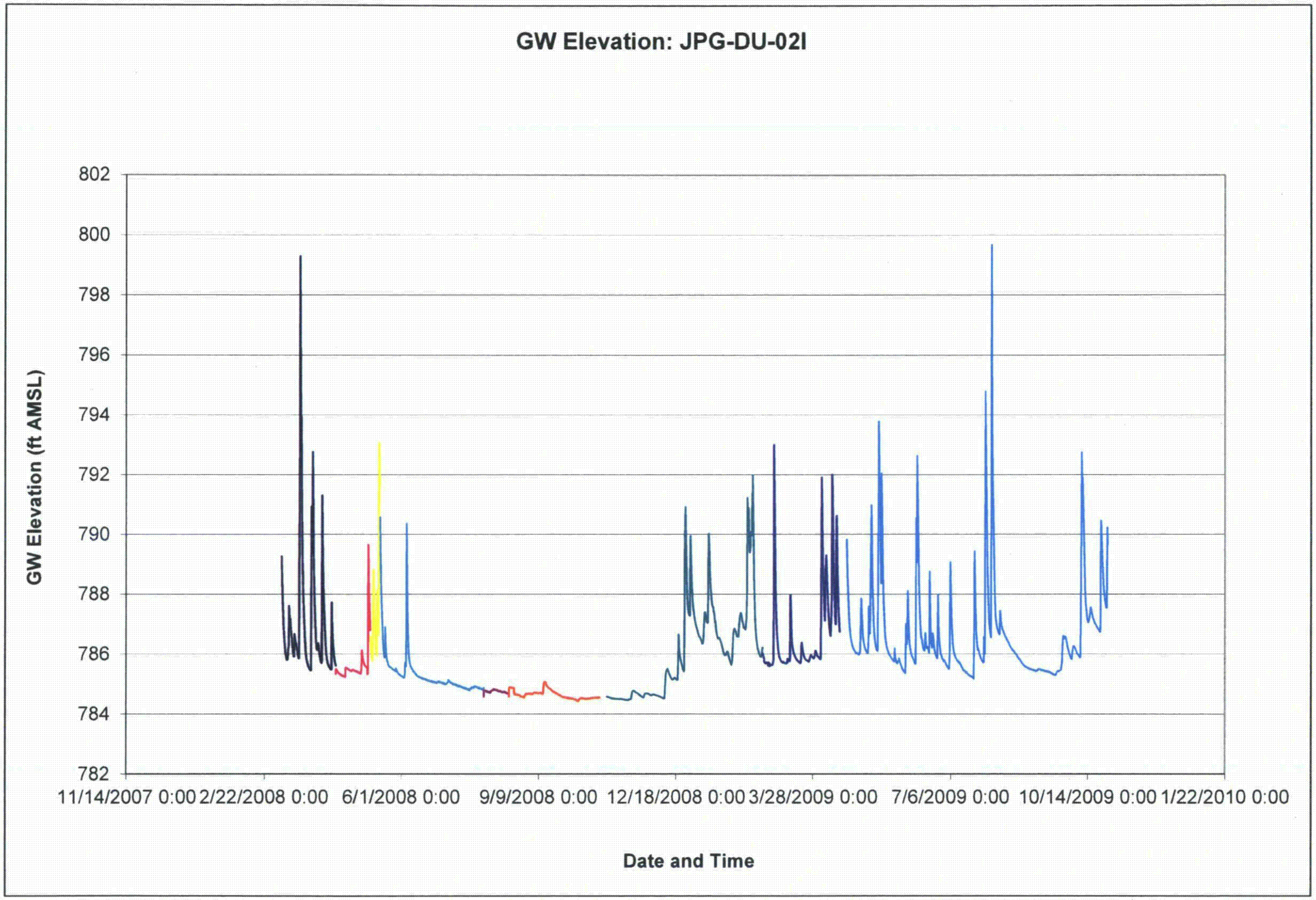
GW Elevation: JPG-DU-02I
GW Elevation (ft AMSL)
802
800
798
796
794
792
790
788
786
784
782
11/14/2007 0:00
2/22/2008 0:00
6/1/2008 0:00
9/9/2008 0:00
12/18/2008 0:00
3/28/2009 0:00
7/6/2009 0:00
10/14/2009 0:00
1/22/2010 0:00
Date and Time

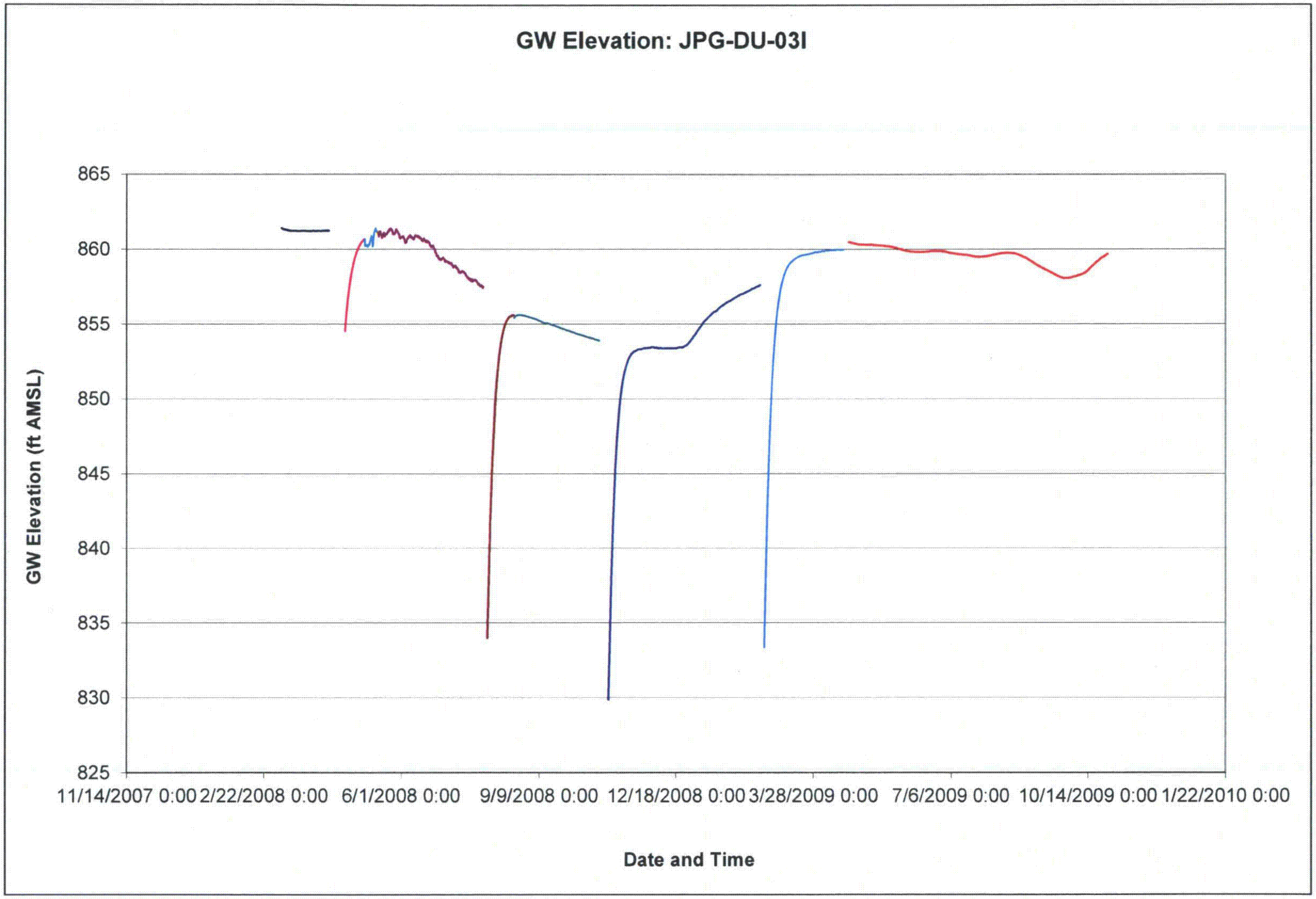
GW Elevation: JPG-DU-03I
GW Elevation (ft AMSL)
865
860
855
850
845
840
835
830
825
11/14/2007 0:00
2/22/2008 0:00
6/1/2008 0:00
9/9/2008 0:00
12/18/2008 0:00
3/28/2009 0:00
7/6/2009 0:00
10/14/2009 0:00
1/22/2010 0:00
Date and Time

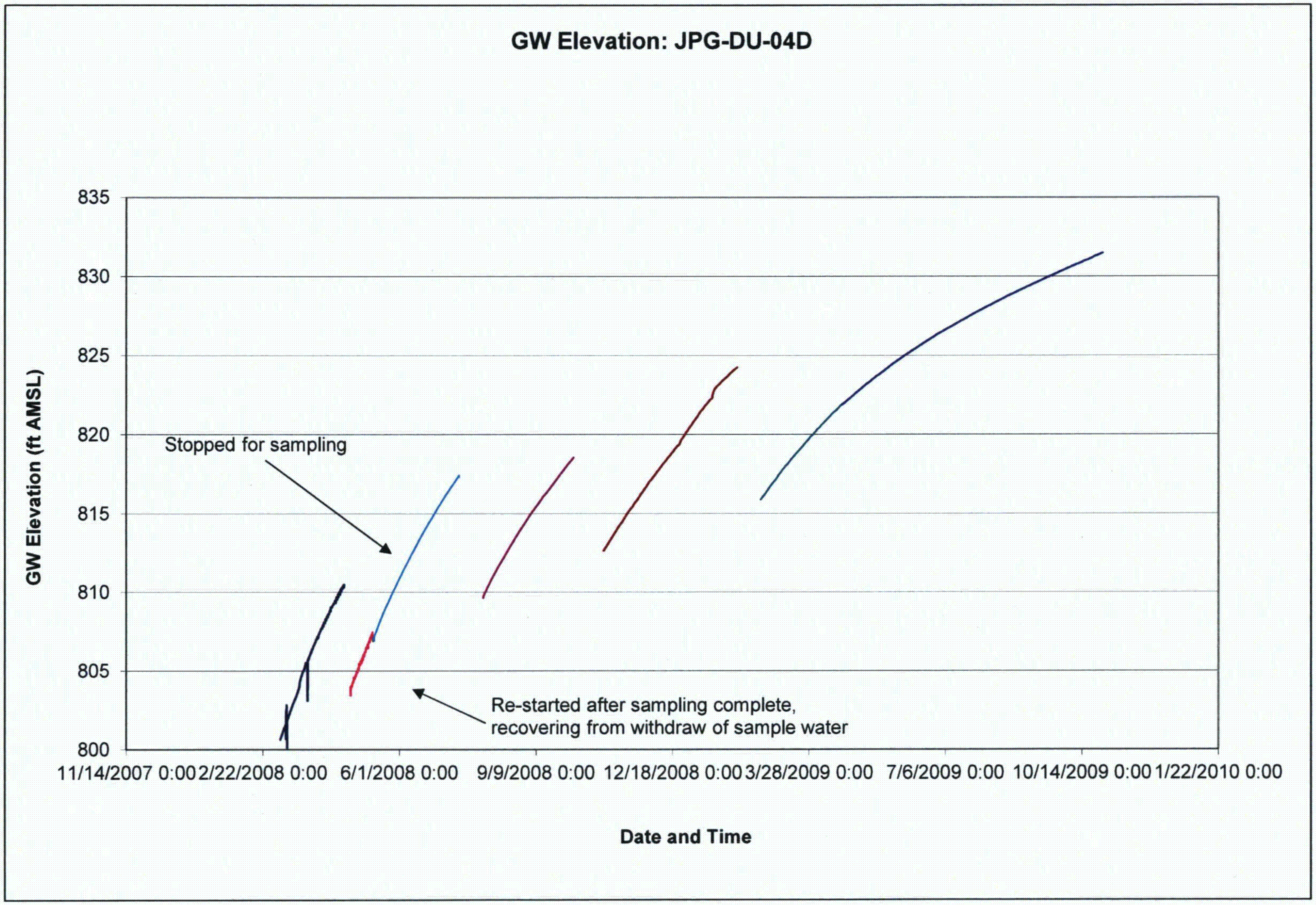
GW Elevation: JPG-DU-04D
GW Elevation (ft AMSL)
835
830
825
820
815
810
805
800
Stopped for sampling
Re-started after sampling complete,
recovering from withdraw of sample water
11/14/2007 0:00
2/22/2008 0:00
6/1/2008 0:00
9/9/2008 0:00
12/18/2008 0:00
3/28/2009 0:00
7/6/2009 0:00
10/14/2009 0:00
1/22/2010 0:00
Date and Time

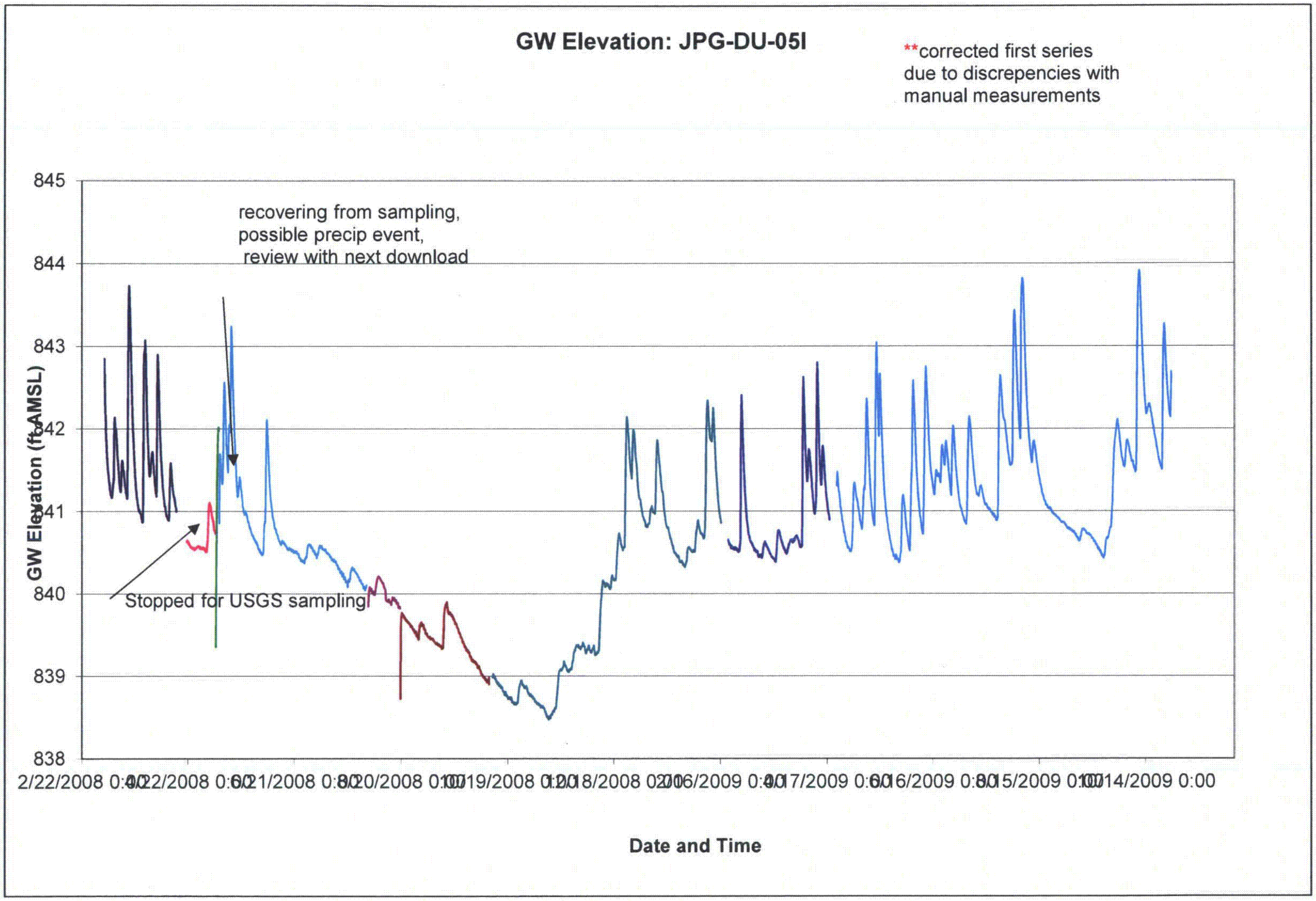
GW Elevation: JPG-DU-05I
**corrected first series
due to discrepencies with
manual measurements
recovering from sampling,
possible precip event,
review with next download
Stopped for USGS sampling
GW Elevation (ft AMSL)
845
844
843
842
841
840
839
838
2/22/2008 0:00
4/22/2008 0:00
6/21/2008 0:00
8/20/2008 0:00
10/19/2008 0:00
12/18/2008 0:00
2/16/2009 0:00
4/17/2009 0:00
6/16/2009 0:00
8/15/2009 0:00
10/14/2009 0:00
Date and Time

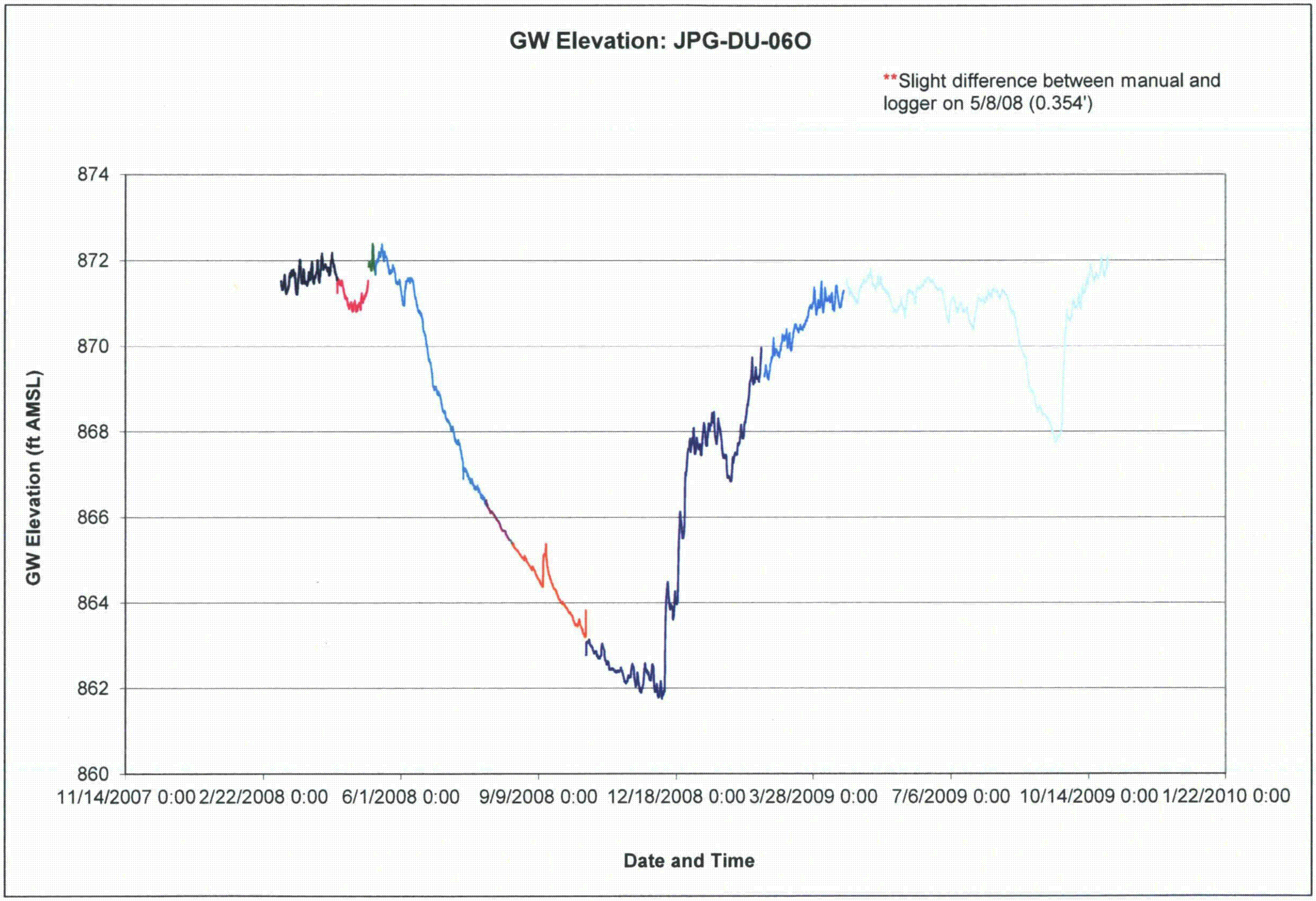
GW Elevation: JPG-DU-06O
**Slight difference between manual and logger on 5/8/08 (0.354')
874
872
870
868
866
864
862
860
GW Elevation (ft AMSL)
11/14/2007 0:00
2/22/2008 0:00
6/1/2008 0:00
9/9/2008 0:00
12/18/2008 0:00
3/28/2009 0:00
7/6/2009 0:00
10/14/2009 0:00
1/22/2010 0:00
Date and Time

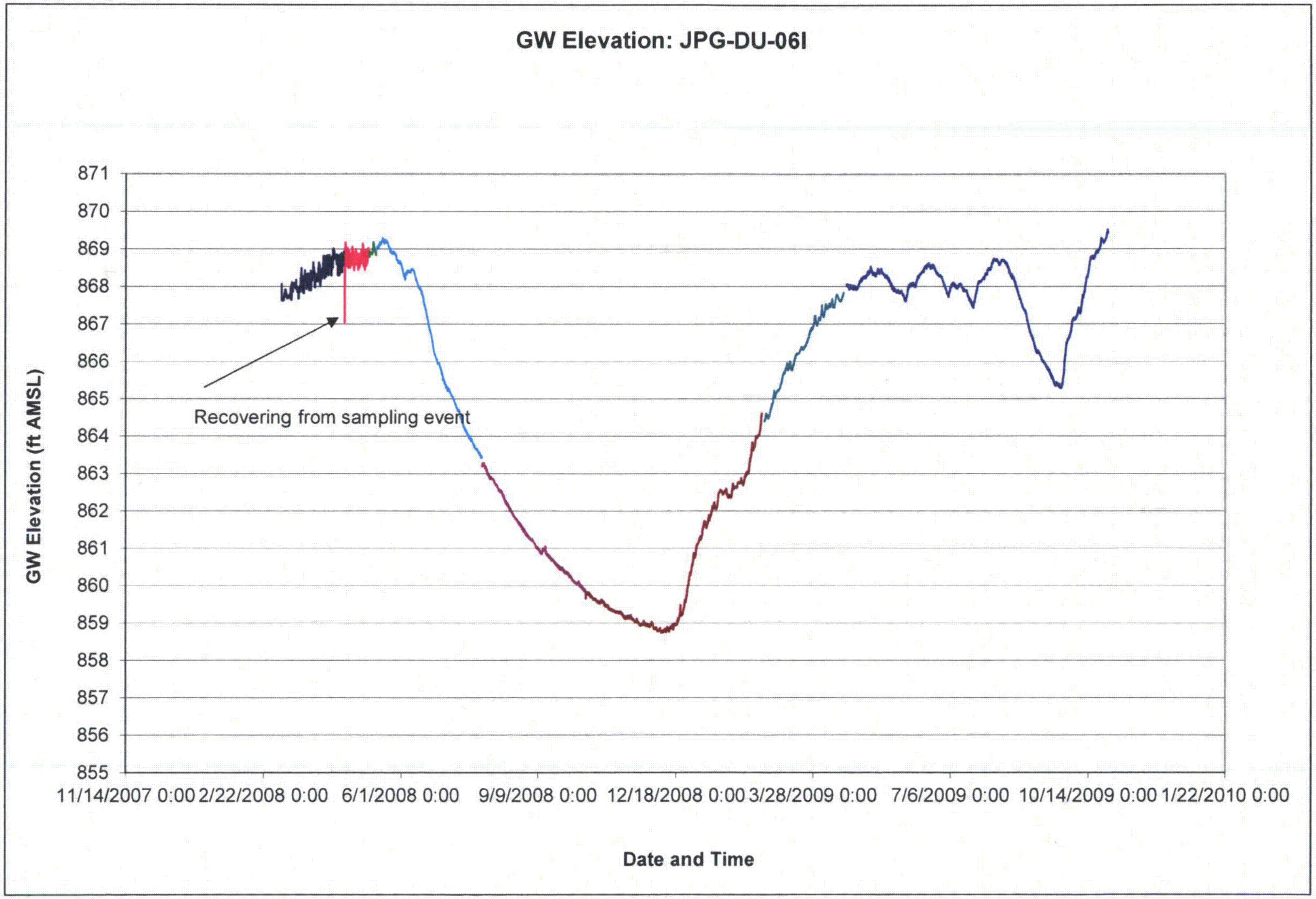
GW Elevation: JPG-DU-06I
GW Elevation (ft AMSL)
871
870
869
868
867
866
865
864
863
862
861
860
859
858
857
856
855
Recovering from sampling event
11/14/2007 0:00
2/22/2008 0:00
6/1/2008 0:00
9/9/2008 0:00
12/18/2008 0:00
3/28/2009 0:00
7/6/2009 0:00
10/14/2009 0:00
1/22/2010 0:00
Date and Time

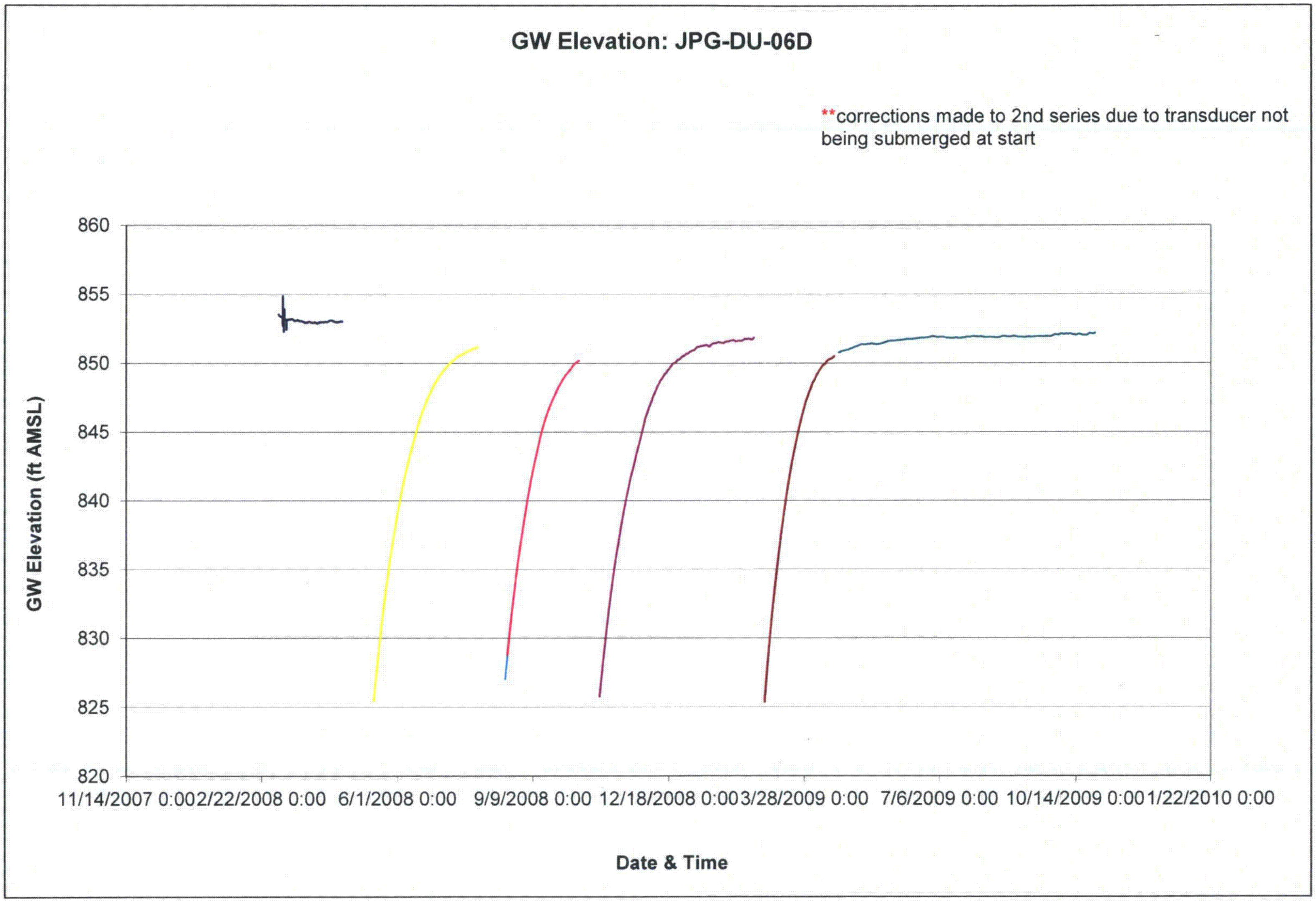
GW Elevation: JPG-DU-06D
**corrections made to 2nd series due to transducer not being submerged at start
GW Elevation (ft AMSL)
860
855
850
845
840
835
830
825
820
11/14/2007 0:00
2/22/2008 0:00
6/1/2008 0:00
9/9/2008 0:00
12/18/2008 0:00
3/28/2009 0:00
7/6/2009 0:00
10/14/2009 0:00
1/22/2010 0:00
Date & Time

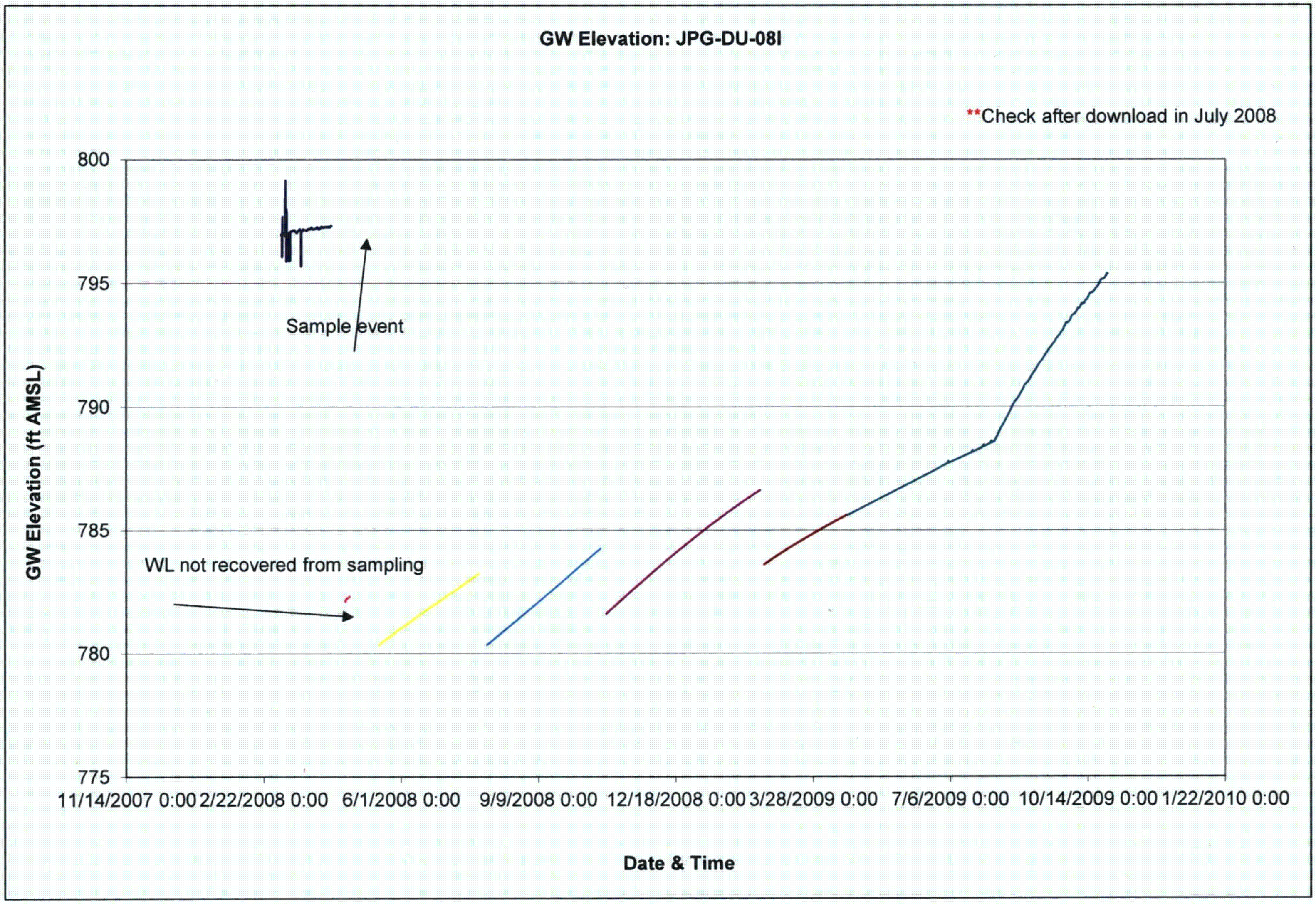
GW Elevation: JPG-DU-08I
**Check after download in July 2008
Sample event
WL not recovered from sampling
GW Elevation (ft AMSL)
800
795
790
785
780
775
11/14/2007 0:00
2/22/2008 0:00
6/1/2008 0:00
9/9/2008 0:00
12/18/2008 0:00
3/28/2009 0:00
7/6/2009 0:00
10/14/2009 0:00
1/22/2010 0:00
Date & Time

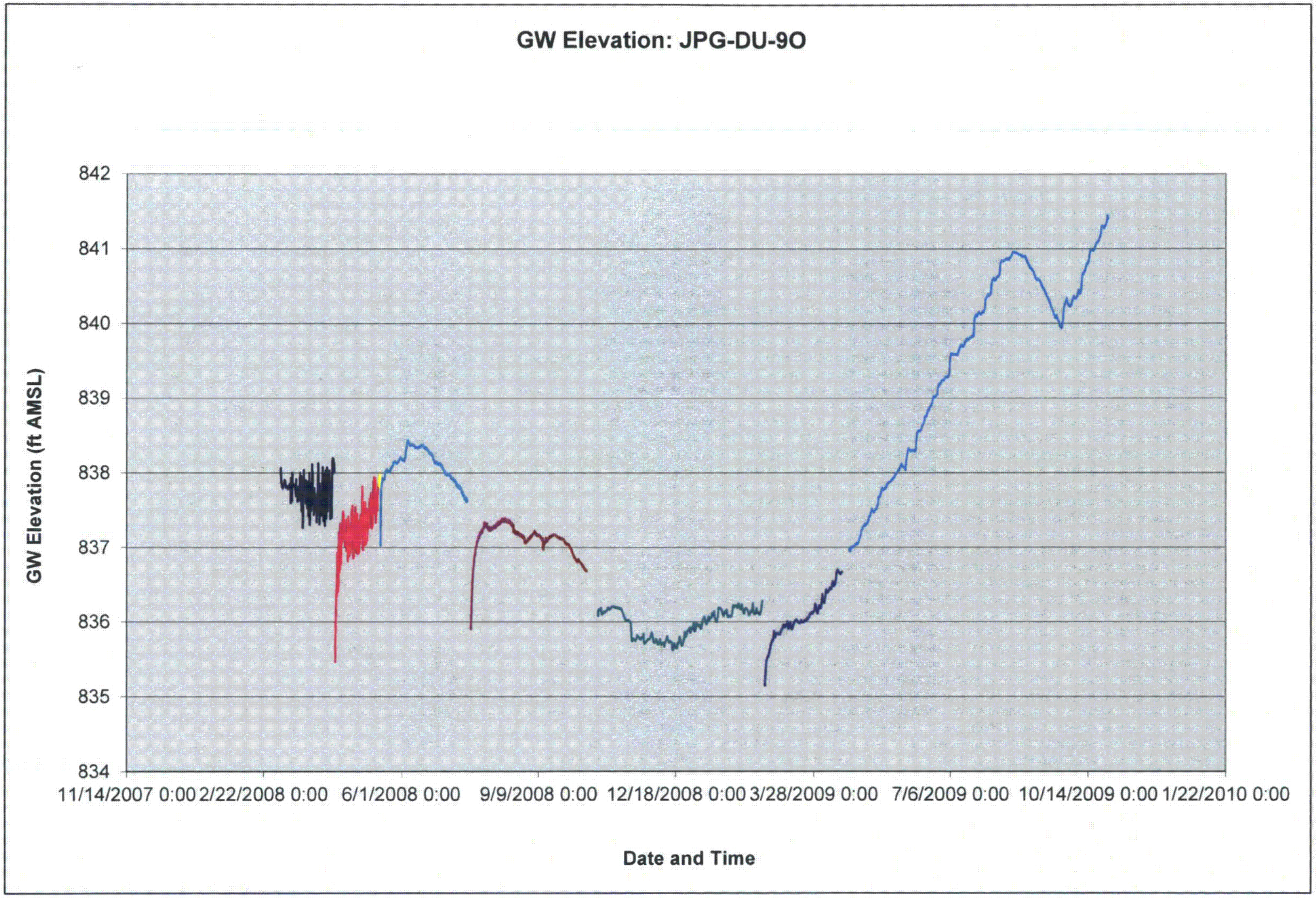
GW Elevation: JPG-DU-9O
GW Elevation (ft AMSL)
842
841
840
839
838
837
836
835
834
11/14/2007 0:00
2/22/2008 0:00
6/1/2008 0:00
9/9/2008 0:00
12/18/2008 0:00
3/28/2009 0:00
7/6/2009 0:00
10/14/2009 0:00
1/22/2010 0:00
Date and Time

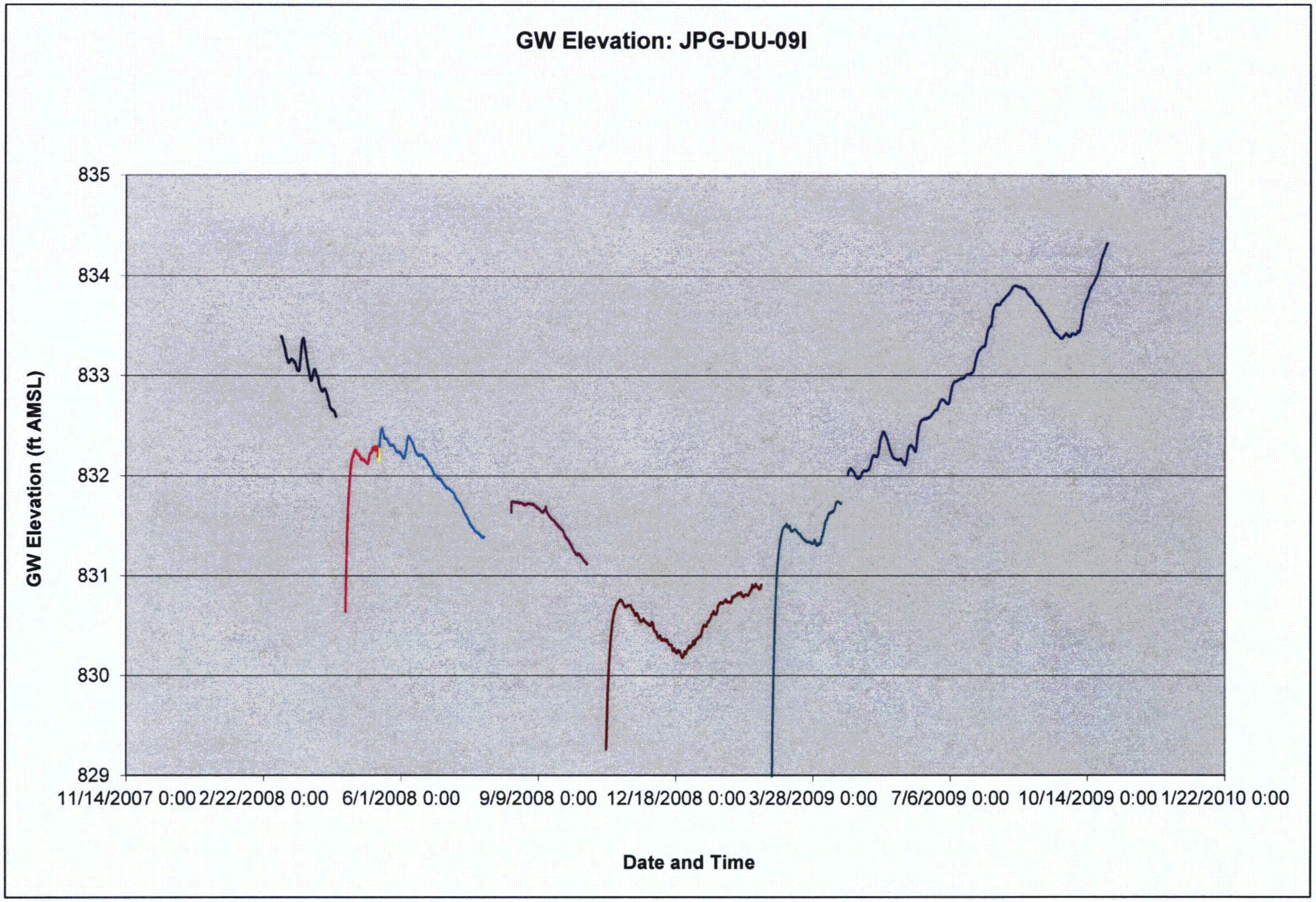
GW Elevation: JPG-DU-09I
GW Elevation (ft AMSL)
835
834
833
832
831
830
829
11/14/2007 0:00
2/22/2008 0:00
6/1/2008 0:00
9/9/2008 0:00
12/18/2008 0:00
3/28/2009 0:00
7/6/2009 0:00
10/14/2009 0:00
1/22/2010 0:00
Date and Time

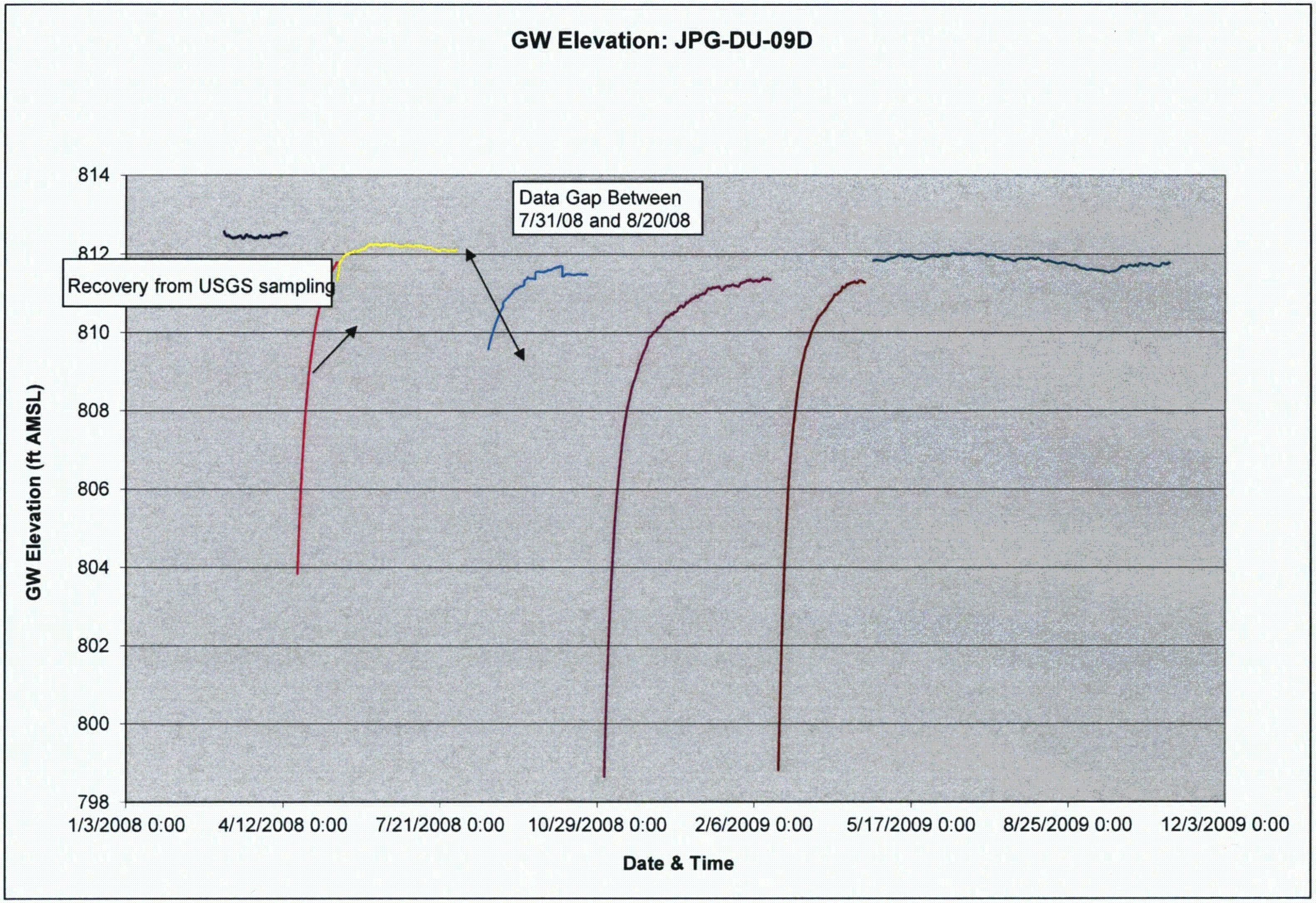
GW Elevation: JPG-DU-09D
Data Gap Between
7/31/08 and 8/20/08
Recovery from USGS sampling
GW Elevation (ft AMSL)
814
812
810
808
806
804
802
800
798
1/3/2008 0:00
4/12/2008 0:00
7/21/2008 0:00
10/29/2008 0:00
2/6/2009 0:00
5/17/2009 0:00
8/25/2009 0:00
12/3/2009 0:00
Date & Time

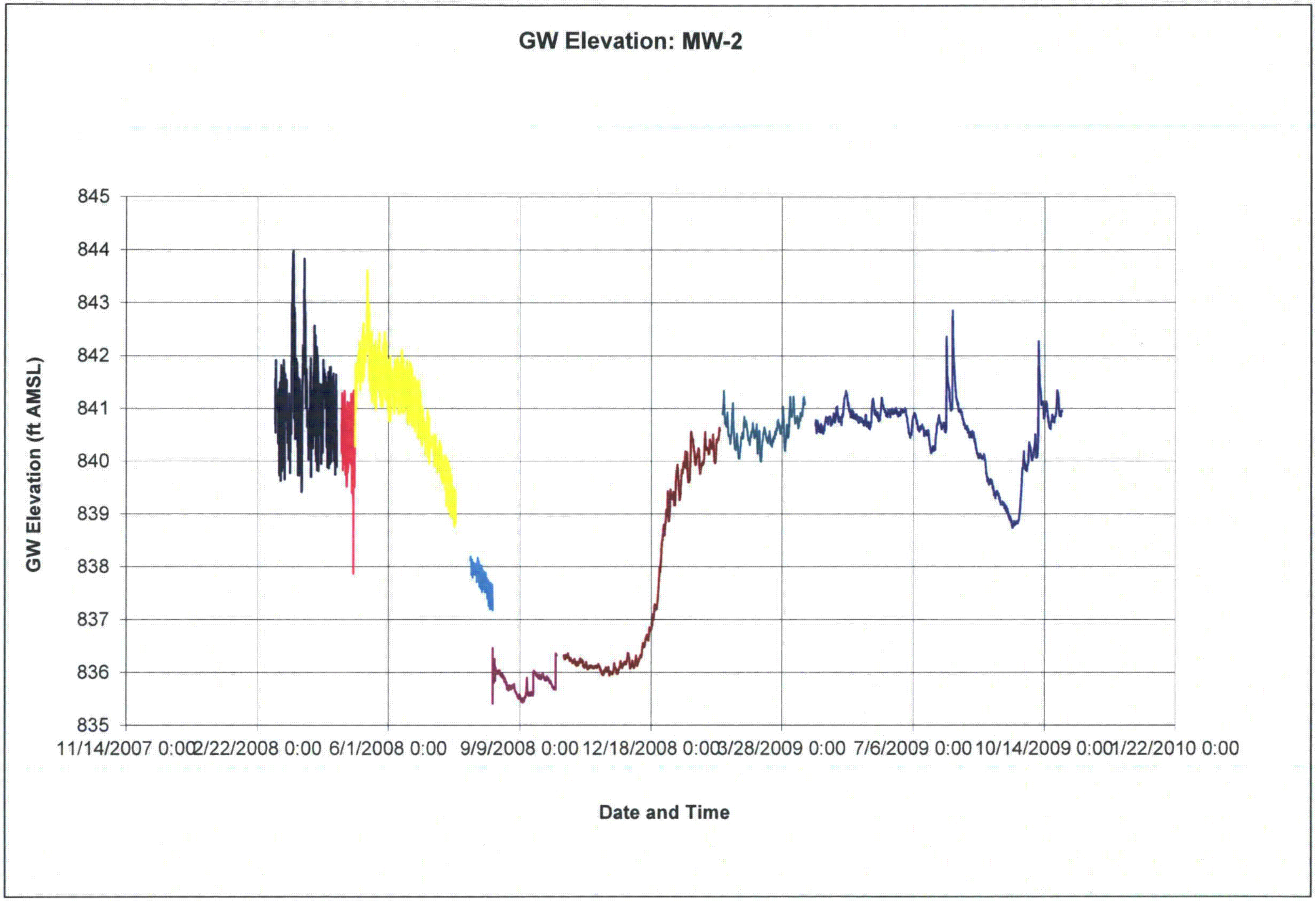
GW Elevation: MW-2
GW Elevation (ft AMSL)
845
844
843
842
841
840
839
838
837
836
835
11/14/2007 0:00
2/22/2008 0:00
6/1/2008 0:00
9/9/2008 0:00
12/18/2008 0:00
3/28/2009 0:00
7/6/2009 0:00
10/14/2009 0:00
1/22/2010 0:00
Date and Time

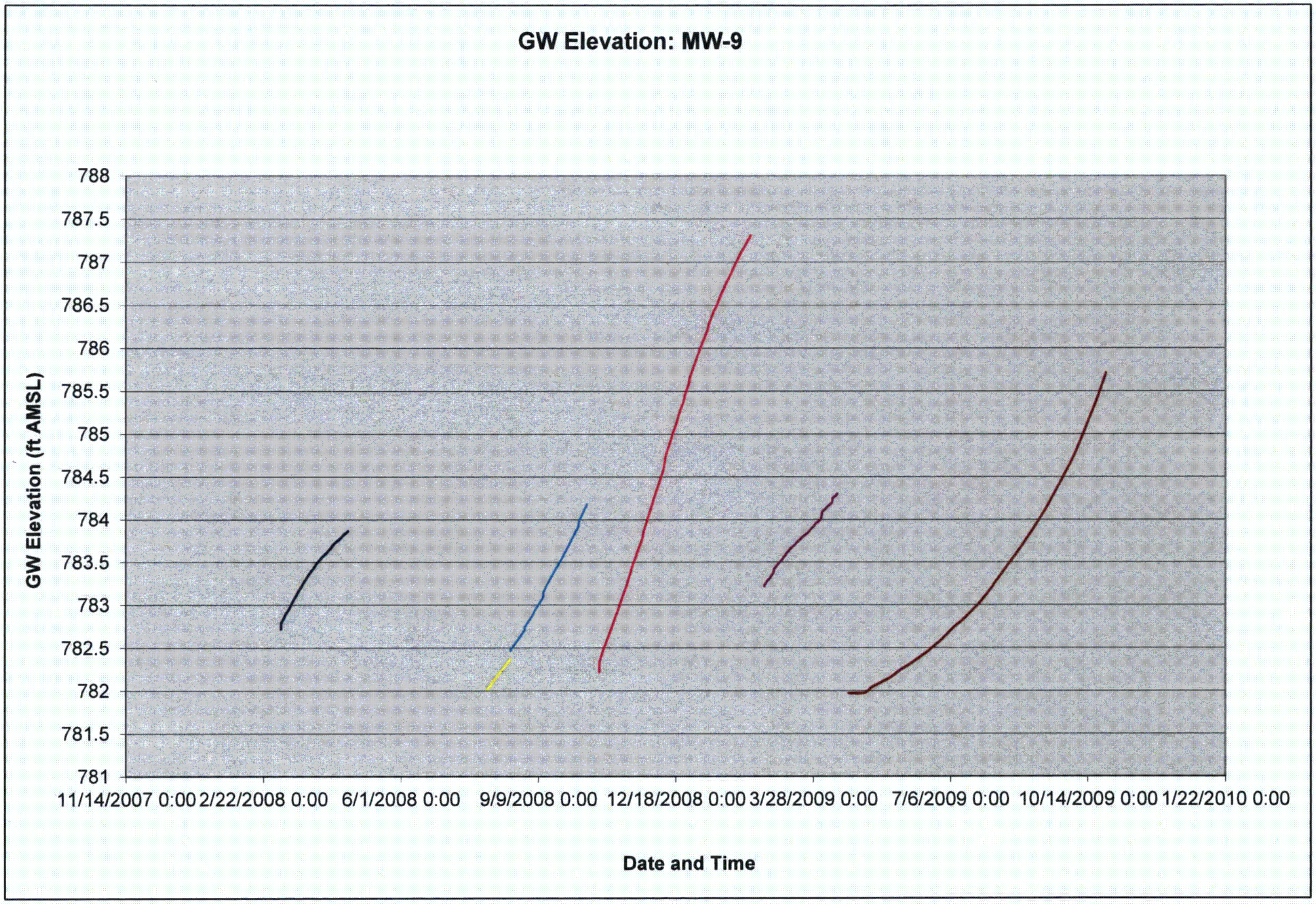
GW Elevation: MW-9
GW Elevation (ft AMSL)
788
787.5
787
786.5
786
785.5
785
784.5
784
783.5
783
782.5
782
781.5
781
11/14/2007 0:00
2/22/2008 0:00
6/1/2008 0:00
9/9/2008 0:00
12/18/2008 0:00
3/28/2009 0:00
7/6/2009 0:00
10/14/2009 0:00
1/22/2010 0:00
Date and Time

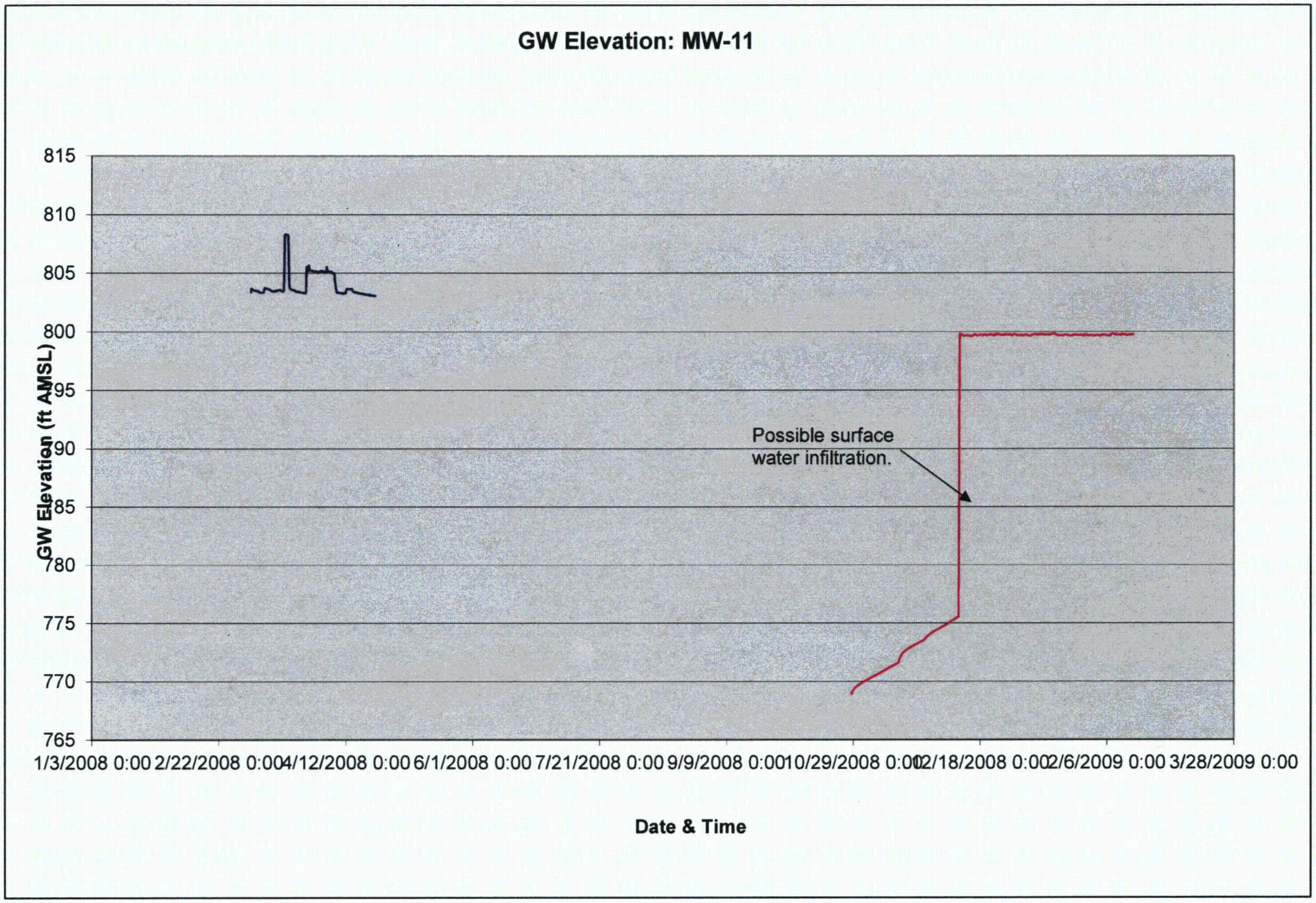
GW Elevation: MW-11
815
810
805
800
795
790
785
780
775
770
765
GW Elevation (ft AMSL)
Possible surface water infiltration.
1/3/2008 0:00
2/22/2008 0:00
4/12/2008 0:00
6/1/2008 0:00
7/21/2008 0:00
9/9/2008 0:00
10/29/2008 0:00
12/18/2008 0:00
2/6/2009 0:00
3/28/2009 0:00
Date & Time